MOLECULAR INTERACTIONS AND BINDING MECHANISMS OF HYDROPHOBIC HOFMEISTER CATIONS TO MACROMOLECULES

A THESIS SUBMITTED TO

THE GRADUATE SCHOOL OF ENGINEERING AND SCIENCE

OF

BILKENT UNIVERSITY

IN PARTIAL FULFILLMENT OF THE REQUIREMENTS FOR

THE DEGREE OF

MASTER OF SCIENCE

IN

CHEMISTRY

BY

UMAY EREN ERTEKIN

AUGUST 2023

MOLECULAR INTERACTIONS AND BINDING MECHANISMS OF HYDROPHOBIC HOFMEISTER CATIONS TO MACROMOLECULES

BY UMAY EREN ERTEKIN
AUGUST 2023

We certify that we have read this thesis and that in our opinion it is fully adequate, in scope and in quality, as a thesis for the degree of Master of Science.

Halil Ibrahim Okur (Advisor)

Emre Büküşoğlu

Burak Ülgüt

Approved for the Graduate School of Engineering and Science:

Orhan Arıkan

Director of the Graduate School

ABSTRACT

MOLECULAR INTERACTIONS AND BINDING MECHANISMS OF HYDROPHOBIC HOFMEISTER CATIONS TO MACROMOLECULES

UMAY EREN ERTEKIN

M.S. in Chemistry

Advisor: HALIL IBRAHIM OKUR

AUGUST 2023

It's been known for over a century that ions specifically affect the bulk properties of solutions, behavior of macromolecules and a myriad of interfacial phenomena occurring in solution. Yet, the molecular mechanisms underlying these so-called Hofmeister effects are only recently being realized within the last few decades. In the resurgence in specific ion effects studies, the role attributed to cations has been relatively understated in comparison to the effects of anions. Whereas various molecular mechanisms have been elucidated for a diverse spectrum of anions, cationic effects have largely remained limited to common metal ions. Within the cationic Hofmeister series for cations, strongly-hydrated cations exhibit very weak binding to polar, electronegative groups, but weakly-hydrated cations in particular are classified as non-interacting. This thesis brings a much-needed expansion to specific cation effects by investigating the interactions between the weakly-hydrated tetraalkylammonium cations and model neutral thermoresponsive polymers, principally poly(*N*-isopropylacrylamide) (PNIPAM). The hydrophobicity of the cations is incrementally tuned by increasing the length of their alkyl chains, thus forming the series of salts investigated herein: NR_4Cl where R = H, Me, Et, *n*-Pr, *n*-Bu, and the anion is kept constant as Cl^-. By using a multi-instrumental approach, it is demonstrated that the largest of these cations exhibit a significant binding to the polymers and that the resulting salting-in effects are comparable in magnitude to those observed for sodium salts of weakly-hydrated anions. Thermodynamic phase transition measurements of the polymers are complemented by ATR-FTIR and quantitative ^{1}H-NMR spectroscopic studies to systematically investigate the nature and molecular-level mechanism of the interaction. In stark contrast to the known behavior of the strongly-hydrated cations, through the temperature-controlled ATR-FTIR investigations it is found that carbonyl moieties are not the primary sites of interaction. Instead, it is found that these weakly-hydrated, 'greasy' cations preferentially interact with the most hydrophobic groups on the polymer: the isopropyl

group on the PNIPAM side-chain, as revealed by a quantitative externally-referenced ^{1}H-NMR methodology developed to elucidate ion-macromolecule interactions. The binding generally follows a Langmuir-type saturation behavior and exhibits site-specific dissociation constants as low as $K_D \approx 0.2$ M. This unprecedented, hydrophobically-mediated interaction between weakly-hydrated tetraalkylammonium cations and neutral macromolecules is then demonstrated to be a general mechanism and is shown to extend to polymers of vastly different molecular architectures. The results presented, thus, signify a new, more expansive view of cationic Hofmeister effects, where the far weakly-hydrated region of the series interacts with a novel mechanism entirely unlike that of other cations.

Keywords: Hofmeister series, specific ion effects, hydrophobic cations, quaternary ammonium cations, thermoresponsive polymers, PNIPAM

ÖZET

HİDROFOBİK HOFMEİSTER KATYONLARININ MAKROMOLEKÜLLER İLE ETKİLEŞİMLERİ VE BAĞLANMA MEKANİZMALARI

UMAY EREN ERTEKIN

Kimya | Yüksek Lisans

Danışman: HALİL İBRAHIM OKUR

AĞUSTOS 2023

Yüzyılı aşkın süredir iyonların çözeltilerin toplu özelliklerini, makromoleküllerin özelliklerini ve de arayüzeylerde gerçekleşen sayısız olayı etkilediği bilinmektedir. Hofmeister etkileri olarak anılan bu olayların moleküler mekanizmaları ancak son birkaç on yılda çözümlenebilmiştir. Spesifik iyon etkileri çalışmalarının yeniden yaygınlık kazandığı bu dönemde katyonlara atfedilen rol, anyonlarınkilere göre nispeten arka planda kalmaktadır. Anyonlar için çeşitli moleküler mekanizmalar ortaya konulmuşken katyon etkileri çoğunlukla yaygın metal iyonlarıyla sınırlı kalmıştır. Hofmeister katyon serisinde görülen kuvvetli-hidrasyonlu katyonlar elektronegatif polar gruplara zayıf bağlanma gösterirken, özellikle zayıf-hidrasyonlu katyonlar etkileşim göstermeyen türler olarak anlaşılmaktadır. Burada, zayıf-hidrasyonlu tetraalkilamonyum katyonları ile başlıca poli(*N*-izopropilakrilamid) (PNIPAM) olmak üzere model nötr termoresponsif polimerlerin etkileşimleri incelenerek spesifik katyon etkileri alanının ihtiyaç duyduğu açık olan bir genişletme sunulmaktadır. İncelenen katyonların hidrofobik özellikleri alkil zincirlerinin kademeli artırılması ile kontrol edilmiş olup, şu şekildeki klorür tuzları serisi olarak ele alınmıştır: NR_4Cl, R = H, Me, Et, *n*-Pr, *n*-Bu. Tuzlardaki anyon klorür (Cl^-) olarak sabit tutulmuştur. Birden fazla enstrümantal metot ile burada gösterilen, ele alınan katyonlar arasındaki en büyük türlerin polimerlere kayda değer bir bağlanma gösterdiği ve ortaya çıkardıkları tuzla-çözünme etkisinin zayıf-hidrasyonlu anyonların etkilerine benzer ölçüde olduğudur. Polimerlerin termodinamik faz geçiş ölçümleri, tamamlayıcı olarak zayıflatılmış toplam yansıma - Fourier dönüşümlü kızılötesi spektroskopisi (ATR-FTIR) ölçümleri ve nicel ^{1}H-NMR spektroskopisi ölçümleri ile birlikte çalışılmış olup böylece görülen etkileşimin moleküler düzeydeki mekanizması irdelenmiştir. Kuvvetli-hidrasyonlu katyonlar için bilinen mekanizmanın aksine, karbonil gruplarının bu iyonlar için birincil etkileşim merkezleri olmadığı sıcaklık kontrolüyle gerçekleştirilen ATR-FTIR

deneyleri ile ortaya konulmuştur. Bundan farklı olarak, bu zayıf-hidrasyonlu, 'yağlı' katyonların polimerdeki en hidrofobik özellikteki gruplar ile etkileştiği belirlenmiştir. İyon-makromolekül etkileşimlerini karakterize etmek için geliştirilen ^{1}H-NMR metodolojisi ile bu etkileşimlerin birincil olarak izopropil yan zinciri ile olduğu açığa çıkmıştır. Bağlanma genel olarak Langmuir türünde bir doyma özelliklidir ve grup-spesifik bağlanma için belirlenen ayrışma denge sabiti $K_D \approx 0.2$ M kadar küçüktür. Zayıf-hidrasyonlu katyonlar ile nötr makromoleküller arasındaki bu hidrofobik özellikteki etkileşim, daha önce hiç gösterilmemiş bir mekanizmadır. Ayrıca, bu mekanizmanın evrensel olduğu çeşitli moleküler yapıdaki polimerler için de geçerli olduğu gösterilerek ortaya konmuştur. Sonuç olarak, bu tezde sunulan buluntular Hofmeister etkileri için zayıf-hidrasyonlu iyonların tümüyle farklı bir mekanizma aracılığı ile etkileşimler gösterdiği, daha geniş, yeni bir model ifade etmektedir.

Anahtar kelimeler: Hofmeister serileri, spesifik iyon etkileri, hidrofobik katyonlar, kuvaterner amonyum katyonları, termoresponsif polimerler, PNIPAM

ACKNOWLEDGEMENT

Looking back on all that I have worked on and achieved over the last three years, I am indebted, first and greatest of all, to my advisor Dr. Halil Okur. His academic experience, breadth of scientific knowledge, and optimistic, practical research attitude have been absolutely invaluable to my growth as a researcher. I know for a fact that I would not be where I am at this point in my life without his guidance. For his endless patience, deep kindness and compassionate mentorship mindset I am infinitely grateful and feel a profound respect. I feel so lucky to have worked with Dr. Okur over the last few years, and hope that our time working together has been as enjoyable for him as it has been for me. I give my sincerest thanks for everything, and hope our correspondence—both over science and in friendship—extends far into the future. From my heart: Thank you, hocam. I wish you all the best.

I wish to thank every member of the Okur Lab, past and present. I believe that good research can only be done in a healthy, supportive environment and that interpersonal exchange leads to mutual growth. Getting to know all of you and working together has been a great joy—as was seeing the research group grow over the years. I wish all current and future members the best!

I would like to thank Dr. Burak Ülgüt and Dr. Emre Büküşoğlu for their kind acceptance of serving on my thesis committee, their feedback and our valuable discussion, which I found most enjoyable and insightful.

I would also like to thank the whole Bilkent Department of Chemistry, which has been my home and my teacher for the last seven years. What a journey it has been.

To my family: thank you, from the bottom of my heart, for your unconditional, unrelenting support. I could not be where I am now without you—I will never forget it. I hope we always share in our pride and our love.

To all my friends, here in Bilkent and beyond: Thank you for giving life meaning and bringing joy. How lucky I am that our paths have crossed. We carry prints of each other in our hearts, our minds and our souls. I will see you again soon. Take care.

Lastly: to myself. Thank you, Umay. You are precious, present, whole. To every person who has felt hopeless, lost, grief-stricken: your story carries meaning, and is being written yet. You can do hard things. To every person who has felt broken, alone, marginalized: thank you for being here, for being your beautiful self. Our journeys continue. How precious that your colors grace the world.

Thank you.

TABLE OF CONTENTS

LIST OF FIGURES

LIST OF TABLES

Chapter 1 – Introduction

1.1 Hofmeister effects: History, Legacy, Present.

Ions in solution affect everything. Such a rather crude but also concise description of the sheer range of specific ion effects (SIE) in aqueous—as well as non-aqueous—physical, chemical and biophysical contexts is perhaps an appropriate summary. Since the publication of a series of studies by Franz Hofmeister and colleagues in the late nineteenth century, the awareness of how dissolved salts affect the behavior of proteins has truly germinated and grown branches that span the breadth of the physical chemistry of solutions, electrolytes, colloids and soft matter. Ions have been shown to modulate protein solubility, folding, aggregation and self-assembly; enzyme activity; stability of DNA helices; surfactant micellization; lipid and colloid self-assembly; as well as solution properties other than those involving macromolecular solutes, such as surface tensions, viscosity and bubble coalescence.[1–5] Hofmeister effects have been invoked in observations involving water retention of wool,[6] bacterial growth,[6,7] and even thundercloud electrification.[8] Named in honor of Franz Hofmeister for his pioneering work, these effects are commonly organized into the so-called Hofmeister series that give the rank order of anions and cations specifically. Figure 1 below shows a typical ordering of anions and cations according to the Hofmeister series.

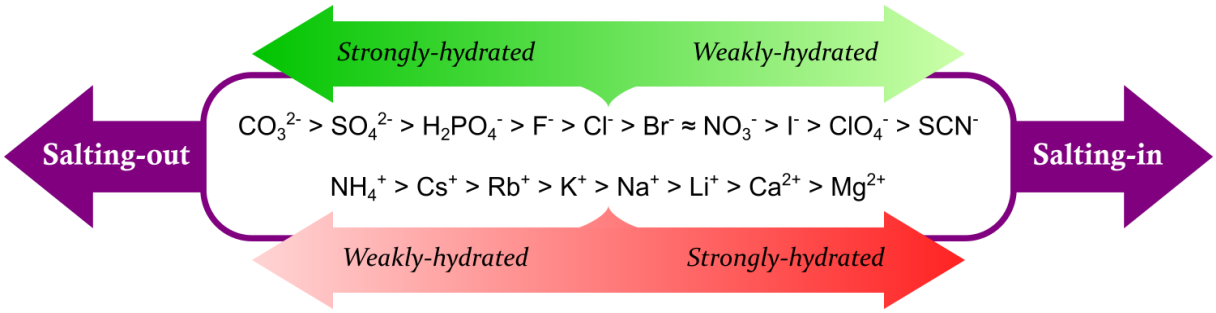

Figure 1: A rank order for Hofmeister anions and cations that one may come across in the literature, ordered from most salting-out (left) to most salting-in (right). The anion series is shown above and the cation series below. Note that the ordering of the two series based on strongly- to weakly-hydrated is inverted, as indicated by the corresponding green (for anions) and red (for cations) arrows. Ion orderings are based on Zhang et al.[9] and Bruce et al.[10]

Indeed, the implications and applicability of the phenomena seemed boundless; from its inception, the importance of understanding the nature of these effects has been recognized, described as the 'highest of sciences'[4,11] To this day, their study has been described as central

to the science of physical chemistry as the work of Mendel is to genetics.[4,12] Yet the continued relevance of the study of specific ion effects is also due, in part, to the complexity of the mechanistic puzzle. Approaching a century and half since their conception, much of the molecular mechanisms underlying Hofmeister effects still remain poorly understood, or otherwise contentious or convoluted. Focus on their study has waxed and waned, and undergone multiple paradigm shifts. For many researchers, the search for a 'holy grail' that describes all of Hofmeister effects continues to this day.

Yet, perhaps the previous analogy to Mendel may also provide an exit: as simplified Mendelian genetics were seen to be, so may the search for a single unifying theory explaining the entirety of specific ion effects—in its myriad contexts—be ultimately too idealistic and, moreover, limiting. In the current revival and continuing progress in the literature—dubbed the "Renaissance of Hofmeister"[13]—the search for a rigorous and encompassing theory continues,[4,12,14] but, in recent opinions, needs to be broken free of in favor elucidating the system-specific molecular-level study of mechanisms where these effects appear.[15,16] In other words, there may not a be one single 'holy grail'.[15] Indeed, significant and heartening strides have been made in systematic studies of specific ion effects on macromolecules in recent years,[10,16] and the field of specific ion effects continually expands beyond the classical species that appeared in Hofmeister's original studies.[17–19]

This chapter will attempt to contextualize the story of Hofmeister effects by providing, firstly, an overview of the historical developments from its inception to the present day and some of the major milestones that appear in our understanding of these phenomena in the following section. Then, the current molecular-level understanding of specific ion effects on macromolecules in aqueous solution, which contextualizes the relevance and motivation of this present work, will be detailed in the sections that follow.

1.1.1 Early Historical Developments in Hofmeister Studies

In a series of papers published starting 1887, Franz Hofmeister and colleagues described their observation of and initial attempts at explaining curious trends in how common salts could increase or decrease the solubility of proteins from aqueous solution. Before the advent of chromatographic methods, crystallization was a very common technique to purify proteins[2] and was thus of interest to Franz Hofmeister, who was a professor of pharmacology. The first of the series of papers—titled 'About the science of the effect of salts'—was authored by Lewith, Hofmeister's student, and was followed by the two most significant papers by

Hofmeister himself, subtitled "About regularities in the protein precipitating effects of salts and the relation of these effects with the physiological behavior of salts", and "About the water withdrawing effect of the salts". In the first two papers, Lewith and Hofmeister described their observed action of salts on precipitating proteins out of blood serum and whole hen egg white.[20–22] Their experiments were particularly informative, not only because they were the first expansive investigation of numerous salts in protein precipitation, but also because they were conducted systematically with sets of salts having common a cation or anion, to isolate and rank the effects of each.[16] In the third paper, Hofmeister attempted to provide an explanation to the mechanism behind their findings, based on what he described as 'water withdrawing ability';[20] ultimately, however, his attempt left him bemused.[4] Hofmeister was aware even at that stage that besides the inherent properties of the ions, encapsulated by the ability to 'hold' water in the bulk solution, specific interactions at the macromolecular interfaces likely also played a role—an aspect which, although he postulated to be the less important effect, he was unable to disentangle from the former.[4,20] Subsequent papers by Hofmeister and coworkers expanded their investigations to other systems, including the effects of alcohols and saccharose.[22–25]

Hofmeister's works were followed by reports by Voet,[26] Green,[27] and Cohn & Edsall[28] which attempted to replicate, systematize and quantify the salt effects on protein solubilities with careful control of conditions, with practical motivation in developing the methods for protein purification via crystallization.[3] They observed that, firstly, at lower concentrations the effect of salts is to salt-in (i.e., increase the solubility) the proteins, in line with Debye-Hückel theory.[3] Above the range of concentrations applicable, however, they reported that the solubility effect followed an empirical law formulated by Setschenow in 1889:[29]

$$\log\left(\frac{S_0}{S}\right) = \log(kc_s) \tag{1}$$

Here, S_0 and S respectively denote the solubilities of the solute in the absence and presence of salt of concentration c_s concentration of salt, and k is known as the salting-in (or out) coefficient. For salts that salt-in, the coefficient is negative, whereas for those that salt-out it is positive.[3] Setschenow was originally interested in the solubility of CO_2 in water in the presence of salts to better understand the transport of the gas in the bloodstream. The Setschenow equation was later also applied the solubility of many other small molecules, typically small nonpolar ones such as benzene.[2,30] Later, the empirical Setschenow equation found a theoretical basis; the form of Equation 1 has been derived from the 'weak interaction

model', where the presence of a salt as cosolute acts as a 'chemical perturbant', and is quantified as an additional term in the solute's chemical potential.[2] Thus, the validity of the Setschenow equation can be taken as a proxy for the weak interaction model being applicable.[2]

Besides solubility, other studies that (re)demonstrated Hofmeister effects were also published in this early period; in 1932, Darmois studied the effects of salts on the optical rotation effects of tartrates and cited Hofmeister for the trends that once more reappeared.[31]

The general goal in this period of time was the establishment of Hofmeister or Hofmeister-like trends in a wide variety of contexts, many of which were listed previously. Studies were able to identify specific ion effects across the physical and biochemical sciences, but mostly struggled or otherwise did not attempt to provide a holistic explanation for the effects. In 1956, Gustavson reported studies of Hofmeister effects on the shrinkage temperature of collagen fibers,[32] and Bello et al. investigated the melting temperature of gelatin gels.[33] Later, these findings were expanded upon and better generalized by von Hippel & Wong, who in the 1960's conducted extensive studies on the effects of various salts on the solution stability and phase transitions of several proteins.[34–37] The melting temperature (T_m) of the globular protein ribonuclease, and the collagen-gelatin transition temperature were measured by von Hippel & Wong against increasing concentrations of salt (c_s), whereby mathematically, their results were found to fit the equation:

$$T_m = T_0 + K_m c_s \tag{2}$$

where T_0 is the critical temperature in the absence of salt, and K_m is an empirical constant.

The melting temperatures observed for both the collagen-gelatin transition and the transition observed in DNA were found to be related to the stabilization-destabilization effects of the salts on the helical native structures of these molecules, namely on the helix-coil transitions. Sinanoğlu & Abdulnur also studied the helix-coil transition.[38] Although their work provided expansive study of solute and cosolute test subjects, von Hippel & Wong themselves did not offer a proposed explanation for the majority of their observed effects.

Robinson & Jenks studied Hofmeister effects in the solubility of an oligopeptide (ethyl ester of acetyltetraglycine) and found that it was an appropriate, simpler model for larger proteins in its recreation of Hofmeister trends.[39] They found that the Setschenow equation (Equation 1) was obeyed, and also investigated for correlations with physicochemical and thermodynamic parameters—however, no clear correlation was found with any such

parameters besides the "internal pressure" of water (cohesion). Robinson & Jenks's study stands out as one of the earlier examples of an attempt at a rational explanation of the Hofmeister effects by relating them to solution and water properties, as well as direct interactions between ions and the solute of interest, in particular with the peptide groups.[3] This latter notion became a popular motif in similar attempts at explaining Hofmeister effects as a possible route to generalization for the protein class of solutes.[16]

1.1.2 Model Paradigms: Kosmotropes and Chaotropes, DLVO Theory, Microcavity-Surface Tension Approaches

The re-emergence of Hofmeister-like patterns in diverse contexts within the literature continued as a trend throughout the 20th century, but the field also waned in popularity in the mid-century era. Collins & Washabaugh's comprehensive 1985 review of the subject comprised almost a thousand references.[1] However, the persistent accompanying trend was the unsatisfactory state of a comprehensive theory to explain these findings—even if not for lack of attempts by researchers. One strong paradigm of the first half of the 20th century was the possible 'structuring' or 'ordering' influence of ions in the general (bulk) structure of water.[40,41] In this model, the typically harder ions (in the hard-soft acid-base sense) having higher charge-to-size ratios (such as SO_4^{2-}, CO_3^{2-} and F^-, amongst anions) induce an *increase* in molecular-level order in the solvent (i.e., increase order in the hydrogen bonding network of water), whereas softer, lower charge density ions (such as SCN^- or I^-) tend to induce a *decrease* in water's order. This gave rise to the terms 'kosmotrope' (from Greek *kosmos* meaning order) and 'chaotrope' (from Greek *chaos*) to describe these classes of two ions, respectively.[1,42] Collins & Washabaugh themselves offered a related model. They conceptually divided the body of water around any interface or solute into three distinct layers; the first layer constitutes the water directly surrounding the solute and thus influenced by it directly, the third layer comprises water that exhibits the general properties of the bulk (i.e., outside the influence of the solute), and the middle second layer a transition between the two. The influence of the solute of interest at the interfacial first layer, as compared to the strength of the influence of the bulk state (which could then be imagined either as pure water or the hydrated cosolute) would determine the ordering of the second layer and the overall direction of preferred interaction, thus generating the Hofmeister effect. Collins & Washabaugh attempted to classify the entirety of systems found in the Hofmeister literature according to these regimes, but arrived at too broad a generalization in the process; not only were many exceptional and inverted cases not examined, their model was also not backed by any form of empirical evidence.

Simultaneously, researchers attempted to develop mathematical models for the physical forces and energy dynamics of species in solution. One approach in this period was Deryaguin-Landau-Verwey-Overbeek (DLVO) theory, originally developed to model colloidal interaction in the 1940's.[43–46] DLVO theory posits that the forces between particles in solution results from the balance between repulsive electrostatic interactions (due to the electrical double layers) and attractive van der Waals forces.[47] The model is adequate to predict interactions at very low salt concentrations, up to ~0.01 M, but fails substantially at any concentration higher, as is typically the case for studies on Hofmeister effects, where physiologically relevant conditions often span a range of milli- to several molars.[5] For example, DLVO theory would predict that serum albumin is repelled by glass, yet it is in fact strongly attracted to it.[3] It also predicts that fibrinogen is water-insoluble, when in reality it is highly soluble (in its non-polymerized form).[3] The essential limitation—and hence downfall—of DLVO theory for predicting Hofmeister effects is that it necessarily makes several strict assumptions: in particular, it uses the Poisson-Boltzmann equation for electrostatic force calculations, which treats ions in solution as point charges.[5] Accordingly, ion specificity is completely lost; furthermore, it treats the solvent bulk as a fixed continuum without granularity; this latter aspect was one of the major criticisms leveled against the predominant theory by Ninham and coworkers in their 2004 review of the state of Hofmeister effect studies.[4] Relatedly, polarization effects in the opinion of Ninham and coworkers were essential and could not be neglected in the manner commonly done by researchers, and the assumed independent additivity of electrostatic and van der Waals force contributions was fundamentally incorrect.[4,14] They introduced modifications into the theory to account for polarization effects alongside electrostatic ones,[48,49] from which they were able to better explain several Hofmeister-related phenomena from experiments such as ion-micelle binding,[50] electrochemical pH measurements of buffer and protein solutions,[51,52] ion-protein[53] ion-polyelectrolyte interactions,[54] and electrolyte surface air/water tensions.[55] In several of their computational studies, Jungwirth & Tobias were able to produce simulations of the air-water interface that showed a preferential exclusion vs. accumulation trend of across the series of halide ions[56] that correctly matched experimental findings by Ghosal et al in their X-ray photoelectron spectroscopy study.[57] Both studies found an increase in the surface concentration of halide anions going from F^- to I^-.

Ninham and coworkers[4] also find some value in the phenomenological identification of correlations between ion physicochemical properties and Hofmeister effects, as instanced earlier by Robinson and Jencks in 1965.[39] Amongst the properties frequently examined are ion

size, water activity, ion polarizability and surface tension increments. According to Ninham, many of these parameters are related to or otherwise factor in to the fundamental polarizability-inclusive forces that dictate the specific ionic effects at the molecular scale. They find it worthy of note that there is indeed some evidence for correlation between quantities such as viscosity B-coefficients, lyotropic number, surface tension increment and water entropy change with polarizability, which they see as support for their analysis of the major shortcoming of the present theory.

Ramsden and coworkers[3] also reference physicochemical correlations when proposing their model, which adopts the surface tension-microcavity approach, and cite the 'solvophobic theory' of Sinanoğlu[58] as the basis of their approach. They categorize three types of forces that must be taken into account: electrostatic, Lifschitz–van der Waals (including dispersion forces) and electron donor-acceptor interactions. The third force expresses the extent of charge transfer during interaction and solvation, and can be alternatively thought of as included within the greater category of polarization effects according to the approach of Ninham and coworkers, albeit here are given more 'chemical' specificity and opportunity for interpretation—such as relating to Lewis acidity/basicity of the species. Ramsden and coworkers argue that the combination of all of these contributing forces can be distilled into the net change in the interfacial tension, i.e., the specific interfacial energy (with units energy per area). These contributions (namely, the Lifschitz-van der Waals potential (γ^{LW}), electrostatic potential (γ^{el}) and donor (γ^{-}) and acceptor (γ^{+}) potentials) can be systematically tabulated from careful measurements, partitioned into contributors and subsequently be consulted for any solute system, whereby they will be recombined (i.e., $\gamma = \gamma^{LW} + \gamma^{el} + \gamma^{-} + \gamma^{+}$). The solvophobic theory approach was utilized by Sinanoğlu & Fernández to correctly predict calorimetric results for the denaturation of lysozyme in water/methanol mixtures.[59,60] Baldwin, in his 1996 review, discusses the surface area-tension work model of solvation (which he calls the 'cavity model') and relates it to the weak-interaction model. Accordingly, salting-in/-out constants obtained from systems that obey the Setschenow equation (Equation 1) can be implemented together with surface tension measurements to calculate apparent microscopic surface areas for solute cavities. One such study by Nandi & Robinson,[61] where salting-out constants were obtained for peptides with side-chains containing 0 to 4 carbon aliphatic chain increments (the structures of some of which are shown in Figure 2c in section 1.2.1), produced results that were then used to calculate apparent surface areas per hydrocarbon unit that matched their known molecular sizes within a factor of 3.[2,62] However, both the solvophobic model and approaches based on

surface tensions in general were met with contention,[2] as conceded even by proponents of the model. Models that assume additivity of forces at the molecular scale were heavily criticized by Ninham and coworkers in context of their critique of DLVO theory.[4,14] The neglecting of microscopic curvature present in considering the molecular scale when generalizing from macroscopic surface tensions is another major issue at the heart of the approach,[62,63] as conceded even by Sinanoğlu,[64] alongside the problem that values from macroscopic measurements of electrolyte solution air-water surface tensions in the literature vary wildly in magnitude and even sign.[4] Perhaps most critically, surface tension-based arguments do not explain the well-known salting-in effect of salts of divalent and other strongly-hydrated metal cations (such as $MgCl_2$) despite their high surface tension increments, as exemplified by Arakawa and Timascheff's studies on protein solubility in various salt solutions that span the Hofmeister series.[65]

1.1.3 Against Structure-Maker/Structure-Breaker Models

The late 20th century saw a shifting away from the structure-maker vs. structure-breaker paradigm of explaining Hofmeister effects. This purported property of the diverse ions of the series that had given rise to the names kosmotrope and chaotrope struggled to find experimental evidence. In turn, with advances in spectroscopic and thermodynamic tools, studies began to show that ions, in fact, did not appear to bring about a change in the structural order of water past their immediate solvation shells; it appeared that the influence of ions in the bulk was not a robust explanation for the source of Hofmeister effects.[12,15,16]

A seminal series of studies in this regard was that of Bakker and coworkers.[66–71] Using femtosecond pump-probe spectroscopy, they were able to investigate the orientational correlation times of water molecules in various concentrations of salt solutions, ranging from both kosmotropic to chaotropic anions and cations. The O-H stretching modes were initially excited with an ultrafast infrared irradiation, and was then followed by a weaker IR pulse to follow the relaxation behavior, with time resolution shorter than that involved in exchange of water molecules between ion solvation shells and the bulk. The findings indicated that while the presence of ions—both kosmotropic and chaotropic—greatly increased the correlation times for water molecules in their first hydration shell (particularly for anions, whereas cations had a more limited effect), neither class of ions had an effect on the dynamics of water in the bulk, even at up to 6 M salt concentration. That is, the structure of the bulk water for unaffected.

A second line of evidence against an all-encompassing structure breaker/structure-maker model of ions came from the work of Pielak and coworkers.[72] They utilized pressure perturbation calorimetry to investigate the heat transfer behavior of aqueous solutions of 17 solutes (including ammonium and guanidinium salts, as well as sugars, urea and other well-known osmolytes) under varied pressure, from which the sign and temperature dependence of partial heat capacity were obtained. The sign of the latter quantity, $(\partial\overline{C_p}/\partial P)_T$, is in indicator of whether a solute increases (if negative) or decreases (if positive) structural order in water, according to the 'two-state' model of water. This model conceptualizes water as a mixture of a less dense, more-ordered state (where water molecules have a greater degree of ice-like, tetrahedral coordination) and a denser, less-ordered state.[73,74] Pielak and coworkers' study found that there was no obvious relation between the expected kosmo-/chaotropicity of the salts tested (or their typical Hofmeister effects) and sign of the partial heat capacity parameter, and thus did not support the structure-making theory of Hofmeister effects.

Cremer and coworkers[75,76] were also able to investigate the water-structuring effects of ions in tandem with their Hofmeister effects, specifically, on the phase transition behavior of a surfactant (octadecylamine) monolayer spread on D_2O and H_2O. They employed vibrational sum frequency spectroscopy (VSFS) to directly isolate vibrational signals corresponding to the interfacial structure. The degree of order in the alkyl chains was elicited by the ratio between methyl and methylene C-H stretch signal intensities, which is greater in more ordered monolayers because the alkyl tails lie parallel to the surface normal, and the reduction of the ratio (which can be due to elevated temperature or added salt) implies increase in disorder and formation of gauche defects in the monolayer packing. In the case of salt effects, enhanced defect formation implied penetration of anions into the monolayer and was also evident in the decrease in the surface potential, which is highly positive in the absence of salt due to the positive charge on the surfactant molecules. For the sodium salts of a series of anions, the degree of alkyl chain disordering and anion penetration was found to follow a direct Hofmeister series (i.e., SO_4^{2-}, Cl^- caused the least de-structuring, whereas SCN^-, ClO_4^- caused the most) but the effect on water structure deviated from this ranking. For instance, a significant degree of water ordering was observed for ClO_4^-, but not as much for SCN^-. Work by Leontidis et al.[77] found similar results for the Hofmeister effects of salts on a 1,2-dipalmitoyl phosphatidylcholine (DPCC) lipid monolayer, where it was observed that the effects of the chaotropic anions correlated with their propensity to penetrate into the lipid structure. Thus, in the case of surfactant and lipid monolayers, the Hofmeister effects of classical salts were found

to not correlate with water ordering, but with specific penetrative behavior into the interfacial subphase.

Nevertheless, the exact nature of the structural effects of ions on water, their distance dependence, and at what concentrations the effects may be manifested are still an active area of study. Neutron diffraction experiments have been able to produce radial distribution functions for hydration around ions and investigate H-H correlations. One study by Neilson et al.[78] found that up to 10 M urea and 1 M LiCl do not significantly change the H-bonding structure of water, whereas with 10 M LiCl the H-bonds between water molecules are reduced by approximately 70%. A different work found that the magnitude of the disordering effect of salt on water was equivalent to that of kilobars of external pressure.[79,80] More recently, elastic second harmonic scattering measurements of salt solutions found evidence for long-range changes in water-water correlations in an ion nonspecific manner.[81–83] Although the subject is, thus, still one of continued study it is true that the structure-maker/structure-breaker model of explaining Hofmeister effects (specifically for salt concentrations above ~100 mM) has largely fallen out of favor due to the lack of credible evidence, and the literature has evolved in favor of pursuing system-specific information regarding molecular-level mechanisms to explain these effects, such as preferential interaction.[12,15,16] The terms kosmotrope and chaotrope are also frequently sidelined in Hofmeister studies, opting for descriptors that are more system-relevant or more generalized, such as strongly- or weakly-hydrated, so as not to imply structural arguments. In accordance with this notion, where it is necessary to use such descriptors, the present thesis will also opt for strongly- and weakly-hydrated in most cases.

* * *

In their prominent and much-cited review, Collins & Washabaugh presented a list of features they believed were common to all Hofmeister effects in their purview of the literature. These properties were:[1] (i) Hofmeister effects become significant at moderate concentrations in the range of 0.01 – 1 M, (ii) Different systems exhibiting these effects produce the same ranking with only slight alterations, (iii) The point of sign inversion (i.e., switch from one direction of effect to another) occurs around NaCl; that is, chaotropes and kosmotropes have opposing effects, (iv) Hofmeister effects are dominated by anions, (v) Hofmeister effects are approximately additive over all species in solution.

The all-encompassing simplicity of these assumptions is certainly attractive; but, as mentioned at the beginning of this section, is as equally limiting and insufficiently evidenced

after nearing 140 years of study. It is this kind of generalization, which will gloss over the true diversity, complexity and chemical richness of specific ion effects, that the literature—in the opinion of Jungwirth and Cremer[15]—should perhaps move away from in order to continue to develop. Indeed, each one of Collins & Washabaugh's 'rules' listed above are challenged today by examples from the known literature, many of which are included here. The following sections of this chapter will cover the present knowledge of specific ion effects on (bio)macromolecular and related systems, and present contemporary studies that are able to hone into the molecular-level mechanisms that are at play, which will then elucidate the motivation and significance of the current study.

1.2 Molecular-level Mechanisms of Specific Ion Effects on Macromolecules: Understanding the Anionic Effects

Understanding the underlying molecular mechanisms of specific ion effects is a difficult endeavor. As the previous section aimed to demonstrate, instances of Hofmeister patterns crop up in a myriad of contexts, making the identification of a single driving factor difficult, if not impossible, partly due to the 'elephant in the room'[15] that is the *specific properties* of the system being studied, whether it be the protein solute, a particular enzyme or a colloidal self-assembling system. In fact, one does not need to search hard to find systems which will immediately bring simple, generalized explanations into question. Lysozyme, one of the most studied proteins, has been known for a long time to follow a 'direct' (i.e., conventional) Hofmeister series for basic pH, but to follow a reversed Hofmeister ordering at acidic or neutral pH conditions.[84,85] This particular system will be discussed further later in this section.

1.2.1 Direct Hofmeister Series, Interactions at the Peptide Bond and α-Positions

Motivated to break down what may be a whole host of system-specific compounding factors, research in the 'renaissance' of Hofmeister has increasingly used simpler systems as a means to study the more complex macromolecules of biological systems. Considering the sheer diversity of protein architectures in nature and the variety of charged, polar and nonpolar amino acid side-chains they contain, one foundational approach in Hofmeister research has been to target the peptide bond (i.e., the protein backbone) as a common motif and originator of Hofmeister effect ubiquity. As mentioned in the previous section, some seminal early research targeted small oligopeptides as models to study more complex proteins, and were able to

elucidate fundamental clues to the greater picture. Amongst these studies are Robinson & Jenks's study[39] of the oligopeptide *N*-acetyltetraglycine ethyl ester (Figure 2a) and Nandi & Robinson's[61,86] studies of oligopeptides mentioned previously (Figure 2b – c). These studies were framed by the researchers as an attempt to investigate the inherent Hofmeister effects on the peptide bond, as a structure common to all proteins. Robinson & Jenks concluded that their findings could best be explained with preferential interaction between the peptide bond and weakly-hydrated anions (such as $I^-$and SCN^-) and strongly-hydrated cations (Li^+ and divalent cations). They found similarity between their calculated salting-out constants for large, weakly-hydrated anions and the determined rank order binding behavior of the same anions to anion-exchange resins,[87] and deduced that a similar interaction/binding must be occurring with the solutes' amide/peptide groups. They also envisioned that the strongly-hydrated cations would interact with the carbonyl groups of the peptide by hydrogen bonding with them via their hydrating water molecules. The papers by Nandi & Robinson reached similar conclusions, finding that their results implied an ion-specific interaction with the peptide bond as the driving force for the Hofmeister effects of salts on the variable-length oligopeptide, with direct proportionality to the number of peptide units in the solute (see the series of oligopeptides studied, as shown in Figure 2b).

Even with the study of oligopeptides, there are compounding factors that convolute the analysis of Hofmeister effects. With smaller molecules, the specific capping groups of the termini[88,89] and the molecular size scale[90] become complicating factors, in particular. To better model protein effects, macromolecular solutes may thus be preferable still. To this end, *thermoresponsive* (or *thermosensitive*) polymers have been of particular use. These materials are soluble in water below their characteristic 'lower critical solution temperature' (LCST), typically existing in random coil conformations, but undergo a phase-transition at and above their LCST point, often observed macroscopically as a cloud-point, and may precipitate out of the solution or undergo liquid-liquid phase separation.[91,92] The utility of thermoresponsive polymers as test subjects is their ability to provide thermodynamic and macroscopic information regarding fundamental Hofmeister effects, in analogy (with varying applicability) with those observed in more complicated proteins and other biomacromolecules, but with allowed control over the solute molecular structure, enabling the tuning of charge, polarity, hydrophobicity and other characteristics. A diverse range of such thermosensitive polymers have found use in the literature: various pyrrolidone-based polymers[93], Tetronic[94] and Pluronic polymers[95], modified cationic poly(vinyl alcohol) polymers[96], and polymers based on poly(2-

oxazoline) with varied hydrophilicty[97] have been studied for the Hofmeister effects on their thermoresponsive behavior. The structures of several examples of these polymers are shown in Figure 3a – c.

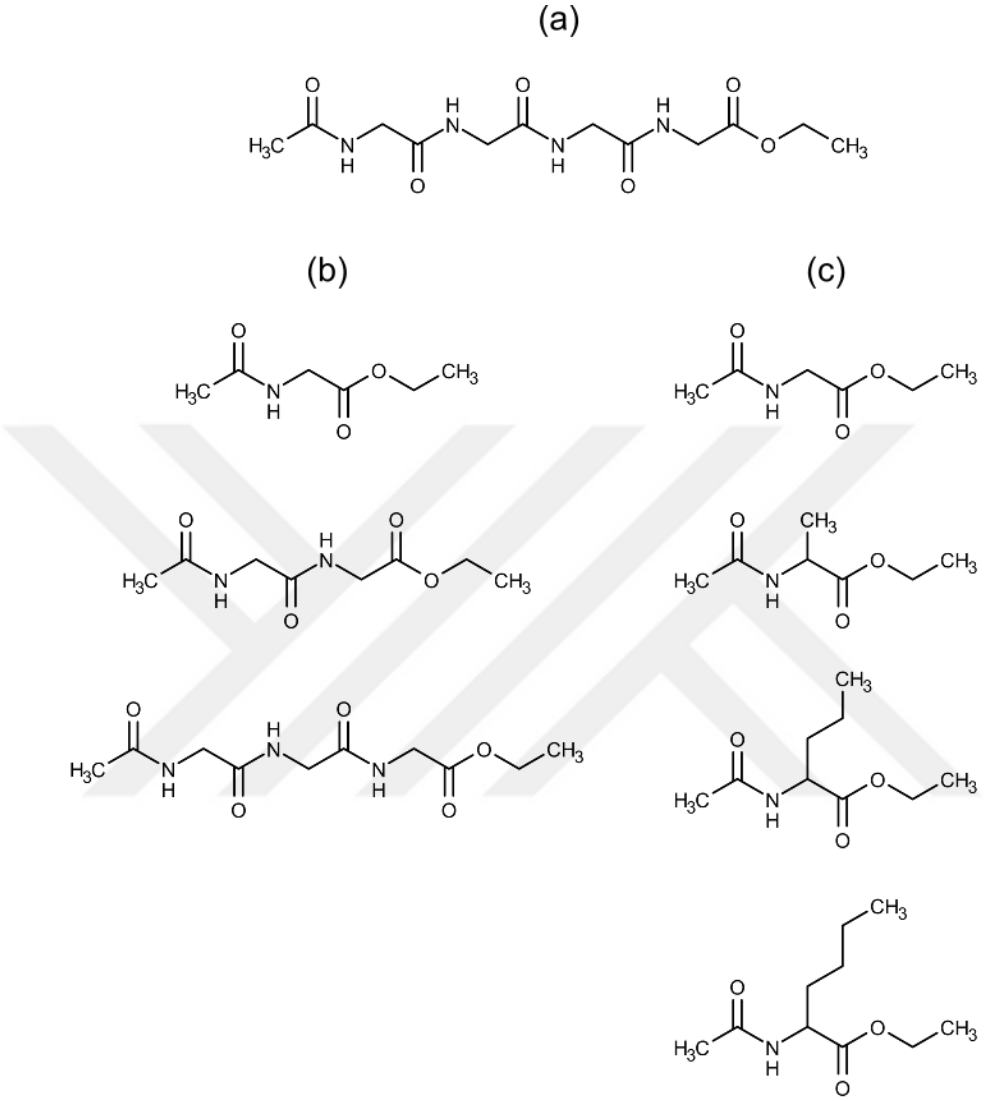

Figure 2: The structures of several of the oligopeptides used in the studies discussed so far. (a) *N*-acetyltetraglycine ethyl ester (ATGEE) as studies by Robinson & Jencks.[39] (b) The series of capped polyglycines as studied by Nandi & Robinson.[86] From top to the bottom, the oligopeptides are the *N*-acetylated ethyl ester derivatives of glycine, diglycine, and triglycine. The fourth oligopeptide studied was the tetraglycine derivative, i.e., ATGEE. (c) Some of the capped amino acids with increasing alkyl side-chain lengths studied by Nandi & Robinson.[61] From top to bottom, the oligopeptides are the *N*-acetyl ethyl ester derivatives of glycine, alanine, norvaline and norleucine. Other amino acids with branching or aromatic side-chains were also studied but are not shown here. The conclusion reached by Nandi & Robinson was

the that number of straight-chain methylene units determined the observed effects; i.e., side-chain branching did not have an effect. Also note that the validity of the ethylated C-terminus as claimed by Nandi & Robinson was later brought into question, as discussed in section 1.2.2.

One of the most well-studied thermoresponsive polymers both as a model macromolecule for specific ion effects as well as in the greater field of temperature-responsive materials is poly(*N*-isopropylacrylamide), or PNIPAM.[12,98] Besides PNIPAM's (and closely related polymers') being well-characterized and easily available, it also holds properties that make it attractive as a model solute: PNIPAM undergoes a sharp phase-transition from a random coil configuration to a globular, aggregated form due to hydrophobic collapse at its LCST (typically 32°C).[5] This behavior is analogous to the cold denaturation phenomenon seen in proteins.[99] Additionally, the structure of PNIPAM (Figure 3d) contains several hydrophobic (backbone groups, the isopropyl group on the side-chain) and hydrophilic (amide group on the side-chain) moieties, thus mimicking the hydrophilic peptide groups and the hydrophobic side-chain groups of natural proteins. The copresence of groups of varying chemical environments and different degrees of hydrophobicity enables PNIPAM-type polymers to be ideal test subjects to investigate the dependence of preferential interactions with ions on the polarity of the polymer groups.

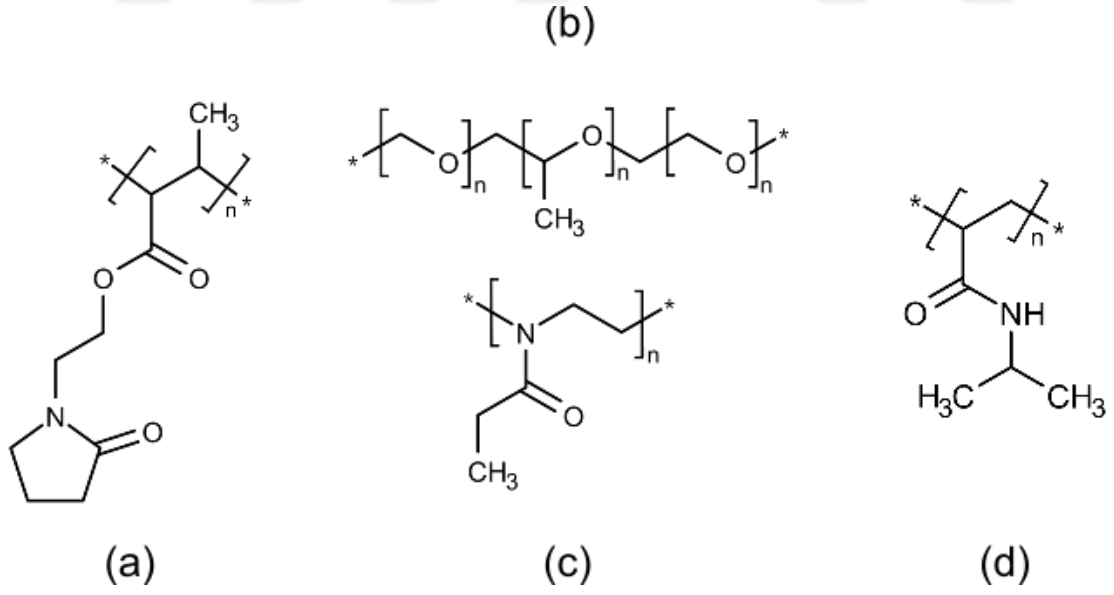

Figure 3: The structures of several thermoresponsive polymers mentioned: (a) poly[*N*-(2-methacryloyloxyethyl)pyrrolidone], (b) Pluronic polymers, (c) poly(2-ethyl-2-oxazoline), (d) poly(*N*-isopropylacrylamide (PNIPAM).

In 2005, Zhang et al. provided a comprehensive investigation of the effects of 11 sodium salts on the LCST of PNIPAM, using their newly-developed microfluidic/dark field microscopy set-up to obtain data of precision not possible before.[5] They found PNIPAM to follow a direct Hofmeister series for anions; the most strongly-hydrated anions were the most effective at salting-out (wherein the LCST of PNIPAM decreased linearly with salt concentration), whereas the weakly-hydrated anions were less effective and exhibited a salting-in component in the LCST curves, manifest as a nonlinearity at lower concentrations. Zhang et al. also provided a model that quantitatively fit the LCST data:

$$T = T_0 + c[\mathrm{M}] + \frac{B_{\max} \cdot K_\mathrm{A}[\mathrm{M}]}{1 + K_\mathrm{A}[\mathrm{M}]} \tag{3}$$

Here, the observed LCST of PNIPAM (T) is given through the relation with the LCST in the absence of any salt (T_0) and molar salt concentration ([M]), where c is a coefficient with units °C/M or K/M and the final term is derived from a Langmuir-type binding isotherm. Accordingly, K_A is the (apparent) association equilibrium constant for ion-PNIPAM interaction and $B_{\max}$ is the maximum change in LCST due to ion binding (i.e., at saturation). Zhang et al. were able to show that the LCST curves for all salts tested could be fit according to this equation— in the case of the strongly-hydrated anions, where the curve is purely linear, the third nonlinear term is simply zero (i.e., $B_{\max} = 0$ or, alternatively, we can say K_A goes to infinity)—and tabulated the relevant parameters as fitted per salt. The authors then proposed three distinct molecular-level mechanisms that together produced the various results, using arguments founded on their comparison of the fit parameters to various physicochemical properties of the ions. The values of coefficient c—which were always negative, and thus expressed a salting-out contribution—correlated well with the *entropy of hydration* for the strongly-hydrated anions, but did so with the *air-water surface tension increment* of weakly-hydrated anions. This was interpreted to mean that there is a distinct mechanism for the salting-out action of the two classes of anions: for weakly-hydrated anions, the salting-out effect derives from destabilizing the hydrophobic hydration of the polymer through elevation of the interfacial surface tension. For strongly-hydrated anions, in contrast, the driving force is interpreted as arising from the ion's ability to polarize water molecules surrounding the polymer, thus weakening their hydrogen-bonding to the amide groups on the side-chains and causing salting-out. The third mechanism they propose to be at play is the specific binding of weakly-hydrated anions at some sites on the polymer, whereby the polymer is thermodynamically stabilized in its soluble (coil) form. This effect is encapsulated by the

Langmuir-type isotherm relation in the final term in Equation 3, hinting that a saturable binding occurs in the system. Additionally, the magnitude of the B_{max} terms for the weakly-hydrated anions matched the order (ClO_4^- > SCN^- > Br^- > NO_3^- > Cl^-) of binding strength reported for polyacrylamide gels,[100] poly(*N*-vinylpyrrolidone)[101] and small peptides.[102]

In 2008, Cho et al. reported a similar study on the LCST behavior of two varieties of elastin-like polypeptide (ELP) with 11 sodium salts.[103] Their motivation was to see whether the distinct mechanisms determined for PNIPAM previously by Zhang et al. held for a different thermoresponsive system, specifically a polypeptide, as a better approximant for natural proteins. Similar to PNIPAM and other thermoresponsive polymers, ELPs undergo a distinct phase transition at their LCST points, which is characteristic to the polypeptide's specific composition and molecular weight.[104] Unlike more complicated polypeptides or proteins, however, ELP's consist of a simpler architecture of repeating five-residue segments of form V-P-G-X-G, where X can be any amino acid residue except proline. Thus, the molecular characteristics—such as charge, polarity or hydrophobicity—of an ELP can thus be designed as desired and obtained from biosynthesis in bacteria.[105] In addition, the phase transition of ELPs has been found to involve significant β-turn- and β-spiral-type secondary structure formation[106–110]; thus, they provide a useful bridging tool between the non-polypeptide PNIPAM and natural proteins. In this study, Cho et al. studied two ELPs of 120 pentad repeats each: a more hydrophobic one that had valine residues at all 'X' guest positions, and a less hydrophobic ELP with valine, alanine and glycine at the 'X' positions in the overall ratio 5:2:3. The general trends for both polymers were very similar to those found for PNIPAM by Zhang et al., such that strongly-hydrated anion salts produced linearly decreasing LCST curves indicative of salting-out and weakly-hydrated anions produced nonlinearities, interpreted as ion-specific binding. The LCST curves could also be fit to the same model (Equation 3). The LCST of the more hydrophobic ELP was lower (~28 °C) than that of the less hydrophobic polymer (~42 °C). After extracting values for the parameters c, B_{max} and K_A for both polymers with each of the salts, correlations with ion properties were screened and the same "excellent" correlations were found to hold for the present system. Namely, the values of the linear salting-out coefficient c correlated well with the entropy of hydration for strongly-hydrated anions and the surface tension increment of weakly-hydrated anions. These results were then interpreted to postulate that the same set of three main mechanisms—polarization and surface tension elevation effective for salting-out, saturable binding for salting-in—were valid for the ELPs.

The authors noted that additional ion properties were checked against the *c* parameters, such as polarizability, ion volume, viscosity *B*-coefficients, hydration enthalpy and free energy, but that no correlations were found. However, an additional correlation was noted between the ratio between the B_{max} values of the two ELPs and anion volume; this was interpreted as a signifier that for larger anions, there was a more significant impedance to binding in the case of the more sterically restrictive and hydrophobic purely-valine substituted ELP. Note, however, that neither Zhang et al. or Cho et al. were able to specify the exact location of the preferential sites of interaction of the weakly-hydrated anions, beyond the speculated localization around the amide/peptide group that was expected. The binding sites for the interactions were investigated and determined more rigorously in following studies. Rembert et al.[111] studied a 600-residue $(VPGVG)_{120}$ ELP (i.e., having the same sequence as one of the polymers studied by Cho et al.; the structure of a pentad fragment can be seen in Figure 4) with the sodium salts of chloride, iodide, thiocyanate and sulfate anions. They combined LCST measurements with quantitative ^{1}H-NMR spectroscopy, as well as molecular dynamics (MD) simulations to characterize the behavior of the ions at different levels of study and provide credible evidence for their proposed model. Their thermodynamic study yielded the same findings as Cho et al., and the LCST curves were fit to a rearranged, identical form of Equation 3:

$$\Delta T = -c[\mathrm{M}] + \frac{B_{\max}[\mathrm{M}]}{K_{\mathrm{D}} + [\mathrm{M}]} \tag{4}$$

Here, ΔT is the change in LCST with respect to the polypeptide in the absence of salt cosolute, and K_D is the *dissociation* equilibrium constant for ion binding. That is, a smaller value of K_D indicates a 'tighter', stronger binding.

The same LCST behavior determined previously by Cho et al. were reproduced. The critical aspect of this study was the implementation of quantitative, externally-referenced ^{1}H-NMR spectroscopy to track the behavior of all protons on the polymer as a function of added salt. In essence, NMR titrations were performed using the same set of salts, using samples in NMR tubes fitted with an additional coaxial insert tube (which contained the chemical shift reference standard sodium 2,2-dimethyl-2-silapentane-5-sulfonate (DSS), providing *external* referencing without chemical contact with the sample solution), and were measured at 5 °C so as to always be below the LCST point of the mixtures. All proton chemical shifts were recorded and analyzed by grouping them by their local chemical environment on the polymer. It was found that the majority of protons exhibited chemical shifts that decreased linearly with added

salt; this included protons on the hydrophobic valine side-chains and the water protons for all salts. However, most informatively, protons at the α- position on the backbone (i.e., on methylene groups adjacent to amide N atoms or carbonyl groups) exhibited nonlinear chemical shift curves with the salts of weakly-hydrated anions. The shape of the curves closely resembled the trend produced by the same salts on the LCSTs of the polymer, and thus constituted clear evidence of preferential interaction at these sites as being the source of the macroscopic thermodynamic effect. The chemical shift curves could then be fit to the following mathematical form, highly similar to Equation 4:

$$\Delta\delta = -c[\mathrm{M}] + \frac{\Delta\delta_{\max}[\mathrm{M}]}{K_{\mathrm{D}} + [\mathrm{M}]} \tag{5}$$

where the change in chemical shift ($\Delta\delta$) is related to a saturable and deshielding (i.e., chemical shift raising) interaction with the weakly-hydrated anions. The dissociation constant (K_{D}) for such interactions were found to be as low as 50 mM, as seen for the binding of SCN^- to α-positions (as indicated on the ELP structure in Figure 4).

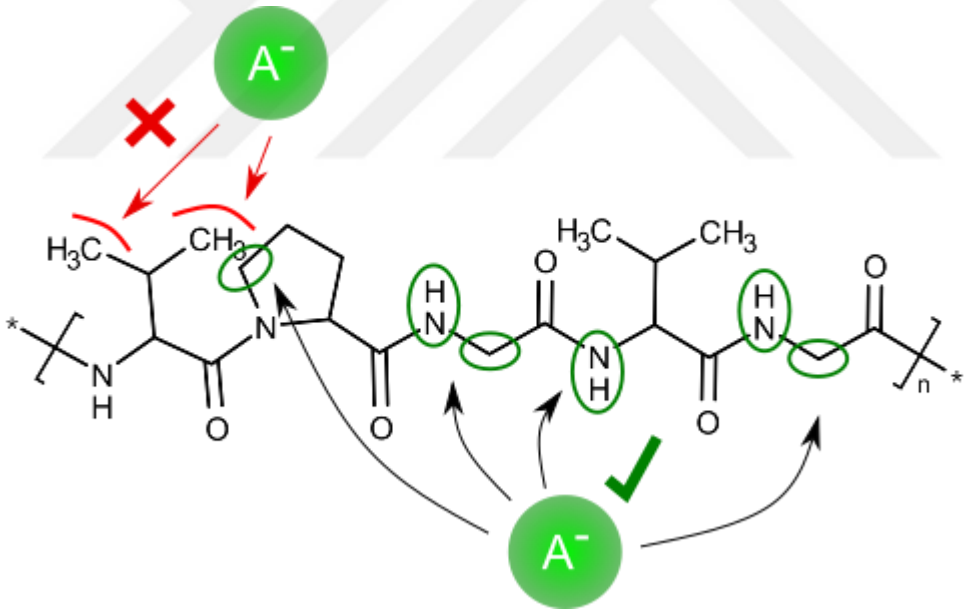

Figure 4: A pentad fragment of ELP studied by Cho et al. and Rembert et al., schematically showing the mechanism for anion binding demonstrated by Rembert et al. Here, A^- is a weakly-hydrated anion such as SCN^- or I^- and is able to preferentially interact with N-H groups and adjacent (α- position) methylene groups. In contrast, the anions are not able to favorably interact with very hydrophobic moieties, such as the terminal isopropyl groups of valine residues.

Additionally, nonlinearity observed in the chemical shift curves implied some interaction with the N-H groups as well. Due to the proximity of these groups to the α- binding sites, additional experiments were done using polyacrylamide and poly(*N,N*-dimethylacrylamide) to clarify the role of N-H groups in the presence of more hydrophobic α-binding sites. The same NMR titration method showed that nonlinearity in the chemical shift curve for the N-H group of the former polymer was quite minimal, but the side-chain methyl protons of the latter exhibited very distinct nonlinear curvature, with the same shape as the ELP α-protons—this was found to be in agreement to the known enhancement of anion binding upon methylation of at least one N-H groups of polyacrylamides in other studies.[100] These findings were together interpreted to conclude that while the polymer's α- aliphatic groups were the primary binding sites, the proximity and partial positive charge on amide N-H (as well as some other neighboring groups) were probably also involved with anion interaction to varying degrees, as represented schematically in Figure 4. MD simulations were used to supplement the information provided by spectroscopic methods, and examine ionic behavior inaccessible to the NMR methodology. A pentapeptide fragment was capped to remove end-charges and fixed in an extended conformation and simulated for 100 ns in an environment containing 1 M NaSCN, 1 M NaCl or 0.33 M Na_2SO_4. The localizations of the ions in space and the distribution functions extracted were quite informative: SCN^- was found to have large regions of enhanced accumulation around the pentapeptide, whereas local distributions were restricted to small volumes near the N-H moiety for Cl^- and SO_4^{2-}, and around the carbonyl group for Na^+. SCN^- was confirmed to cooperatively interact with N-H and adjacent α-methylene groups, and to have an overall net inclusion around the polymer, whereas the Cl^- interaction was weaker and SO_4^{2-} was excluded from all $-CH_n$ groups, and both of the latter ions were depleted from the polymer interface overall. Allowing for polarization in the simulation of the ions produced a significant difference only for SCN^-, where binding was strengthened to some extent in this case.

The findings of this study by Rembert et al. were significant in that they both confirmed and challenged different assumptions about ion-peptide interactions that had previously not been experimentally verified. The salting-in effect of weakly-hydrated anions was indeed found to arise from specific interactions, but not directly—or, at least solely—with the polar amide/N-H moieties. Instead, a 'hybrid' binding site that included adjacent α-aliphatic hydrocarbon units were identified; these sites carry partial positive charge due to the inductive effects of the neighboring electronegative and electron-withdrawing groups, thus providing the basis for

interaction with anions, but are also less tightly hydrated than the most polar amide groups. Thus, there is a smaller enthalpic dehydration penalty for them to shed some of their solvating water in favor of anion binding. The enhancement in anion binding to polyacrylamide upon methylation, also demonstrated in the same Rembert et al. study, is further proof of the significant role played by less strictly hydrated, partially-charged 'hybrid' aliphatic binding sites. In 2015, Cremer and coworkers[112] performed analogous thermodynamic and spectroscopic studies of a ethylated derivative of PNIPAM, poly(*N,N*-diethylacrylamide) (PDEA), which is similar in structure to PNIPAM but does not possess an N-H group in its side-chain. Their findings essentially agreed with the conclusions of Rembert et al. and further decentralized the role of N-H moiety in the dynamics of anion binding. By employing the same quantitative ^{1}H-NMR methodology, they were able to elucidate that the backbone α-CH group—adjacent to the amide carbonyl—is the main binding site for weakly-hydrated anions like SCN^- and I^-, with binding K_D's 70 and 260 mM, respectively. Other sites, including those on the *N*-ethyl groups exhibited monotonic linear chemical shift curves, indicating no specific interaction with the anions.

In 2017, Okur et al.[16] further characterized and supported the dynamics of ion inclusion/exclusion by studying PNIPAM and the same valine-substituted ELP as Rembert et al. in 1 M solutions of eight sodium salts using VSFS measurements. Using Gibbs monolayers of the macromolecule, they observed that the OH stretch bands at 3200 and 3400 cm^{-1} exhibited significant enhancement in oscillator strength upon introduction of the weakly-hydrated anions, whereby the perturbation followed a direct Hofmeister series. This served as evidence of the preferential adsorption of these anions to the air/polymer/water interface over sodium counterions. The effect was much less significant for strongly-hydrated anions, indicating they were not being strongly partitioned to the interface.

1.2.2 Inverted Hofmeister Series: Charged Small Molecules, Macromolecules and Proteins

The long-standing mystery of the reversed anionic Hofmeister effects occasionally encountered has also been greatly elucidated by recent studies: in essence, it is often a product of (positively) charged solutes.[16,113,114] In these cases, it is strongly-hydrated anions that lead to more effective destabilization/denaturation/salting-in (or rather, as in some studies discussed in this section, less effective at aggregating/salting-out) in many instances by preferential interaction with the sites of positive charge.[16] One such case where this effect is encountered

is, in fact, with small oligopeptides, as done by Nandi & Robertson.[61,86] In their original study, Nandi & Robertson used tripeptides they reported as capped at both the N- and C-terminus, in order to isolate the inherent Hofmeister effects of ions on the peptide groups specifically. However, as later discussed by Hladílková et al.[88], the original methodology employed by Nandi & Robertson to cap the C-terminus of their triglycine solute was found to be ineffectual. MD investigations performed by Hladílková et al. examined the Hofmeister effects of salts on uncapped, half-capped (N-terminus capped, C-terminus uncapped) and fully-capped triglycine solutes and found that the results reported by Nandi & Robertson indeed resembled those of the half-capped solute and not the fully-capped solute. As determined by Hladílková et al., the effect of capping at either terminus of the solute is quite dramatic; in the uncapped case, all salts cause salting-in, whereas for the fully-capped solute only the weakly-hydrated anions contribute salting-in, through interaction with the peptide bonds. The strongly-hydrated anions and also cations instead salt-out, due to limited interaction with the peptide groups. The half-capped solute with C-terminus a 'naked' carboxylate is negatively charged, which results in attractive interactions with cations and repulsive interactions with anions, in particular, strongly-hydrated anions like F^- and SO_4^{2-} that go so far as to overpower the favorable interaction with Na^+, resulting in a net salting-out effect for these salts. The researchers also performed NMR titration experiments with the half-capped solute, and confirmed that even with NaSCN, there was no binding at the α-carbon positions—known as particularly susceptible sites for SCN^- interaction—likely due to unfavorable repulsion from the negatively charged C-terminus.

The effects of capping the charged termini of triglycine, as a model small peptide, was investigated in further detail by Paterová et al.[89] Similarly, they found in their MD simulations that the fully-capped triglycine (acetylated N-terminus, C-terminus converted to amide) followed a direct Hofmeister series for anions, whereby strongly-hydrated anions are preferentially excluded from the vicinity of the molecule, whereas weakly-hydrated anions exhibit affinity for interaction with the peptide groups, particularly with α-methylene groups closest to the N-terminus end. When the peptide is uncapped, the trend becomes a reversed Hofmeister series instead; interactions between the positively charged N-terminus and strongly-hydrated anions impart a stronger salting-in than weakly-hydrated anions, in particular amongst the halides—strikingly, SCN^- ion had surprisingly significant affinity for the charged N-terminus despite being weakly-hydrated. They also performed NMR titration measurements, finding interaction between the weakly-hydrated anions and the α-carbon positions that

corroborated the MD simulations for the capped tripeptide. The uncapped peptide largely had no appreciable binding at α- positions, with the possible exception of SCN^- at the middle position.

Amongst the 20 canonical amino acids used in the encoding of proteins, three bear side-chains that are usually positively charged under physiological conditions: these are lysine (bearing an ammonium-type group), arginine (with a guanidinium-like terminal group) and histidine (having an imidazolium moiety). Negatively charged side-groups, in contrast, are only present as carboxylates. This additional diversity in the former likely points to cationic amino acid residues being amongst the important players governing the Hofmeister effects of proteins, and perhaps raises intriguing questions about the possible richness of charged residue-ion effects in biology that organisms may have evolved to employ.[16] Resembling the findings of the studies on oligopeptides already discussed, MD simulation studies of single amino acids as well as polypeptides found that strongly-hydrated anions interact preferentially (i.e., form ion pairs) with positively charged amino acid residues over weakly-hydrated anions.[115,116] Okur et al.[16] describe their experimental study of an ELP solute containing approximately 3% lysine residues at the variable guest position (the 97% remainder was occupied by neutral valine, glycine and proline), where they observed that the LCST of the macromolecule was swiftly depressed by salts with ranking following a reversed Hofmeister series. This was attributed to neutralization of the charge on the cationic residues by the anion cosolutes, and a correlation between the anionic partial molar volume and the effectiveness of ion pairing with the ELP was found. However, strikingly, above salt concentrations of ~0.2 M, the sharp fall of the LCSTs either plateaued or could even reverse, and the trend inverted to a direct Hofmeister series. In this region of salt concentration, the weakly-hydrated salts (NaSCN, NaI in particular) salted-in the ELP more effectively than strongly-hydrated anion salts, which was understood as due to interactions of the former with the peptide backbone in accordance with the mechanism for neutral polypeptides,[111] and correlated (qualitatively) with the anions' air-water surface tension increments. While a detailed molecular-level mechanism for the system was not given by Okur et al., this study is nevertheless noteworthy in its corroboration of a different study of a natural protein, which is discussed below.

The pattern of Hofmeister effects exhibited by many proteins and why the rank order of salts sometimes reverses (most often when pH < pI of the protein) has been known for a long time and has been a significant scientific challenge to explain.[117] The behavior of lysozyme as one such case and one of the most classical examples of the phenomenon was

investigated by Zhang et al.[118] by studying the evolution of its liquid-liquid phase separation (LLPS) transition temperature over the concentrations of various salts as cosolutes. Lysozyme has an isoelectronic point (pI) of 11.2. Zhang et al. studied the LLPS of lysozyme at pH 9.4 using a 20 mM tris buffer, where the protein is net positively charged. Below the LLPS temperature of the protein, it aggregates in coacervate droplets (observed macroscopically as a cloud point) and may even fully settle into a distinct lower phase upon standing. Above the cloud point, the protein resolubilizes—note that this behavior is the opposite of the LCST phase transition exhibited by PNIPAM, ELPs and other typical thermoresponsive polymers. It was observed that at low salt concentrations, all salts greatly increased the cloud point (i.e., favored the soluble form) because of electrostatic charge screening. Here, a reversed Hofmeister series was indeed followed, where the weakly-hydrated salts were found to salt-out (i.e., charge neutralize) most effectively. The cloud point curves, however, exhibited a maximum (or, in the exceptional case of NaCl, an inflection) at about 200-300 mM salt, where the authors argue that the charge screening effect is no longer dominant and the feasible sites for anion association have been saturated, whereby the magnitude of the effect no longer changes with additional salt. Instead, at higher concentrations the effect was better explained by the modulation of surface tension at the protein-water interface by the added salt. All of the weakly-hydrated anion salts were interpreted to decrease the interfacial tension, and thus salt the protein back in (i.e., lower the cloud point back down) except for NaCl, which elevated surface tension and thus continued to raise the cloud point, and moreover the observed ordering in this region switched back to a direct Hofmeister series. It was found that these relatively complex dynamics could nevertheless be encapsulated in a single equation which modeled the cloud point – salt concentration data:

$$T = T_0 + \frac{B_{\max}[\mathrm{M}]e^{-b[\mathrm{M}]}}{K_\mathrm{D} + [\mathrm{M}]e^{-b[\mathrm{M}]}} + c[\mathrm{M}] \tag{6}$$

As can be seen, the form of the relation is similar to that reported for the modulation of LCST of PNIPAM and ELPs (Equations 3 and 4), and the term with coefficient c is here likewise interpreted as a linear component related to the interfacial tension effect of the salts. According to Zhang et al., it is reasonable to model anion binding to positively-charged lysozyme as a Langmuir-type event, to a first approximation, but the additional exponential multiplier is included because electrostatic neutralization is involved. The added term b here has units of inverse concentration and it along with $B_{\max}$ express the effectiveness of an ion to associate with and neutralize the charge of the protein. The authors then discuss correlations

between their fit parameters and physicochemical properties of the ions and draw mechanistic conclusions. Firstly, it is seen that both B_{max} and b values correlate well with anion partial molar volumes; this property of ions has previously been interpreted as a measure of the size of the hydrated ion, and is taken as a parameter proportional to the free energy of hydration.[119] It is seen, thus, that the larger, more weakly-hydrated anions are more effective at associating with lysozyme and consequently salting-out, because the energetic cost for their dehydration whilst transferring from bulk solution is smaller. This conclusion is also consistent with observations regarding other charged protein – charge screening salt effects in the literature.[120]

The parameter c values on the other hand, were found *not* to correlate with macroscopic air-water surface tension increments of the salts, as was previously observed for weakly-hydrated anions in studies of PNIPAM and ELPs.[5,103] In fact, all c values determined were negative (indicating that term expresses a salting-in effect on the LLPS transition), except for NaCl, whereas all of the salts studied *increase* the air-water surface tension, as previously discussed. Instead, the values of c were found to correlate well with anion polarizabilities. The former was interpreted by the authors as an indication that the effect of the most polarizable, weakly-hydrated anions was to *lower* the protein-water surface tension, and therefore promote lysozyme dissolution in a direct Hofmeister ordering. The authors also calculated apparent lysozyme-water surface tension increments for the various ion using their c values and the assumption that the value for NaCl can be taken as equivalent to that of its air-water surface tension increment.

1.2.3 Molecular Length-Scale and Local Curvature Effects, Binding to Host Pockets

The previous section described systems where inverted Hofmeister series were observed in the effects of salts on proteins and smaller molecules. In reading the discussion of the various studies presented above, however, it is worth noticing that the molecular mechanisms given for the reversed Hofmeister trends observed in smaller, oligopeptide solutes and larger, charged proteins are in fact not the same. For smaller molecules, the mechanism suggested was the predominant ion pairing of charged groups with strongly-hydrated anions,[88,89] as opposed to the preferential association of weakly-hydrated anions in the case of charged ELPs[16] and lysozyme.[118] Better understanding of complex systems is still underway, and in this sense it is hard to generalize such models; however, a recent study may shed light on an additional aspect of Hofmeister systems that is likely to be intimately involved in the

divergence—molecular length-scale (i.e., size) and topology of the solute or interface. In a 2022 paper,[90] Cremer and coworkers studied the interactions of NaSCN with poly(ethylene oxide) (PEO) solutes of various degrees of polymerization (i.e., number of monomer units). Using ^{1}H-NMR spectroscopy and fitting their results to the same model as used by Rembert et al.,[111] i.e., Equation 5, they were to identify a critical distinction: the weakly-hydrated SCN^- ion binds strongest to the central residues of the longer PEO chains, but not to terminal groups or to smaller oligomers, from which it is excluded. The water-structural characteristics of hydration are length-scale and curvature dependent; the bulk water network is more easily able to accommodate smaller, more convex solutes within its intermolecular network, but is disrupted by and forms more disordered hydration around larger and flatter solutes and interfaces.[121–124] This was shown experimentally by Cremer and coworkers by performing multivariate curve resolution (MCR) Raman spectroscopy measurements on aqueous solutions of various chain-length PEO solutes, finding that the termini of the polymer were indeed associated with more highly-structured hydrating water. Finally, MD simulations were utilized to confirm the preferential accumulation of SCN^- ions around central residues, but not at termini, and to correlate the tendency for this adsorption to the water tetrahedral order parameter q,[125] confirming that the heterogeneity could be explained by the more ordered water at the termini disfavoring the adsorption of SCN^- ions.

The implication of length-scale and local curvature as determinants of the characteristics of hydration, and consequently of specific ion effects, by these results underlines that these aspects bring an additional dimension to Hofmeister phenomena. The length-scale concept inherent to the study by Cremer and coworkers can be considered in connection to additional insightful studies on the link between Hofmeister effects (particularly those of weakly-hydrated anions) and local topology and curvature of the macromolecular interaction sites. Gibb & Gibb[126] published the first thermodynamic and spectroscopic characterization of the strong binding behavior of weakly-hydrated anions to a model 'cavitand' host molecule with a hydrophilic outer surface (functionalized with carboxylic acid groups) and a highly hydrophobic inner concavity. Using isothermal titration calorimetry and ^{1}H-NMR spectroscopy, they found that the effectiveness of the binding of a series of sodium salts followed a direct Hofmeister series for the anions. The most strongly binding amongst the anions (ClO_4^-) was observed to liberate 2.70 kcal/mol of free energy upon binding, with association equilibrium constant 95 M^{-1} (i.e., $K_D \approx 0.011$ M). Gibb & Gibb emphasize that while this is a relatively modest free energy gain, it is larger than the energy change found for

association with the polar amide groups in studies using PNIPAM (~0.41 kcal/mol),[9] and also that, interestingly, the binding of the anions is driven by a large favorable enthalpic gain, with a significant unfavorable entropic cost. Moreover, Gibb & Gibb found that the binding of weakly-hydrated anions competed with that of prototypical hydrophobic guest molecules (in the study, adamantane carboxylate), and thus would appear to 'weaken' the hydrophobic effect. They propose the system studied as demonstrative of a possible mechanism for the Hofmeister effects of weakly-hydrated anions or chaotropes in general. A later study by Gibb and coworkers[127] investigated the binding of a larger range of anions to the same host cavitand, and found results that largely agreed with their interpretations and also pointed to dynamics of the partial dehydration of the anions during binding as an important factor for their affinity. A very recent study by Sullivan et al.[128] expanded the investigation further to additional host molecules (including other cavitands, as well as cyclodextrins) and found that while a Hofmeister series was observed for the binding of anions to all hosts, the complete consideration of the hydration dynamics of the free host and of the guest, the bound complex, as well as counterion effects were needed to explain the full, emergent trend in anion affinities.

Fox et al.[129] studied the interactions between a spectrum of sodium salts and human carbonic anhydrase II (HCAII)—which contains a Zn^{2+} cofactor site capable of binding anions, as well as various hydrophilic surfaces and hydrophobic cavities—using isothermal titration calorimetry. Their results were in strong agreement with Gibb & Gibb: anion binding to Zn^{2+} in the enzyme active site was stronger for weakly-hydrated anions, such that the free energy gain of binding correlated inversely with the free energies of anion hydration (i.e., the more weakly-hydrated anions had a smaller cost of dehydration and thus a larger free energy driver for binding), and the binding of the anions was once again associated with favorable enthalpic and unfavorable entropic grounds—that is, demonstrated an 'enthalpy-entropy compensation'. X-ray crystallography was employed to determine that SCN^- and ClO_4^-, which bound most strongly, interacted primarily with Zn^{2+}, whereas for I^- and Br^- additional binding sites were found in the hydrophobic declivities near the active site, a fact which was interpreted as indicating that anion shape and size also affected the specific affinities. Interestingly, whilst strongly-hydrated anions were indeed observed to exhibit little to no binding (e.g., for SO_4^{2-} and HPO_4^-, no binding was observable), the behavior of HCO_3^- and CH_3COO^- deviated from the trend; this was explained by the former being the substrate of HCAII and the latter an analogue, and thus specifically selected by the enzyme through hydrogen bonding with amino acid residues in the active site. This serves to demonstrate that as much as Hofmeister effects

are universal, nature may also modify or appear to 'flout the rules' through specific ion selectivity of coordination environments.[16]

1.2.4 A New Branch of Hofmeister Effects: Superchaotropic Anions

The investigation of local topology effects on Hofmeister phenomena, as in binding to pocket structures as described in the previous section, was also instrumental in the identification of what is considered by some researchers as a new, distinct class of Hofmeister ions. In recent years, disparate research groups studying various related systems have observed a range of curious and significant effects related to chaotropic anions and their binding to hydrophobic surfaces, particularly concave surfaces, reminiscent of the findings by the researchers discussed in the previous section. These effects were seen to be strikingly strong for special, 'nonclassical' large polyatomic anions. Citing the growing body of work characterizing the behavior of such anions—for which they were described with the burgeoning term "superchaotropes" or "superchaotropic ion"[130,131]—and their newly recognized widespread applicability in a variety of chemical contexts, this (supra)molecular motif was termed the "chaotropic effect" by Nau and coworkers.[17,130] Early hints of this phenomenon include a study by Taraszewska & Wójcik,[132] where the binding of several anions to α- and β-cyclodextrin (CD), in competition with *ortho*-nitrobenzene serving as organic guest species was investigated using ^{1}H-NMR spectroscopy and polarography. The ClO_4^- anion was found to bind the strongest, with $K_D \approx 0.11$ M, and the anion binding affinities were also related to the Hofmeister ranking of the anions by the authors. The same effect was even more prominent in studies of dodecaborate anions ($B_{12}X_{12}^{2-}$ where X = H, Cl, Br, I) by Assaf et al.,[130] where the affinity for binding to γ-CD was comparable to that of hydrophobic guests such adamantane and triamantane. The thermochemical character of the behavior was also investigated, finding an associated entropic cost (similarly to that which was reported in the study by Fox et al.[129] discussed previously) and was attributed to the dehydration process of the anions. The binding behavior of the same dodecaborates was then extended to larger CDs,[133] and other hosts (such as calixarenes[134] and tetrathiafulvalene[135]) as well as to other related anions, including larger borate clusters[136] and thiol-substituted dodecaborates.[134] These anions have also been shown to interact with hydrophilic column materials,[137] in-line with the behavior of chaotropic anions from classical studies.[138]

A large group of studies in this field have investigated polyoxometalates (POMs) as a different class of similarly behaving ions: these species are discrete, inorganic metal-oxygen

clusters with sizes that are often nanometric or larger.[139] Naskar et al.[131] attempted to classify POMs in terms of Hofmeister effects and observed adsorption of POMs onto micelles of nonionic surfactants and to the water-surfactant monolayer interface, as evidenced from small-angle X-ray scattering (SAXS) and ion flotation, and independently arrived at the descriptor of 'superchaotropic anions' for these species. Stoddart and coworkers[139] showed the complexation of the well-known Keggin-type POM $[PMo_{12}O_{40}]^{3-}$ with γ-CD both in solution and in the formation of solid-state inclusion complexes. Many supramolecular complexes of POMs were investigated by Cadot and coworkers,[140] including a particularly striking 'hierarchical' architecture comprising a Dawson-type POM $[P_2W_{18}O_{62}]^{6-}$ surrounded by two γ-CD units, then altogether contained within a giant 'Mo-blue' ring ('Mo_{154}').[141] Both dodecaborates[142,143] and POMs[144,145] were also found to interact with the exterior convex hydrophobic surfaces of cucurbit[*n*]uril (CB*n*) macrocycles, often interacting with multiple solutes in a multidentate manner, thereby inducing precipitation in solid-state exclusion complexes—which can be described as a reverse Hofmeister effect.[17] The biologically-relevant behavior of these superchaotropic anions has also been investigated: Kuperman et al.[146] found very strong binding of dodecaborates to bovine and human serum albumins, with K_A's $10^4 – 10^6$ M^{-1}, and the binding was found to be even stronger for metallocarboranes by Goszczyński et al.[147] Both boron cluster anions[148] and POMs[149] have been found to interact with lipid membrane structures, and the former were recently proposed as novel, highly desirable candidates for membrane-transport agents.[150]

All of the studies described in this section which considered the thermochemistry of superchaotropic ion binding found the same enthalpically-driven, entropically-costly signature that Assaf et al. emphasize is the hallmark of the chaotropic effect and the key distinguisher from hydrophobic effects, which are conversely associated with entropic driving forces and enthalpic penalties.[17] They and other research groups prioritizing the study of POMs understand the superchaotropicity of these nanometric ions (or 'nanoions'[151]) as related to the effective dispersion of charge over the ion outer surface, producing low overall charge density without 'burying' charge centers within bulky hydrophobic layers, which might entail that more hydrophobic-type properties are relevant for ions such as $AsPh_4^+$ and BPh_4^-.[17] Study of the physical chemistry of these ions continues; their preferred classification as either superchaotropic ions or charged nano-colloids was the subject matter of one recent paper,[152] where evidence for both conceptualizations were presented, whereas a different article argued that POMs were better considered as colloidal particles.[19] In the view of Assaf et al.[17],

superchaotropic ions constitute an expansion of the far weakly-hydrated end of classical Hofmeister (anion) series, lying in a unique intermediate region between the classical chaotropes and the hydrophobic ions, neutral hydrophobes and cavities that extend beyond them. Their unprecedented affinities for binding to hydrophobic sites, as well as their behavior as surfactants in some systems[153] (on the basis of which they have been described, owing to their starkly different geometry than classical head-and-tail surfactants, as 'intrinsic amphiphiles'[17,154,155]) and ability to self-assemble[156,157] highlight both their uniqueness and the rich prospects for uses in supramolecular, materials science and even medicinal contexts.[17]

The recent research on superchaotropic ions also highlights that the boundaries posed by classical, limited understandings Hofmeister ion effects are ripe for expansion. As is evident, the research outlined in this section has focused on many novel anions and, as will be discussed shortly in the following sections, the current state of the study of Hofmeister cations directs us to pursue a similar broadening beyond the classical models for positively-charged ions as well—a sentiment that is central to the motivation of this work.

1.3 Cation Effects: Interaction, Exclusion and Beyond the Classical Metal Cations

As compared to anions, cations have always held a comparatively understated role in the Hofmeister literature.[1,3,12,158] As can be seen from Collins & Washabaugh's[1] aggregated list of common Hofmeister features mentioned in section 1.1.3, anions' dominance over the influence of cations was a common sentiment across the Hofmeister literature. Through the mid- to late-twentieth century, experimental and theoretical work has attempted to characterize and explain these purported differences based on general, intrinsic arguments. Conceptually, the simplest argument might be that anions are typically larger and more polarizable than cations, and therefore would predominate in contexts where polarizable/non-electrostatic interactions are favored—this is, for instance, the reason why large, soft anions may locally accumulate at air-water interfaces, whereas cations typically do not.[56,159,160] The difference between anions and cations in water can also be explained, according to some views, as a consequence of the polar asymmetry of water itself: Collins et al.[161] postulate that due to the water oxygen's high electronegativity, it readily accepts the net electron charge transfer from anions, but is less inclined to donate charge to cations during hydration—that is, hydration of anions is stronger than that of cations. Extra-thermodynamic methods to apportion separate ionic quantities from values measured for salts often reach the same conclusion.[162] The

difference may also arise from the structural orientation of water in the cationic (oxygen-oriented) vs. anionic (hydrogen-oriented, often linear due to hydrogen bonding) hydration shell: according to a (relatively early) computational work by Combariza et al.,[163] whilst water in the hydration clusters of cations only form inter-shell hydrogen bonds, anionic clusters may have intra-shell hydrogen bonding as well due to the differing geometry. It is also possible to find references in the literature that conclude cations affect the structure of water less than anions based on interpretations of experimental studies, such as IR spectroscopy measurements of salt solutions carried out by Luck,[164,165] and a systematic Raman spectroscopy study of a set of alkali halide salts by Terpstra et al.[166]

Indeed, reports on diverse systems have often determined that cations are not the main drivers of prominent differences in salt effects. Changing the identity of the cation was found not to cause any effect in the orientational ordering of water near the PNIPAM monolayer at the air/water interface by Cremer and coworkers in a VSFS study,[167] wherein a broad range of cations were tested by means of comparing each of their chloride salts (LiCl, NaCl, KCl, CsCl, NMe_4Cl, $CaCl_2$, $MgCl_2$). Onorato et al.[168] conducted a study of the adsorption of SCN^- anion to the air/water/dodecanol monolayer interface, and found no difference between NaSCN and KSCN within error. A paper by Fesinmeyer et al.[169] investigated the salt effects on the agitation-induced aggregation of IgG2 monoclonal antibodies. Aggregation was determined to increase in the order $F^- < Cl^- < Br^- < I^- < SCN^- \sim ClO_4^-$ for anions, whereas for the cations tested (Li^+, Na^+, K^+, Rb^+, Cs^+) there was no differential effect. Interestingly, the authors posited that the aggregation process primarily occurred at the air-water interface, and that agitation then cycled protein aggregates into the bulk and provided a convective supply of protein for further aggregation. Thus, ion accumulation/depletion behavior at the air/water/protein interface is likely part of the mechanism here as well.

Yet, this is hardly the full story. In a comprehensive theoretical treatment that considered the full space of ion size, surface hydrophobicity and polarity properties, Schwierz et al.[170] make the following prominent remark: “As a matter of fact, the Hofmeister series is not intrinsically weaker for cations compared to anions; it just so happens that ordinary cations are smaller than anions typically considered.” Indeed, they found that the behavior of cations is just as relevant and complex as that of anions—perhaps most of the literature has placed emphasis on anionic effects because of this incidental ‘quirk’ of the metal cations encountered in common salts. Moreover, recent studies have revealed that even the behavior of the common metal cations in relatively simple systems belie widespread generalizations and over-

simplification of cations as passive Hofmeister components: Shahir et al.[171] reported a cation-specific effect in the sum frequency generation (SFG) signal intensity of water OH bands at the solution/monolayer (of methyl isobutyl carbinol) interface, which they explained by the increasing tolerance of the larger alkali cations (like Cs^+) to approach the air-water interface, thus cooperatively allowing more Cl^- counterions to penetrate it, as evidenced by the decreased surface potential. Hua et al.[172] investigated a similar air/water interfacial system, and determined the strength of the interfacial electric field generated by cation-anion separation increases $Li^+ \approx Na^+ > NH_4^+ > K^+$, in line with the conclusions of Shahir et al. A striking recent study by Perrine et al.[173] produced experimental evidence that, in fact, Li^+ is able to better adsorb to the air-water interface than K^+ in alkali metal halide solutions, and is present at the interface. The behavior of Li^+ has been regarded as anomalous in multiple reports; in their VSFS study of the fused-quartz surface-water interface, Flores et al.[174] determined the cation ordering $Li^+ > Cs^+ > Rb^+ > NH_4^+ > K^+ > Na^+ > Ca^{2+} > Mg^{2+} > Zn^{2+}$ for the attenuation of the OH stretch peak—the unexpectedly extreme position of Li^+ is particularly striking. Moreover, when the surface was changed to TiO_2, several stark differences were captured: Li^+ behaved more in line with Na^+ and K^+, Mg^{2+} and Ca^{2+} switched positions, and NH_4^+ interacted most strongly amongst all the cations. The authors remark that the observed manifold reordering likely relates to the differences in charge density, polarizability, basicity, and hydrogen bonding capacity of the two surfaces, and illustrates the specific complexity that may arise within cationic effects. A different study (Götte et al.)[175] used vibrational sum frequency generation (VSFG) to determine that the solvent-shared ion pair formation in $MgSO_4$ solutions (but not other magnesium salts) lead to a local accumulation of Mg^{2+} near the air-water interface, with implications for aerosol chemistry and thundercloud electrification. Recently, van der Vegt and coworkers[176] simulated the salting-out effects of alkali chlorides on benzene in an attempt to provide and explanation for the experimental salting-out order NaCl > KCl > RbCl, LiCl > CsCl, where Li^+'s position once again stands out. They found that unlike the strictly repulsive Na^+, Li^+'s hydration shell was able to accommodate and share hydration with benzene. Additionally, it was found that the larger cations had an affinity for cation-π type direct interactions with the aromatic benzene ring. A different study by Altekar[177] serves as another interesting examination of the larger alkali cations: the researchers investigated the effects of chloride salts of monovalent cations on the fluorescence of nine proteins. The effects were generally complex, and categorized as occurring through 'direct' and 'indirect' interactions with aromatic amino acid residues. In this regard, Cs^+ was identified as the only cation to quench fluorescence through direct interaction with residues such as tryptophan. Na^+, K^+, Rb^+,

Li^+ and NH_4^+ did not produce this particular effect, although various degrees of quenching or dequenching were seen for most proteins, attributed to salt effects on the general structure of the proteins. 4 M LiCl in particular induced fluorescence changes in bovine serum albumin (BSA), papain and trypsin that were indicative of protein structural changes.

It is a striking observation in biology that the mammalian intracellular environment is rich in K^+ but poor in Na^+, and the inverse is true for the extracellular medium. In fact, cells actively maintain this gradient through membrane ion-channel proteins. Moreover, whilst outside the cell Na^+ is largely electro-neutralized by Cl^-, this is not the case for inside the cell; instead, much of the negative counter-charge is comprised of negatively charged proteins and lipids—this phenomenon is known as the "anionic gap". The exact biochemical and evolutionary explanation is still unknown, and remains an active area of research today; the difference in the cation specific affinities of K^+ vs Na^+, toward charged amino acid residues has been proposed as one explanation.[178] Motivated to investigate cation-phospholipid effects, Klasczyk et al.[179] studied alkali metal chloride – palmitoyl oleoyl phosphatidylcholine (POPC) vesicles using ITC and found a direct Hofmeister effect, whereby Li^+ had the greatest tendency to associate with lipid head-groups. At molar concentrations, the alkali chlorides shifted the phase transition temperature of the lipid system by several degrees. Lo Nostro & Ninham[12] remark that such studies may hold significance for elucidating the poorly-understood mechanisms behind the pharmacological effects of Li^+, Rb^+ and Cs^+ cations.

With regards to proteins specifically—the original template for Hofmeister studies—we should recognize that attempts to explain Hofmeister effects on the basis of the peptide bond that began in the 1960's (often using model oligopeptides) already concluded that cations appeared to play a role, as discussed in the previous sections.[1,3,12,16,39,61,86] Additional evidence for interactions with cations came from Bello & Bello:[180,181] in a series of studies, they reported unusually high viscosities in solutions of *N*-methylacetamide (NMA) and *N,N*-dimethylacetamide (DMA) with lithium and calcium chlorides, and also obtained crystallized adducts of the amides with these and other salts. X-ray analyses revealed that the crystal structures contained cations coordinated with four amide carbonyls and two water molecules, with anions hydrogen-bonded to water and amide N-H groups.[182] Kurtz & Harrington[183] were able to isolate complexes of LiBr with polyproline, polyhydroxyproline, polysarcosine, polyglycine and polyalanine, though structures were not reported. In column chromatography studies by von Hippel and coworkers,[100] the affinity of various salts for polyacrylamide column material was investigated, and directly reproduced the Hofmeister series; specifically, amongst

the cations, the strongly-hydrated Ca^{2+}, Mg^{2+} and Li^{+} were observed to retain most strongly when eluted as their chloride salts. Interestingly, amongst the larger monovalent cations, there was a volcano-curve like pattern, where the affinity minimum was observed at K^{+}, after which affinity increased once again. CsCl was observed to have a stronger retention than NaCl. NMR studies of amide proton exchange provided additional evidence for both cation and anion complexation to NMA,[184,185] alongside the direct cation Hofmeister ordering observed in ^{13}C-NMR chemical shifts (specifically, the deshielding) of the carbonyl resonance of small amide molecules.[186] Timascheff and coworkers conducted extensive studies on the Hofmeister effects of numerous proteins; in two of their studies in the early 1980's,[65,187] using densimetric measurements they were able to observe direct Hofmeister orderings for cations and anions with BSA, lysozyme and β-lactoglobulin. The cations tested were found to be influential in the effects, specifically inducing salting-out in the order: Mn^{2+}, $Ni^{2+} < Ca^{2+}$, $Ba^{2+} < Mg^{2+} < Na^{+}$.

In more recent years, we find spectroscopic studies of cation-amide interaction that unambiguously demonstrate the often weak but measurable affinity of strongly-hydrated cations for the amide carbonyl. In 2013, Okur et al.[188] examined the small molecule butyramide—as a simple model for the peptide group—in high concentration solutions of metal chloride salts, using attenuated total reflectance (ATR)-FTIR spectroscopy and VSFS measurements. In the ATR-FTIR measurements, the amide I band of the deuterium-exchanged butyramide, which appears at 1620 cm^{-1} in neat D_2O and consists almost entirely of the carbonyl stretching mode, remained unchanged in the presence of 5 M NaCl and 5 M KCl, but generated a new shoulder peak at 1645 cm^{-1} with 5 M $CaCl_2$. With increasing salt concentration, this shoulder peak grew in intensity whilst the intensity of the main peak decreased. The shoulder peak was thus assigned to carbonyl groups that had formed contact pairs with Ca^{2+}; the authors explain that replacement of water in the coordinating environment of the carbonyl oxygen with most other species results in a net blueshift, due to hydrogen bonding with water having a significant charge transfer (from the carbonyl oxygen to the water σ* antibonding orbital) and thus a comparatively larger redshift associated with it. The amide I band behaved in a similar manner with 5 M $MgCl_2$ and 9 M LiCl; both salts generated shoulder peaks that were a few wavenumbers further blueshifted than $CaCl_2$, indicating that their polarization of the carbonyl group was slightly weaker.

Okur et al. were also able to show the change in the population of cation-bound carbonyl groups against salt concentration. The relation was linear for all three binding salts, and even for the strongest binding $CaCl_2$ only ~30% of carbonyl sites were occupied by cations at 5 M

salt. Although accurate dissociation constants cannot be determined from this concentration range, the K_D's for cation-carbonyl association was approximated to be 8.5 M, 9.5 M and 20.2 M for $CaCl_2$, $MgCl_2$ and LiCl, respectively through extrapolation—note that these values are above saturation limits, and the cation-carbonyl affinities border on being merely statistical. Whereas ATR-FTIR measurements had revealed contact pair formation, VSFS measurements of butyramide Gibbs monolayers at the air/solution interface was able to provide information on overall partitioning of ionic species to the solute interface. Indeed, the intensification of OH bands in the VSFS spectrum observed in $CaCl_2$, $MgCl_2$, and LiCl solutions in that order confirmed that the cations partitioned to the interface with this order of effectiveness. The spectra for NaCl and KCl were no different than that of pure water as solvent within experimental error; overall, a direct Hofmeister series is obeyed. The FTIR findings of the study were later corroborated by an *ab initio* theoretical study (though for *N*-methylacetamide as the studied molecule), which also determined that Na^+ also interacted locally with amide carbonyls, but did not produce detectable shifts in the amide I band of NMA.[189]

The most detailed characterization of cation effects on model neutral macromolecules was reported in 2020, where Bruce et al.[10] investigated the phase-transition effect of nine different metal chloride salts on PNIPAM and also studied the same systems with all-atom MD simulations. The general effect of all salts tested was to salt-out the polymer, i.e., monotonically lower its LCST. However, at higher salt concentrations an upwards-oriented curvature was observed in the LCST vs salt concentration curves. This partial salting-in contribution was largest for the strongly-hydrated cations (in order, $MgCl_2$, $CaCl_2$, $SrCl_2$, LiCl), and followed a direct Hofmeister series. Based on the mechanistic correlation found previously for anions, the strongly-hydrated cation salts would be expected to salt-out PNIPAM more strongly; since the anionic salting-out effect was correlated to surface tension, the divalent metal chlorides in particular would be expected to salt-out twice as effectively at the same concentration, in agreement with their air-water surface tension increments. Yet, this is not the case. Moreover, the Langmuir-type saturable binding model found applicable for anion binding (Equations 3 and 4) was clearly not obeyed; instead, the LCST curves fit the empirical form:

$$T_c = T_0 + ac_s + dc_s + fc_s^2 \tag{7}$$

where the LCST (T_c) is related to the concentration of a given salt, c_s through both linear and quadratic terms. The linear term ac_s was interpreted as a surface-tension related salting-out contribution on the basis of correlations with salt tension increments, whereas the final two

terms—which were significant only for the salts with significant salting-in contributions at higher concentrations—were linked to specific ion accumulation. The MD simulations illuminated this effect in more detail: salt (including both ions) was depleted overall from the PNIPAM vicinity in all cases, but in the specific case of the strongly-hydrated cation salts the depletion was significantly attenuated at higher concentrations. Radial distribution functions demonstrated that, indeed, there were local accumulations of cations around amide oxygens and of anions around the amide nitrogen and terminal methyl groups. The ions were generally found to retain their hydration shells during the interaction, and a cooperative effect was observed whereby the strongly-hydrated cations also enhanced the chloride accumulation. The formation of solvent-shared ion pairs (SIPs) was found to also occur in local maxima around the ion hotspots, but only with strongly-hydrated cations. Probability density maps for Ca^{2+} SIPs near the polymer and Ca^{2+} overall were nearly identical, indicating that the charged ions preferred to approach the macromolecular interface in ion-pairs so as to neutralize (or reduce) charge separation (as represented schematically below in Figure 5). Additionally, the implication of SIPs brings light to the quadratic (fc_s^2) concentration dependence of the salting-in term in Equation 7, as ion-pair formation probability is related to both cation and anion concentrations in solution, and thus scales quadratically. This work was significant in that it both experimentally and theoretically demonstrated the general mechanisms of the direct cation Hofmeister series on a well-studied, neutral model macromolecule—it serves, thus, as credible evidence that such cationic effects are likely present in many systems, as background contributions that may be contextually overshadowed by stronger effects.

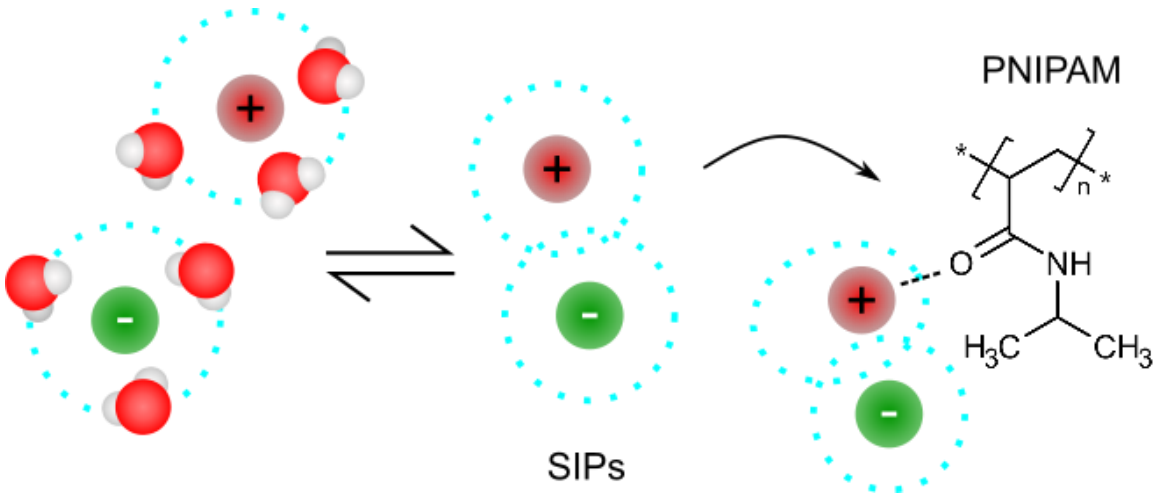

Figure 5: Schematic representation of the molecular mechanism (Bruce et al.[10]) found for interaction of strongly-hydrated cations with PNIPAM facilitated through the formation of solvent-shared ion pairs (SIPs). Figure was partially inspired from Bruce et al.[10]

1.3.1 Cationic Effects on Negatively Charged Solutes: Enhanced Effects and Strong Binding to Peptide Chains

Does the relatively weak affinity of even strongly-hydrated cations for the peptide bond and model neutral molecules mean that they are not of substantial influence in protein Hofmeister effects? When, if ever, are cation effects more significant than anion effects? In fact, there are reports in the literature that claim cation interactions with small molecules are actually stronger than anionic ones. Balos et al.,[190–192] for instance, used dielectric relaxation spectroscopy to conclude that cations appeared to bind more strongly than anions to NMA molecules, based on their greater restriction of the rotational mobility of the molecules' amide groups. Yet, the majority of the studies presented in the preceding discussion have maintained that anion interactions are stronger—this notion appears to hold a stronger consensus. Even so, cationic effects are greatly enhanced in the presence of negatively charged groups on a solute,[10,16] which is quite frequently the case in nature. Interactions with the negatively charged (carboxylate) side-chains of amino acid residues tend to be the main effectors, for which cation affinities tend to follow the Hofmeister series, i.e., strongly-hydrated cations have greater affinity.[15,178,193] X-ray absorption spectroscopy and computational studies of small negatively-charged amino acids, as well as formate and acetate in aqueous solution have confirmed this trend.[194–196] Binding of strongly-hydrated cations to negative polyelectrolytic peptides can be strong enough to lead to over-charging, as determined by simulations and electrophoresis experiments.[197] With longer polypeptides, the structural implications of cationic effects become even more evident: cations with larger affinities for backbone carbonyls and charged carboxylate side-groups (typically, the more strongly-hydrated cations) may destabilize preferred conformations of polypeptide chains—which rely on intrachain hydrogen bonding and salt bridges between ionic residues—and significantly affect chain folding kinetics, according to the findings of MD simulations,[114,116,198–201] circular dichroism (CD) and Förster resonance energy transfer (FRET)[202] studies. The dynamics are quite complex and chemically rich; salts may impart a nonspecific stabilization effect to secondary structure elements such as α-helices at low concentrations due to their screening of charges on the chain, but destabilize the same conformations due to competitive ion-specific interactions at higher concentrations, such that the effect overpowers the former stabilization contribution.[203]

Furthermore, in systems like those described the contributions of anions and cations are often both important, and are observed to be nonadditive and synergistic; binding of one species may amplify the denaturing efficacy of the other.[116,203] A recent study by Cremer and

coworkers[204] looked at the phase transition of an 64-pentad ELP containing 16 aspartate residues (as well as 32 valine and 16 phenylalanine residues in the remaining guest positions) in the presence of 12 monovalent and divalent metal chloride salts at basic pH. The LCST behavior of the ELP was fit according to Equation 6, and VSFS measurements of a Gibbs monolayer of the ELP in presence of low concentrations of the salts generated the same ordering (based on the water OH signal attenuation as a signifier of charge neutralization of the ELP by cation accumulation) as that of the LCST depression ranking at the same concentration. There were some significant changes in the LCST-based rank order of ions in the higher concentration regime, though an explanation was not pursued by the authors. The binding strengths of the cations mostly followed a direct Hofmeister series, in particular for the divalent cations, which bound several orders of magnitude tighter (~1.4 – 7.6 mM) than the monovalent cations (~78 – 345 mM). NH_4^+ was anomalous in its behavior, in that it was the most strongly binding monovalent cation, which was attributed to its capacity for hydrogen bonding with carboxylate groups. As a control, the same measurements were conducted at low pH (where all aspartate residues are protonated) and no significant difference between any of the salts were found with either experimental method. Thus, the study illustrated that cationic specific effects can be very pronounced for systems with negative charges, wherein cations are observed to bind to such moieties very tightly.

1.3.2 Beyond Classical Hofmeister Effects: Nonadditivity, and the Cationic Denaturant Guanidinium

The discussion in the previous sections have highlighted that cations in fact do play a significant and often understated role in varied contexts, with significance depending on charge, polarity, size and other specific features of the systems studied. Where many studies have indeed reproduced direct Hofmeister series, or series resembling it, the previous discussion also contained several instances that hint at the limitations of such a framework. The behavior of ions in solution is frequently more complex than the static, strictly additive (cation-anion independence) understanding of the classical Hofmeister framework as outlined by Collins & Washabaugh.[1]

Nonadditivity of cation and anion effects are one major area where classical Hofmeister series fall short. As mentioned in the previous sections, ion pairing is found to be fundamental to understanding the effects of salts on proteins, polypeptides and neutral model polymers, as well as ion behavior at interfaces—and, indeed, ion nonadditivity has significant implications

for the (biophysical) chemistry of electrolytes at large,[205,206] as increasingly mentioned in the recent literature.[15] Such an effect was also recently manifested in the familiar system of the PNIPAM phase transition. In a 2021 study, Bruce et al.[207] observed that varying the cation in PNIPAM LCST measurements in iodide salt solutions had an unexpected effect: amongst the iodide salts, the order of salting-out was CsI > NaI > LiI, with large differences between salts particularly at high salt concentrations. All-atom molecular dynamics were employed to bring light to this phenomenon. Preferential binding coefficients depicted the greatest depletion of both types of ions from the polymer surface for CsI, and least for LiI. It was found that with increasing size of the cation (i.e., weaker hydration) a stronger propensity for contact ion pairing led to a competitive sink for I^-, and thus a diminution of its (dominant) salting-in effect. 1 m solutions of the salts (without PNIPAM) were computed to have 83% CIP formation for CsI, but only 11% and 7% for NaI and LiI, respectively. Varying the propensity for ion pairing (by modulation of the "cation-anion Lennard-Jones size parameter") demonstrated that the depletion of CsI from the interface was less severe with ion pairing effectiveness reduced. The thermodynamic consequences of ion pairing were investigated further by using Kirkwood-Buff integrals (KBI). Nonideality factors were calculated, which were then used to calculate the influence of the salt on the chemical potential of the PNIPAM polymer via the Wyman-Tanford/Kirkwood-Buff relation. In brief, it was seen that, intriguingly, ion pairing had two, opposing effects: a salting-out effect due to mitigation of the influence of I^- on the polymer, and a salting-in effect due to the lessening of the effect of the ions on water overall—that is to say, decrease in the activity of the ions or their solvent excluded volume effect. While the net effect establishes that salting-out due to ion pairing dominates, it is not as severe as would have been the case where only the first contributing factor was in effect. This study illustrates how the Hofmeister effects of even commonly-studied ions can be complex, and the consequential role cations may play even when their direct effects are not dominant.

In moving toward future studies of Hofmeister effects it is also important to identify and characterize ions that break the mold of known mechanisms—some of them novel (as with superchaotropic anions discussed in section 1.2.4) and some of them quite well-known. Guanidinium cation (Gnd^+) is one such species, as an example of the latter. Gnd^+ represents, by itself, an exception and a challenge to the anion-predominant viewpoint of Hofmeister effects, as its salts have long been recognized and used as potent denaturants.[2] Structurally and topologically, this weakly-hydrated[208] cation is quite distinct from monoatomic metal cations, having flat hydrophobic faces and the ability to participate in hydrogen bonding through its

three end groups. It has been discovered to deplete less extensively from the air-water interface and form ion pairs with itself in solution; both of these properties involve stacking interactions, via parallel orientation of its flat faces.[209,210] It has also been shown to interact specifically with aromatic groups,[211] and is even present as a motif in proteins themselves as seen in the arginine side-chain. One of the intriguing aspects of Gnd^+ is that its denaturant behavior depends very strongly on the counterion its salts; Gnd^+ salts with weakly-hydrated anions such GndSCN and GndCl are commonly used as denaturants,[212] with the former being particularly effective, whereas strongly-hydrated anions make for salts that are far less denaturing, and in the well-known exceptional case of $GndSO_4$, actually stabilizing. For this latter Gnd^+ salt, multivalent ion pairing into aggregates in solution has been implicated as a possible mechanism for the quenching of Gnd^+'s denaturant ability.[213–215]

Recently, substantial strides have been made in understanding the unique properties of these salts. Heyda et al.[216] systematically investigated the phase transition of an ELP polymer (120 pentads with glycine in all guest positions) in solutions of five different Gnd^+ salts. The results were striking: vastly different behavior was observed for the different salts. The LCST of the polymer was observed to rise linearly for GndCl, remain largely unchanged for $GndNO_3$, decrease linearly for Gnd_2CO_3 and Gnd_2SO_4, and exhibit a unique non-monotonic trend for GndSCN, wherein the LCST fell at low concentrations but rose again at 1.5 M and higher salt concentrations. At low concentration, GndSCN was in fact the strongest salting-out agent, followed by Gnd_2SO_4 and Gnd_2CO_3. It was clear that the Langmuir-type binding model used previously for the same ELP (Equation 4) was not applicable, and that a Hofmeister series was not followed amongst the anions. The researchers conducted ATR-FTIR measurements of the ELP in solutions of low salt concentration above its LCST, as well as control measurements in neat solvent. By looking at the signature bands belonging to each of the species, they found that both Gnd^+ and SCN^- ions were enhanced in the ELP-rich phase that developed in the samples above the LCST; that is, the ions were accumulated/preferentially included in the collapsed form of the polymer. Additionally, the vibrational information extracted from the polymer indicated it was in a less structured state than standard collapsed form in the absence of salt. Analogous measurements for Gnd_2SO_4 demonstrated instead that the ions were depleted from the collapsed form of the ELP. Finally, measurement using GndCl found slight depletion of the Gnd^+ ion from the ELP-rich phase, as well as lower intensity of the ELP amide I band, which could indicate that there was less effective aggregation of polymer due to slight charging. Together with coarse-grained Langevin dynamics and all-atom MD simulations, these results

were used to propose a holistic model of denaturation/stabilization mechanisms for Gnd^+ salts. Salting-out salts such as Gnd_2SO_4 are depleted from the polymer interface and thus operated via an excluded volume mechanism. In the GndSCN case where both ions had a high affinity for interaction with the ELP, at low concentrations of salt the polymer collapses due to the strong binding and bridging (or 'gluing') effect of bound ions. At higher concentrations, the polymer relapses into its extended form because sufficient ion saturation is reached so as to make cross-linking ineffective, and also to further maximize the number of unbound sites accessible to the solution.

1.3.3 The Weakly-Hydrated Extreme of Hofmeister Cations: Quaternary Ammonium Cations and the Present Work

As illustrated throughout this chapter, specific ion effects on macromolecules occupy a rich and complex space of competing, cooperating and modulating driving forces, and the growth of the knowledge of these effects often requires extensions of the classical and well-studied Hofmeister series. The unique and potent effects of the weakly-hydrated cation Gnd^+ are indeed a salient indicator of the diverse phenomena that may arise from the balance between weak forces in 'soft' systems. As evident from the discussion in section 1.2.4, even the better-studied field of anionic effects has grown rapidly in recent years through exploration of the far chaotropic end of the Hofmeister anion series; for cations, this realm remains largely untouched and unknown. It is with this motivation, thus, that the present thesis was undertaken, with the goal of producing the first systematic study of the Hofmeister effects of very weakly-hydrated, large and (tunably) hydrophobic cations that belong to the quaternary ammonium class. By varying the chain length of the alkyl groups attached to the nitrogen atom, the size and weakly-hydrated nature (the 'greasiness') of the cations are concomitantly modulated and thus provide an avenue for systematic study.

Mention of quaternary ammonium (QA) cations—which consist of a central nitrogen atom connected to four alkyl, aryl or organyl groups, as can be seen for the case of several tetraalkylammonium cations in Figure 6—appear only very rarely in scattered reports from the Hofmeister literature. We should distinguish here that we are specifically interested in quaternary ammonium species and, in particular, symmetrical tetraalkylammonium cations. Ammonium cations with less than four alkyl substitutions (named primary, secondary or tertiary ammonium, or 'aminium' ions) have, firstly, the complication of weak acidity/deprotonation, inherent asymmetry, as well as less hydrophobic character. QA cations

decorated very asymmetrically with both long and short alkyl substitutions, on the other hand, frequently exhibit surfactant behavior—for example, consider the well-known surfactant cetyltrimethylammonium bromide—and thus belong in a different class than non-surfactant Hofmeister cations. In typical Hofmeister cation series, ammonium cation (NH_4^+) is often included, at the chaotropic/weakly-hydrated end, i.e., as the least salting-in cation, according to a direct Hofmeister rank order. One much less frequently finds other QA cations, most likely tetramethylammonium ($N(CH_3)_4^+$, or NMe_4^+) if any, which is usually ordered farther than NH_4^+. Inclusion of any other QA cations is quite rare.

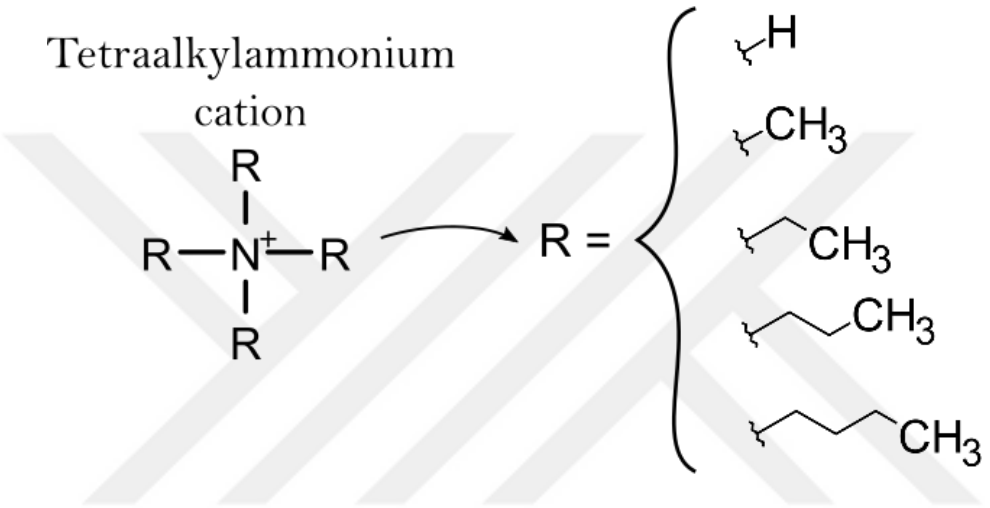

Figure 6: The structure of quaternary tetraalkylammonium cations, with up to 4-carbon unit alkyl chains lengths. When the R group is each of the substituents shown on the right-hand side, the corresponding cation is, from top to bottom: ammonium (NH_4^+), tetramethylammonium (NMe_4^+), tetraethylammonium (NEt_4^+), tetra-*n*-propylammonium (NPr_4^+), tetra-*n*-butylammonium (NBu_4^+) cation.

One area of the Hofmeister literature that one can come across QA cations in is solubility studies of small molecules. Study of salt effects on the solubility of polar and nonpolar organic nonelectrolyte solutes gained traction as a methodology to investigate and model Hofmeister effects in the early to mid-twentieth century. Some discussion of such studies was given in the previous sections. Alongside dissolved gases, benzene and its derivatives were typically chosen as representative nonpolar solutes.[30,217] It was shortly determined that the majority of salts decrease the solubility of these solutes (in accordance to the Setschenow relation, Equation 1, above) whereas some large, organic ions salted-in—this was the origin of Neuberg's proposition of 'hydrotropism'.[218] QA cations constituted the main class of cations that salted-in benzene-like molecules and multiple studies included QA salts in their

measurements, analyses and theories.[217] Saylor et al.[219] found in 1952 that NMe_4Br salted-in aqueous solutions of benzene and nitrobenzene, and commented on the difficulty of explaining this fact with the extant electrostatic approaches in the literature of the time. Bockris et al.[220] conducted a systematic survey of the solubility of benzoic acid in solutions of NR_4I salts for R = H, Me, Et, *n*-Pr, *n*-Bu, and observed that all salts other than NH_4I salted-in benzoic acid, with the order of increasing salting-in determined as: $NMe_4I < NEt_4I < NPr_4I < NBu_4I$. They also reported a linear correlation between the NR_4^+ cationic radii and Setschenow salting-in constants derived from the measurements. Linderstrom-Lang[221] conducted a systematic study of the solubility effects of various alkylated ammonium chlorides on quinone and hydroquinone, finding that hydroquinone was salted-in by these salts—with the effect increasing with number of alkyl groups and chain lengths—whereas quinone was not; this striking fact may perhaps be interpreted to mean that aromaticity is integral for small-molecule salting-in by NR_4^+ salts. Deno & Spink[222] found that NMe_4Br salted in benzene, tetralin and diphenylmethane, and that benzene was also salted-in by NEt_4Br and NPr_4Br. Bergen & Long[223] measured solubilities for several acidic and basic benzene derivatives (salicylic acid, phthalic acid, benzoic acid, phenol, benzene, aniline, benzylamine, piperidine) in solutions of four different QA salts (NMe_4Br, NEt_4Br, NPr_4Br, and NMe_3PhBr where Ph = phenyl). Salting-in was observed in all cases and was more prominent for the larger cations, except in benzylamine and piperidine, where the effect was weaker and the ordering was more convoluted. Desnoyers et al.[224] carried out an extensive study of the solubility of benzene in solutions of tetraalkylammonium and other ammonium salts, mainly finding that larger QA and longer-chain primary ammonium salts salted-in the nonpolar molecule more effectively. The number of *n*-Pr substitutions was also examined, finding that the Setschenow salting-in constants roughly doubled with each additional substitution on the ammonium cation.

In the opinion of Conway et al.,[225] however, using aromatic compounds for nonpolar solubility studies is inadvisable because of the complications of potential π-water interactions. For this reason, they investigated the solubility of argon (Ar) as a better inert, ideal and spherical nonpolar solute in solutions of different QA salts. Most surprisingly, it was found that the larger tetraalkylammonium bromides in particular salted-out Ar dramatically, but nonmonotonically reverted to salting-in at high concentrations. Wen & Hung[226] investigated the water solubility of a series of small hydrocarbons (methane through butane) in solutions of NR_4Br salts (spanning R = Me to *n*-Bu) and $N(C_2H_4OH)_4Br$. The results were once again rather complex; the hydrocarbons were generally salted-in by the larger QA salts, more significantly

at higher temperatures. Smaller hydrocarbons were salted-in less effectively, and at low temperatures (5°C) CH_4 was observed to be salted-in by low concentrations of NBu_4Br but salted-out by higher concentrations.

Where QA salts are included in Hofmeister series for macromolecule systems, it is likely that the cited source traces to the work of von Hippel and coworkers, who in several of their 1960's studies had the insight to include some QA salts alongside metal cation salts. In 1962 and 1963, von Hippel & Wong[34,35,227] studied the effects of various salts on the kinetics and transition temperature of the random-coil gelatin to helical collagen transition using optical rotation measurements, and included ammonium and several tetraalkylammonium salts. They observed a complex pattern amongst QA cations (albeit without keeping the anion sufficiently constant in all cases for proper control), whereby NMe_4^+ increased the transition temperature (i.e., salted-out), whereas NH_4^+, NEt_4^+, NPr_4^+, NBu_4^+ lowered it (with the latter two, in fact, no transition could be observed within the tested range). Von Hippel & Wong[36,37] later studied the melting/unfolding transition of ribonuclease, and again included QA salts in their survey. Similarly, they found increasing alkyl chain lengths brought about destabilization, salting-in in the order $NMe_4^+ < NEt_4^+ < NPr_4^+ < NBu_4^+$, whereas NMe_4^+ and NH_4^+ were ranked more stabilizing than strongly-hydrated metal cations Li^+ and Ca^{2+}. They mainly tested the Br^- salts for the QA series, though included NMe_4Cl, from which they argued that cation and anion effects were roughly additive. The assigned contribution of the Br^- ion from other measurements was subtracted from each QA salt in order to isolate the cation portion, which were then compared to the effects of several small alcohols, inspired by previous work on ribonuclease.[228] Von Hippel & Wong tested ethylene glycol, methanol, ethanol and 1-propanol and found that the denaturant effect increased in this order and was roughly linear with alcohol concentration. By assigning 'effective number of methylene groups' for each alcohol and to QA cations with the equivalent number of alkyl groups (i.e., one-fourth the concentration of the alcohol), they presented an argument that the melting-point lowering effect of both substances reflected the property of the alkyl chains. Both their inclusion of and proposed explanation for the effects of especially the larger QA cations is undoubtedly rooted in the work of Frank & Evans[229] who put forward large QA cations as noteworthy substrates for their conception of large, ordered clathrate-like 'iceberg' structures in water around hydrophobic solutes, which may be interpreted as a driver of excluded-volume related salting-out effects.

Another one of the few noteworthy studies of QA cation Hofmeister effects is by Jain & Ahluwalia,[230] who in 1996 studied the thermal denaturation temperature of lysozyme in

presence of a set of QA salts with varying chain lengths and anions using differential scanning calorimetry (DSC). Amongst the salts tested, longer-chain QA cation salts were found to lower the transition temperature more, and the lowering was monotonic for most salts. Br^- salts (which were the majority of the salts tested) produced the more significant effects, and NMe_4^+ and NH_4^+ chlorides were generally the least denaturing salts and exhibited nonmonotonic behavior, whereby they lowered the transition temperature at lower concentrations but raised it at higher concentrations (and caused precipitation at highest concentrations). Jain & Ahluwalia made a remark similar to von Hippel & Wong,[37] that additional methylene groups farther from the central nitrogen (e.g., going from NPr_4^+ to NBu_4^+) has a greater effect than methylene groups closer to the nitrogen atom.

It is clear the QA cations have unique properties and that their very sparse presence in studies shows that the far weakly-hydrated side of Hofmeister cations has been neglected in the modern era of research. The hydration and solution dynamics of these ions has also attracted interest, though remains needing further study. As mentioned, in the early hydration theories these ions were regarded as examples of hydrophobic hydration within cage-like water structures—the Frank & Evans 'iceberg' hypothesis.[229,231] Although strict, literal interpretations of the ice-like quasi-crystallization of water around large solutes has fallen in and out of favor, the hypothesis is not utterly without basis; the hydration entropies of QA salts are very negative and decrease with the size of the cation.[232,233]

A striking property of QA salts was discovered in about the same time as Frank & Evans'[229] proposition: the larger QA halide salts (NBu_4^+ and $N(i\text{-Pe})_4^+$ salts, where *i*-Pe = isopentyl group) were discovered to form 'high hydrates'—crystalline hydrates with number of hydration waters as high as 60 and melting points lying in 3 – 60°C.[234] Several stable hydrates with various hydration water numbers for different salts were identified. Later, McMullan & Jeffrey[235–240] also obtained crystalline hydrates of tetraalkylphosphonium and trialkylsulfonium salts, and characterized a substantial number of tetraalkylammonium salt (mainly NBu_4^+ and $N(i\text{-Pe})_4^+$) hydrates, determining melting-points, hydration numbers and crystal structures using X-ray diffraction. They found that the lattice structures were generally tetragonal, orthorhombic or cubic, although the vast diversity of clathrate hydrates possible (and polymorphism amongst known structures) complicates matters. They posited that these hydrates were indeed of 'clathrate' type, analogous in structural and chemical features to gas clathrate hydrates known for many small gas molecules (where molecules of gas reside in cells inside an ice-like lattice[241]. Later, Wen and coworkers[242,243] studied different properties of the

aqueous and clathrate hydrate forms of the QA salts, aiming to relate solution properties to broader ion-solvation models and clathrate formation tendency; for instance, a minimum in the partial molar volume of NBu_4Br was observed, at a cation-to-water mole ratio of ~1:60, that was apparent at lower temperatures but diminished above 35°C, and was not observed for several salts for which no clathrate hydrate had been isolated. This was interpreted by Wen as indicating that the solvation of these ions had characteristics of pre-organization for clathrate-type structuring, thus qualitatively supporting the 'iceberg' model of their hydration.

* * *

The study of the Hofmeister effects of QA cations is important not only because it provides a better understanding of the full scope of cation-specific Hofmeister effects, but also because QA motifs exist in biological systems already, and their physicochemical properties are not well understood. QA centers are indeed not hard to find in both small and large biomolecules—for example, in the essential nutrient choline and its many derivatives across biochemistry including the neurotransmitter acetylcholine, in the head-groups of choline phospholipids, and in the structure of the betaine class of osmolytes. In a 1994 study, Nair et al.[244] determined that the $-NMe_3^+$ substituent on an acetylcholinesterase inhibitor interacted with a tryptophane residue; the specific ion properties of QA groups are, thus, already utilized by biology. The tetraalkylammonium cations also exhibit physiological activity;[245] they are generally toxic, and tetraethylammonium and tetrabutylammonium specifically are potent inhibitors of some cation channel proteins,[246–249] but the reason is not well understood. This is all to say that nature already uses greasy, hydrophobic cation centers, and thus it is one of the motivations and goals of the present study to contribute to our understanding of this unique class of cations.

Chapter 2 – Materials and Methods

2.1 Materials

2.1.1 Salts

All salts were purchased from Sigma-Aldrich, the majority having purities ≥ 99%, except for tetrapropylammonium chloride (98%), tetrabutylammonium chloride (≥ 97%), and 2,2-dimethyl-2-silapentane-5-sulfonate sodium salt (DSS) (97%).

Salts were used as received without further purification, except for tetrapropylammonium chloride, which was found to have a small amount of water-insoluble additive. Before use, stock solutions of tetrapropylammonium chloride (initially having a slight turbidity) were filtered through 0.2 μm cellulose acetate syringe filters (Sartorius Minisart®). Before use, the syringe filters were rinsed several times with a few milliliters of deionized water and air was pushed through between rinses. A small amount of sample solution was also used for rinsing before filtering the rest through the syringe filter. Filtered solutions were perfectly clear in appearance, as expected.

2.1.2 Polymers

All polymer samples were lyophilized according to the procedure detailed in the section below (2.2) before usage.

Poly(*N*-isopropylacrylamide) (PNIPAM) used for LCST measurements was purchased from Polymer Source Inc., with reported number average molecular mass of 118,500 Da and polydispersity index (PDI) of 2.16 (determined via gel permeation chromatography). PNIPAM used for all other measurements (ATR-FTIR spectroscopy, ^{1}H-NMR spectroscopy) and the initial LCST test measurements was purchased from Sigma Aldrich, with reported number average molecular mass of 85,000 Da (from certificate of analysis for specific batch: 71,262 Da) and PDI of 1.5 (specific batch).

Poly(*N,N*-diethylacrylamide) (PDEA) was purchased from Polymer Source Inc., with reported number average molecular mass of 55,000 Da and PDI of 1.16.

Poly(ethylene oxide) (PEO) was purchased from Acros Organics, with reported molecular mass of 250,000 – 400,00 Da. Specific batch molecular mass and PDI were not included.

Poly(*N,N*-dimethylacrylamide) (PDMA) was purchased from Polymer Source Inc., with reported number average molecular mass of 85,500 Da and PDI of 1.45.

2.2 Lyophilization of Polymer Samples

Stock solutions of the polymers were prepared by weighing the appropriate mass of solid material into a volumetric flask and dissolving fully in deionized water to target solution volume. Solutions were homogenized thoroughly by use of a vortex mixer and then refrigerated at least six hours, with additional intermittent mixing where necessary, to ensure complete dissolution. Aliquots of required volume (based on mass of polymer desired in final sample) were carefully transferred to the bottom of a 2 mL Eppendorf tubes/microtubes by means of a micropipette and then sealed with a punctured tube cap, as shown below in Figure 7 (these punctured caps were kept separate for each polymer type).

Figure 7: Polymer samples before and after lyophilization. Left: 2 mL Eppendorf tube closed with punctured cap for freezing in liquid nitrogen and subsequent drying under vacuum. Right: sample removed from vacuum and closed with original cap. Lyophilized polymer can be seen as small amount of solid at the bottom of the tube.

The closed tubes were then frozen in liquid nitrogen for several minutes. The samples were then placed in a desiccator chamber connected to a vacuum pump and completely dried under continuous vacuum for at least eight hours (see Figure 8 for the set-up). Afterwards, they were removed and closed with original (non-punctured) tube caps and stored in the refrigerator until usage. To prepare any particular sample, the freeze-dried solid polymer samples were re-dissolved in their Eppendorf tube by addition of relevant solution and homogenized thoroughly by vortex mixer.

Figure 8: The vacuum set-up used for polymer lyophilization consisting of vacuum pump, connection and desiccator chamber. The desiccator chamber was ensured a tight seal by frequent application of vacuum grease to the chamber and lid lips.

2.3 LCST Measurements

Lower critical solution temperature (LCST) measurements were made at minimum in triplicate, using samples (as solutions in deionized water, unless specified otherwise) injected into fine capillary tubes. Measurements were carried out using an OptiMelt MPA100 instrument (Stanford Research Systems, see Figure 9 below for frontal view). The instrument records frequent camera images and scattering vs. temperature data during measurement which was accessed and controlled through its MeltView 2.0.7 software (see Figure 10 for screenshots from the program window). Temperatures were always ramped at a rate of 1°C during measurements.

Below the LCST point, thermoresponsive polymer samples are clear and homogeneous solutions with low scattering intensities that remain largely constant with temperature. At the LCST transition, there is a sharp increase in scattering and noticeable opacity increase, which rises further until a limit. Macroscopically, the transition is visually observed as a cloud point (i.e., appearance of cloudy turbidity; see Figure 10 for an example of the view from the instrument camera before and after the transition). LCST points were defined and taken as the onset of the rise in detected scattering, approximated as the intersection points of the linearized curves before and during the transition (depicted in Figure 11).

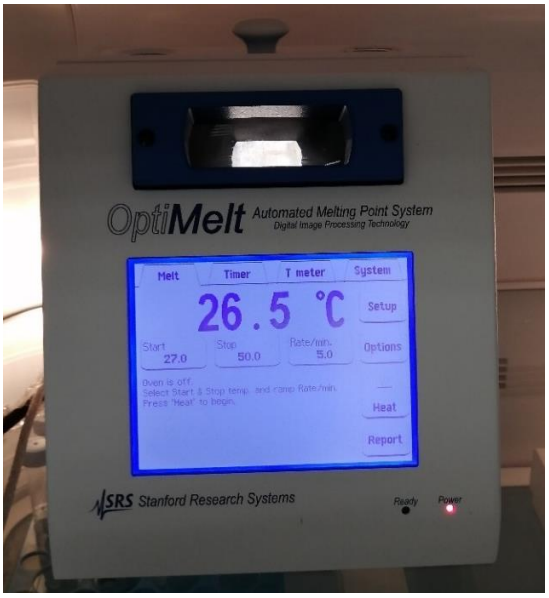

Figure 9: OptiMelt instrument, frontal view. The instrument was placed inside the refrigerator or freezer during operation.

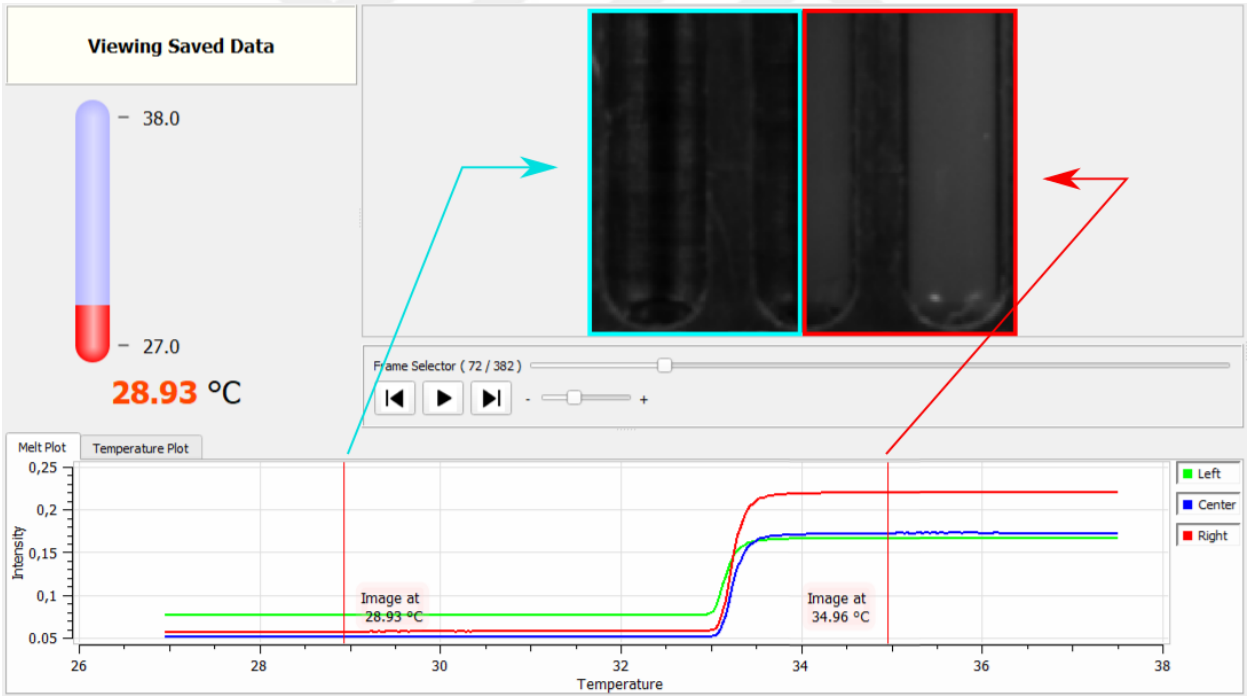

Figure 10: MeltView window showing scattering intensity vs. temperature plot and camera view, split in half to show typical camera images of samples below (left; translucent capillaries) and above (right; opaque capillaries) the LCST phase transition.

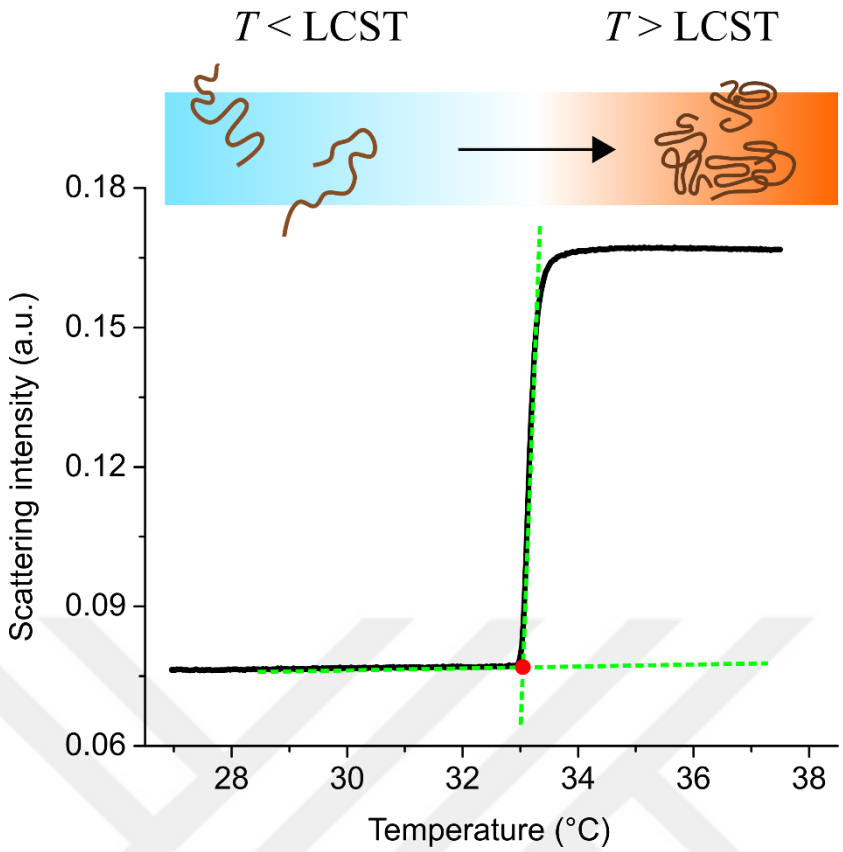

Figure 11: Representative scattering intensity vs. temperature plot for PNIPAM in neat water, with tangent lines to the curve before and after the LCST onset drawn. The point of intersection (red dot) is taken as the LCST point of onset. Top illustration schematically depicts the transformation of the polymer from a random coil (T < LCST) to aggregated globules (T > LCST) state through hydrophobic collapse, resulting in intra- and interchain interactions at and above the LCST temperature.

LCST – cosolute concentration curves were fit using OriginLab 2016 nonlinear function fitting with Levenburg-Marquadt iteration algorithm. Where necessary, bounds were imposed on certain parameters to obtain physically meaningful fit values. Additional specific considerations regarding the fitting process are discussed in the related section (3.2.1).

2.4 ATR-FTIR Spectroscopy Measurements

Attenuated total reflectance Fourier transform infrared spectroscopy (ATR-FTIR) measurements were conducted using a Bruker ALPHA FTIR spectrometer, equipped with a Platinum ATR module (which contains a monolithic diamond crystal soldered into tungsten carbide and a rotatable arm for securing samples), pictured below in Figure 12a. The instrument was used in conjunction with a custom temperature control set-up consisting of a water-circulator (CLRC-05C, CLS Scientific), connected via tubing to a cylindrical metal head-piece, to control and regulate the temperature of the spectrometer plate, ATR crystal and sample. During measurements, the circulator head was fixed over the plate by means of the rotatable arm, and the opening was covered with a cap for minimal air contact (see Figure 12b). The circulator head does not come into contact with the crystal directly or with the liquid sample after delivery (see Figure 12c), but is in contact with the metal ATR plate. The circulator was run in this position for at least 2 hours prior to measurements to ensure the instrument temperature was stabilized at the desired value. The CLRC-05C circulator is able to maintain both cold and hot temperatures, and thus was used for both cooling below and heating above the LCST of particular samples, as specified in further detail in subsequent sections.

ATR-FTIR spectra were obtained from 50 μL liquid samples prepared in D_2O, at 2 cm^{-1} resolution in the region 400 – 4000 cm^{-1} from the average of 32 scans and with frequent background spectrum measurement, as well as automatic atmospheric compensation. Data acquisition was managed through the instrumental software OPUS 7.2, but all further analysis and processing of spectra were performed in OriginLab 2016.

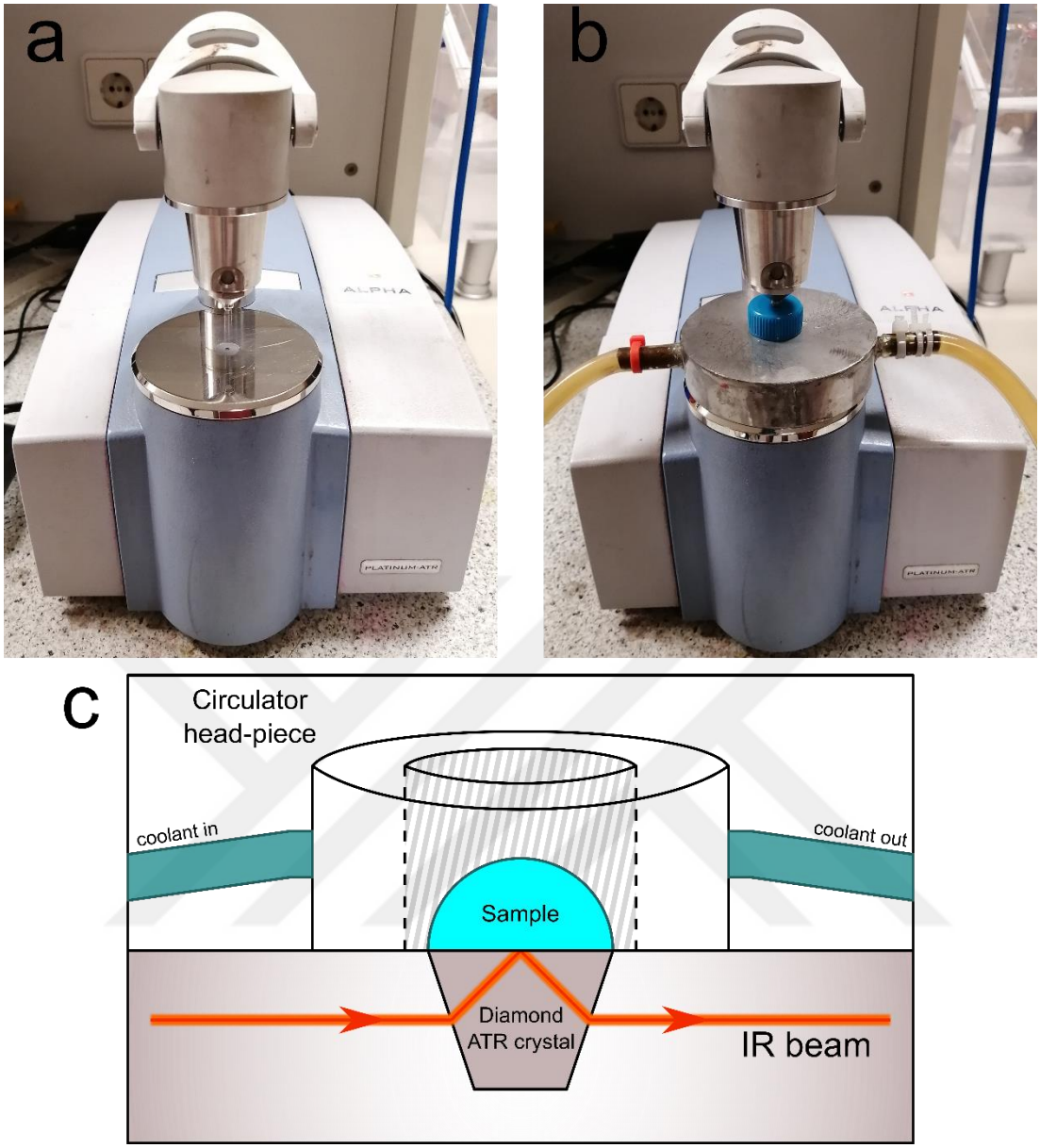

Figure 12: (a) ATR-FTIR spectrometer used for measurements. (b) Spectrometer with water circulator head secured in place. (c) Schematic representation of temperature-controlled ATR-FTIR set-up. The circulator fluid flows through the cylindrical head, which thus regulates the temperature of the ATR crystal and sample via conduction through the metal plate.

2.5 ^{1}H-NMR Spectroscopy Measurements

^{1}H-NMR measurements were conducted using a Bruker AVANCE III 400 MHz spectrometer at ambient/room temperature. Samples were prepared in D_2O as solvent and measured in SP Wilmad-LabGlass 5 mm thin-walled precision 7″ NMR tubes, fitted with SP Wilmad-LabGlass coaxial inserts for external chemical shift referencing (to 2,2-dimethyl-2-silapentane-5-sulfonate sodium salt (DSS) in D_2O solvent). The reference solution was always contained in the inner insert tube and the measurement sample in the outer tube, as shown below in Figure 13. The two solutions were thus measured together simultaneously without any physical or chemical contact. Sample and reference solutions were prepared such that the height of both solutions in the fitted ensemble were ~5 cm, thus matching the measurement range of the spectrometer detector coils. NMR spectra were obtained from the average of 32 scans. Standard procedures, such as solvent deuterium-signal locking, shimming (for Z, Z^2 and Z^3 shim magnets, primarily), and automatic tune matching were completed in full before every measurement. Details of the NMR data analysis and processing that were employed are given in section 3.1.1.

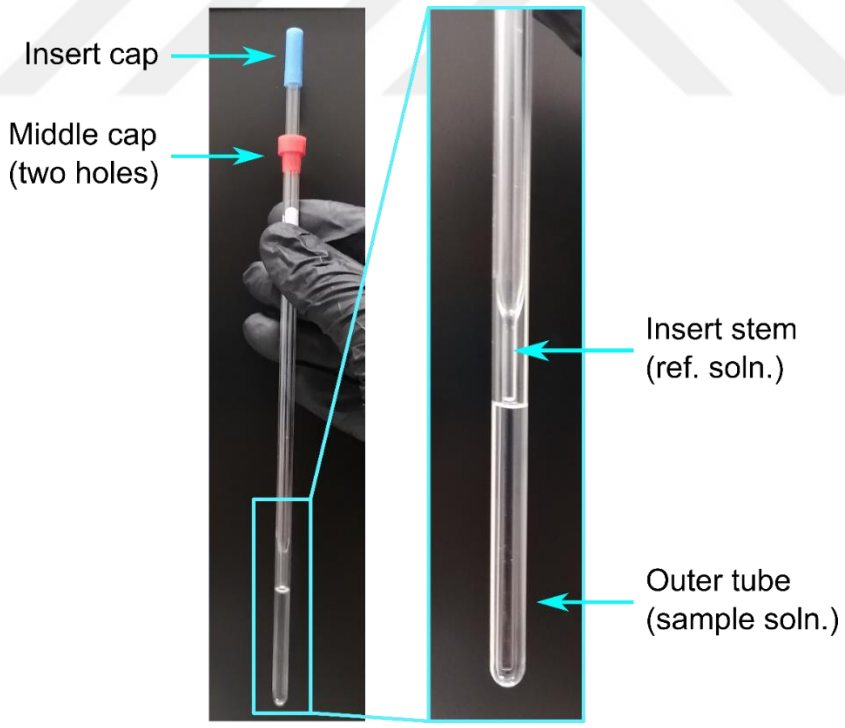

Figure 13: 7″ 5 mm outer NMR tube (containing the sample to be measured) fitted with inner coaxial insert (containing chemical shift reference solution), and close-up view. The insert stem has a length of 50 mm, outer diameter of 2 mm and inner volume of 60 µL. The outer tube has a sample volume of 530 µL once fitted with the coaxial insert.

Chapter 3 – Results

3.1 Development of a Methodology for Characterizing Ion-Macromolecule Interactions Using ^{1}H-NMR Spectroscopy

As the first step of the project, it was necessary to develop the necessary methodology based on quantitative, externally referenced ^{1}H-NMR spectroscopy to characterize ion-macromolecule interactions in solution. NMR spectroscopy has found prominent use in generating both qualitative and quantitative evidence for specific ion effects in the bulk solution and interactions at macromolecular interfaces,[88–90,111,112,126,233] as described previously in Chapter 1 – Introduction. Our aim here is to quantitatively characterize the site-specific binding behavior of an interacting ion with a model macromolecule and to distinguish it from a non-interacting ion. For the salts, we chose NaSCN and NaCl as our non-binding and binding test cosolutes, respectively. NaCl is very commonly regarded as a neutral midpoint of Hofmeister salts, and studies have shown that neither Na^{+} cation nor Cl^{-} exhibit any significant binding to neutral macromolecules in aqueous solution, and the net effect manifested by the salt is a moderate salting-out.[1,9,10,16] SCN^{-} anion, on the other hand is amongst the classical binding weakly-hydrated Hofmeister anions, showing affinity for neutral small and macromolecules as well as charged solutes.

The experiments were performed with poly(*N*-isopropylacrylamide) (PNIPAM) as the model macromolecule. As discussed before, PNIPAM is one of the most well-studied and frequently used thermoresponsive polymers in the Hofmeister literature, and is frequently used a simplified, neutral model for more complicated polymers.[98,99] Although not directly relevant to the solution-phase NMR study in this section, the thermoresponsive behavior of the polymer is also analogous to the cold denaturation of proteins and is an invaluable tool to gain thermodynamic information about the macromolecular and interfacial dynamics in solution. Thus, PNIPAM is the principal model polymer used predominantly in our studies herein before testing with other polymers, as described in section 3.3.

3.1.1 ^{1}H-NMR Data Processing

The instrumental and measurement specifics of ^{1}H-NMR spectroscopy employed were described in section 2.5. The measurement operations were managed through the instrumental Bruker TopSpin 2.1 software interface. The initial processing for the data were also performed via this program. Namely, after the acquisition of the 'raw' ^{1}H-NMR spectrum in the form of a

‘free induction decay’ (FID) waveform in the time domain, a Fourier transform was performed on the data to obtain the spectrum in the frequency domain. Afterwards, an initial phase correction was applied using the automated commands available within TopSpin, followed by exponential windowing (multiplication by an exponential function) to improve signal-to-noise and resolution. Then, a baseline correction was done through the TopSpin command and the results inspected. It was often necessary to iteratively perform additional cycles of phase and baseline corrections at this point to achieve better spectral lineshapes.

Typically, additional manual correction and processing of the spectra are necessary after the automated functions performed in TopSpin, and these were carried out alongside general spectrum manipulations and formatting in the program MestreNova v6.0.2. By inspection, semi-manual baseline corrections were applied if the spectrum baseline appeared distorted upon high magnification. For this purpose, Whittaker smoother function with filter frequency set manually (typically to ~100 Hz) was usually preferred due to it giving the best results for most spectra—however, each spectrum was best corrected by inspection; so, other baseline corrections (e.g., polynomial, Bernstein polynomial) were occasionally utilized. Baseline distortions, if present, were typically broad features (spanning >1 ppm) with intensities < 5% of typical sample signals and thus did not noticeably affect peak positions.

Then, further phase corrections were performed if deemed necessary by inspection. In the ideal case, all NMR resonances should appear positively-phased, sharp and having symmetrical, flat tail-ends on both sides. If an asymmetry or distortion was observed, zeroth order and first order phase corrections were performed manually according to the largest peak in the spectral region as reference, or according to multiple peaks in the case of complicated spectra with large signals lying in the middle frequencies. MestreNova’s built-in automatic phase correction algorithms were also occasionally used (‘Global’, ‘Selective’, ‘Metabonomics’ or a combination thereof) if a minor touch-up of the spectrum phases appeared sufficient.

The fully corrected spectra were then chemical shift referenced to the DSS main reference signal, set by convention to 0.0 ppm. This large signal arises from the three Si-bonded methyl groups on the DSS molecule, and is a sharp, highly shielded (low chemical shift) singlet resonance that can be conveniently identified and referenced without interference. In some cases, slight distortions near the peak apex could be observed and could not be sufficiently eliminated through rigorous shimming, exponential window multiplication or phase

corrections. These were likely due to instrumental fluctuations or magnetic drift effects that could not be corrected for by routine shimming and would require deep recalibration of all shim magnets by a technician. Although the effect of such small features should be minor, to best account for any error that may be introduced the weighted average of the main peak position and any small 'shoulder' deviations were calculated and taken as the reference point. This is illustrated by the representative peak shape shown in Figure 14a.

Unlike the resonances exhibited by small solute molecules, the NMR signals generated by large, less mobile species in solution such as polymers appear as broad bands. In this case, the chemical shift assigned to such signals is best defined as the peak apex point, but may not be sufficiently precise when determined automatically or by hand during data processing, as is commonly done for small molecules. Furthermore, due to the broadness of such polymer signals, small levels of spectral noise not relevant for sharper signals may coincide and convolute the peak apex region. To ensure robustness and maximum precision, polymer bands were analyzed separately in OriginLab. A Savitzky-Golay smoothing function ('points of window' parameter set manually, typically ~50 pts[*]) was applied to each band to attenuate the effects of noise. Then, a horizontal intersection line was drawn at a height between the half-maximum and the full-maximum, and the peak apex position was taken as the average of the two (left and right) intersection points, thus obtaining a symmetrical best estimate for the peak position. The methodology is illustrated below in Figure 14b. Overall, although one can argue that there is a measure of 'subjectiveness' in the various corrections by inspection, in a 'blind' repeated processing of the same spectrum twice, the final peak positions agreed within ~0.0001 ppm (i.e., ~1% of typical differences between samples). Additionally, in an alternative method, the bands were fit to a Gaussian function within appropriate bounds, which determined peak (center) positions that agreed with those from the intersection method within ~0.0001 ppm. Thus, it can be concluded that the data processing methodology employed was largely systematic and consistent.

[*] We tested various smoothing parameters (5 – 120 pts) and saw that ~50 pts was approximately the smallest smoothing window that could eliminate the effects of random noise. A smoothing window greater than ~90 pts resulted in visible deviation from spectral line shape, for instance in the maximum intensity of the peak.

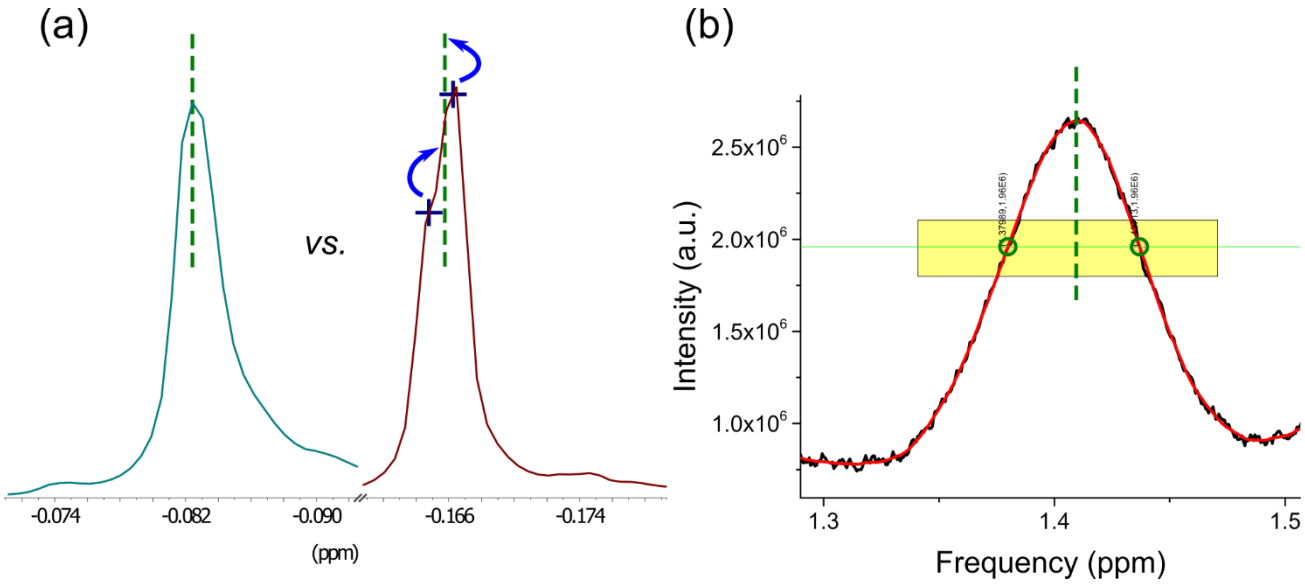

Figure 14: (a) Two examples of the DSS reference signal, zoomed in and scaled to the same intensity for comparison. The left signal is an example having very good spectral line shape. Its apex point is readily apparent. The right signal has a small amount of distortion, where a portion of the signal has shifted and formed a 'shoulder'. To account for this small effect, the weighted average of the estimated peak positions was taken as the 'true' position of the signal before setting it to 0 ppm. (b) A snapshot from OriginLab representative of polymer band processing. The 32-scan spectrum (black) is first smoothed (red) and intersected with a horizontal line (green) close to the apex. The best estimate for the peak position is then taken as the average of the two intersection points between the line and the smoothed band curve.

3.1.2 ^{1}H-NMR Spectrum of PNIPAM

Figure 15 below depicts a representative ^{1}H-NMR spectrum obtained for a sample containing 3.3 mg/mL PNIPAM in neat D_2O solvent, externally referenced to DSS in D_2O according to the measurement procedure described in section 2.5. Several characteristic peaks belonging to different species are clearly visible and merit an overview here. First, note that four of the resonances that appear in the spectrum belong to the DSS reference molecule, whose structure is also included, inset in Figure 15 below the spectrum. As mentioned in the previous section, the sharp, singlet reference peak (set to 0.0 ppm) corresponds to the set of nine terminal -CH_3 hydrogens on the Si atom. There are three additional multiplet signals that DSS generates, corresponding to the three backbone methylene positions, and these are also marked on the molecule and the spectrum. The highest chemical shift multiplet (3), at ~2.90 ppm, corresponds to the methylene closest to the electron-withdrawing sulfonate end-group, which causes this deshielding effect inductively. Multiplet (2) appears at a lower chemical shift (~1.75 ppm) due

to its additional distance from the sulfonate group, and multiplet (1) at a lower chemical shift still (~0.624 – 0.625 ppm), due to being farthest from the sulfonate and closest to the Si atom, which imparts a small shielding effect due to its lower electronegativity.

Secondly, we may notice that two relatively large, broad singlet-like peaks appear at ~4.5 – 5.0 ppm. These peaks originate from the small amount of exchangeable hydrogen (protium, ^{1}H) contamination in the solution environment; this contamination is inevitably present at a low level in all deuterated protic solvents or is otherwise gradually picked up from the air or surface contact during sample preparation. In the present case, a significant source of ^{1}H contamination is the polymer itself, due to the protic amide -NH moiety. These exchangeable H's are rapidly dispersed in the solution upon dissolution in D_2O, although interestingly it was rarely observed that a small broad feature at ~7.5 ppm was visible in the spectra of very freshly-prepared samples, likely originating from some residual unexchanged -NH groups.

The neat D_2O water (HDO) peak appears at 4.8 ppm.[250] However, the presence of solutes affects the chemical and magnetic environment of the solvent molecules and thus shifts the water peak. In the PNIPAM/neat D_2O spectrum depicted in Figure 15, the sample HDO peak appears at ~4.78 ppm, however the water peak is generally shifted further (to lower chemical shifts) in salt-containing samples, as will be seen shortly. The reference solution HDO peak is constant (unless the solution concentration is changed) and appears at ~4.75 ppm.

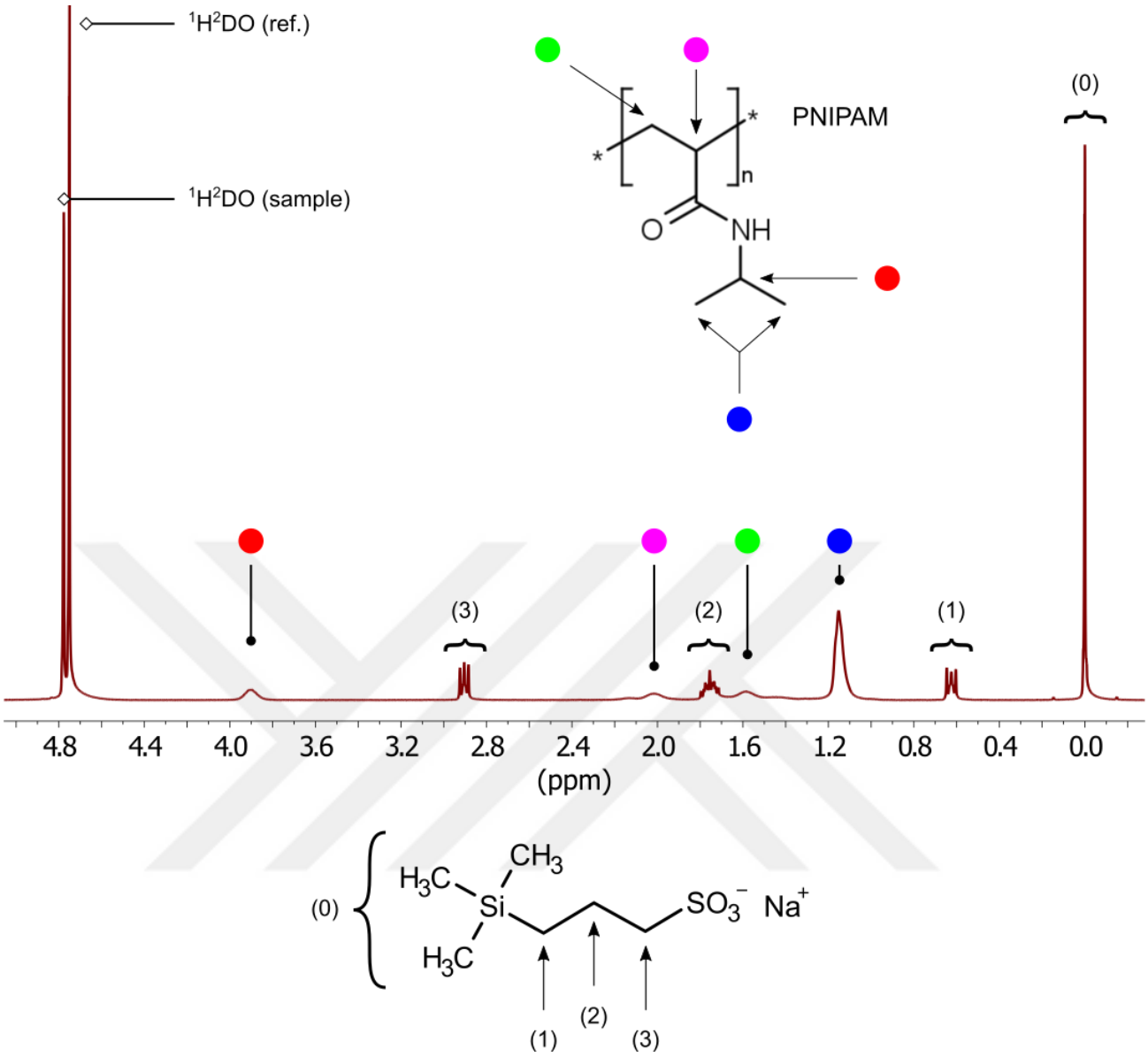

Figure 15: A representative ^{1}H-NMR spectrum obtained for a sample of PNIPAM in neat D_2O, externally referenced to DSS. Note that signals corresponding to the polymer, DSS and water H-contaminant are all present. The structure of PNIPAM is included near the top with color-coded annotations for its four signals. The bottom shows the structure of DSS and numbers the four sets of H's that give rise to the four resonances, labeled likewise in the spectrum. The two water peaks (HDO in sample, HDO in reference solution) are also indicated on the spectrum. Specific peak positions are given in the text.

Finally, we can observe that the polymer PNIPAM gives rise to four distinctive bands. Peak assignments can readily be found in the literature,[250–252] and will be briefly discussed here. In neat D_2O solvent, the lowest chemical shift signal at ~1.15 ppm (blue circle in Figure 15) is also the largest, and corresponds to the six *i*-Pr terminal methyl hydrogens. The hydrogens are

in the most hydrophobic local environment and, relatedly, are the farthest away from electronegative groups. The next highest chemical shift signal appearing at ~1.58 ppm (green circle) is a smaller band corresponding to the backbone methylene (-CH_2) group, which is also relatively far from the influence of electronegative groups. The signal corresponding to the position alpha to the amide carbonyl (backbone -CH-, magenta circle) appears slightly higher at ~2.02 ppm owing to its proximity to the electron-withdrawing carbonyl group. The highest chemical shift polymer signal belongs to the -CH- group connected to the amide N-atom (red circle; hereon frequently abbreviated to N-CH) and appears at ~3.90 ppm.

3.1.3 NMR Titrations with NaCl and NaSCN: Evidence for SCN^- Binding

To test that our methodology for quantitative ^{1}H-NMR spectroscopy is able to characterize ion-specific interactions with PNIPAM, we conducted NMR titrations of 3.3 mg/mL PNIPAM with solutions of NaCl and NaSCN in D_2O solvent. That is, incremental concentrations of each salt solution were used as the solvent in PNIPAM samples, and the changes in the chemical shifts with salt concentration were tracked. The results from our measurements are shown below in Figure 16, which plots the change in chemical shift ($\Delta\delta_H$) for each polymer signal against the concentration of NaCl and NaSCN. The same color-coded labels for polymer positions as Figure 15 is used.

Notice that for both salts, the chemical shift vs. concentration curves for most positions is an entirely linear, monotonic decrease. For NaCl, this is the case for all polymer signals but, strikingly, for NaSCN the backbone α-position -CH- curve (Figure 16b) exhibits an obvious, significant nonlinearity. At lower concentrations there appears to be a positive (chemical shift increase) contribution, that levels off and is dominated by the negative (chemical shift decrease) contribution at higher concentrations.

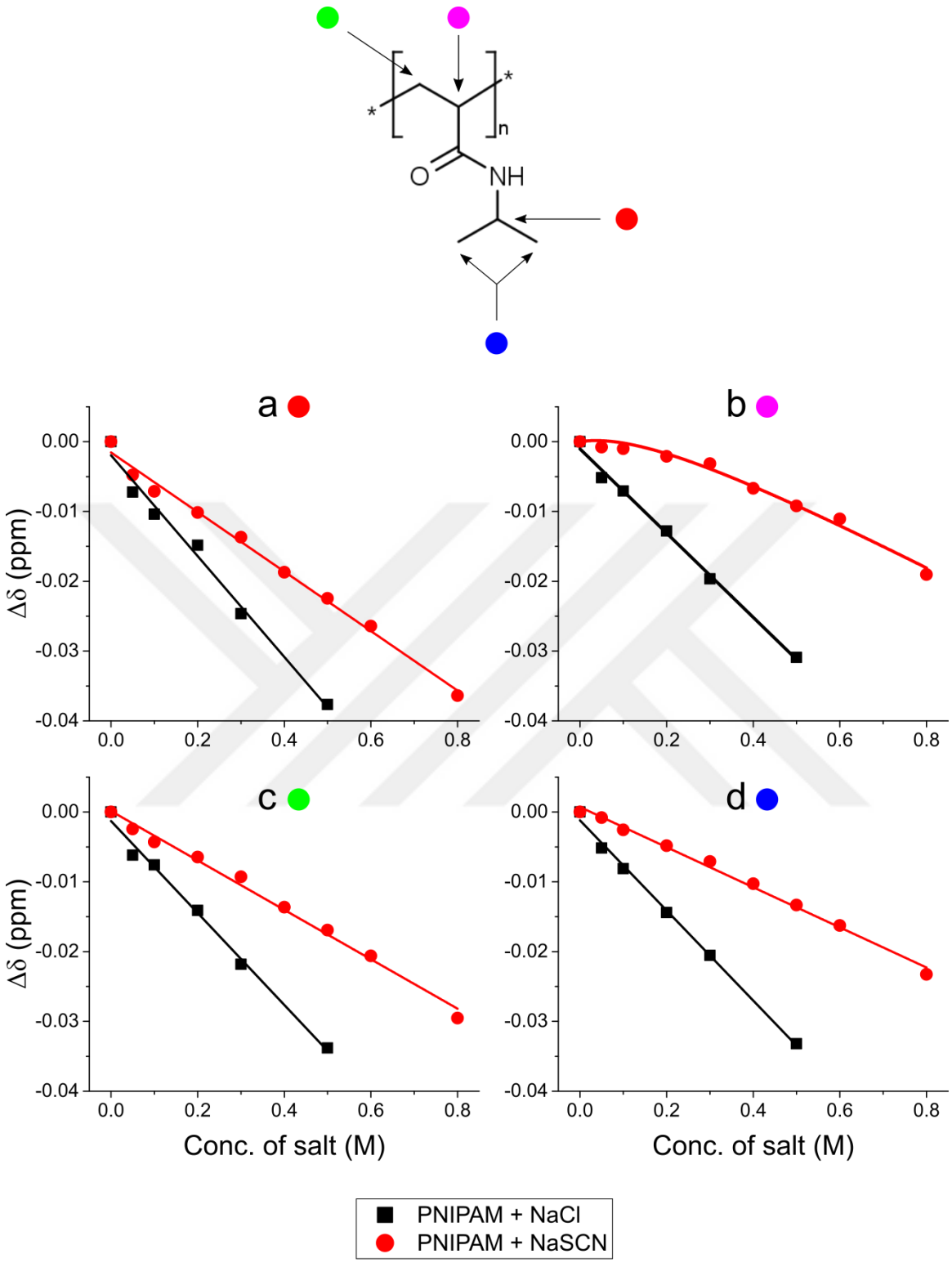

Figure 16: Results of ^{1}H-NMR titrations of PNIPAM with NaCl and NaSCN solutions in D_2O. Top: structure of PNIPAM with color-coded position labels. Panels depict change in chemical shift vs. concentration of NaCl and NaSCN for: (a) the N-CH group, (b) the backbone -CH- group (alpha position to carbonyl group), (c) the backbone -CH_2- group, (d) *i*-Pr terminal -CH_3 groups. Bottom: legend for all panels (a) – (d).

This is in fact precisely the result that we expect to obtain, in that it is indicative of the binding of SCN^-. As discussed previously, a very similar methodology was employed by Cremer and coworkers[111,112] to demonstrate that weakly-hydrated anions preferentially bind to the α-carbon positions of simple polypeptide ELPs as well as the polymer PDEA—the latter is highly similar to our model, PNIPAM. They also reported that the chemical shift changes at most positions is a linear fall (i.e., non-interacting/non-binding) but the singular binding site exhibited a nonlinear response. It is thus possible to interpret the shape of the nonlinear curve as the sum of contributions resulting from a salting-in specific-binding effect and the general salting-out driving force. We can fit the nonlinear chemical shift curve to an equation that captures both effects, as demonstrated before,[111,112] of the following form:

$$\Delta\delta_{\mathrm{H}} = c[\mathrm{M}] + \frac{\Delta\delta_{\max}[\mathrm{M}]}{K_{\mathrm{D}} + [\mathrm{M}]} \qquad (8)^{\dagger}$$

The results of the fitting ($R^2 \approx 0.99$) are as follows: $c \approx -0.034 \pm 0.001$ ppm·M^{-1}; $\Delta\delta_{max}$ (the maximum change in chemical shift, i.e., at saturation) ≈ 0.012 ppm; and finally, K_D (the ion-polymer binding dissociation equilibrium constant) ≈ 0.28 ± 0.06 M. The determined K_D for NaSCN is comparable in magnitude to the one determined for interaction with several different α- sites on ELPs[111] and reasonably similar to the K_D = 0.070 M reported for binding to the PDEA α- position[112]. The level of difference in the values can likely be explained by the difference in the polymers used in the studies, as well as their use of non-deuterated H_2O as solvent.

It is also worth discussing here the specific reason behind the changes in the chemical shifts of various solution species as a function of salt. As mentioned, the hydron chemical shift of water (^1H_2O, $^1H^2DO$ or ^2D_2O) itself exhibits a shift in the presence of salts; this can be understood, principally, as the electronic manifestation of water's coordination environment.[90] Gaseous water molecules exhibit a marked increase in their chemical shift (i.e., deshielding) upon transfer to the liquid phase because they enter a highly coordinated, hydrogen-bonded state, which shifts the electron density around the hydrogen atoms such that the net attenuation of the applied external magnetic field is diminished. As compared to water's self-coordination in the neat liquid, water molecules hydrating ions almost always have a less 'bonded', i.e., partial-covalent/hydrogen-bonded character, and thus the deshielding of the hydrons is partially relaxed, and a net negative chemical shift change (shielding) is observed. It is known that

† This is a restatement of Equation 5 given in section 1.2, with a minor modification to the expression.

anions shift the ^{1}H-NMR signal of water to lower chemical shifts, and due to their domineering effect over cations dictate the net effect of many salts.[253] However, some strongly-hydrated cations may have sufficiently high charge density or complex-forming ability to induce positive chemical shift changes.[253,254] In the present study, both salts indeed demonstrated a very similar linear shielding effect on the water signals, as depicted below in Figure 17 (left panel).

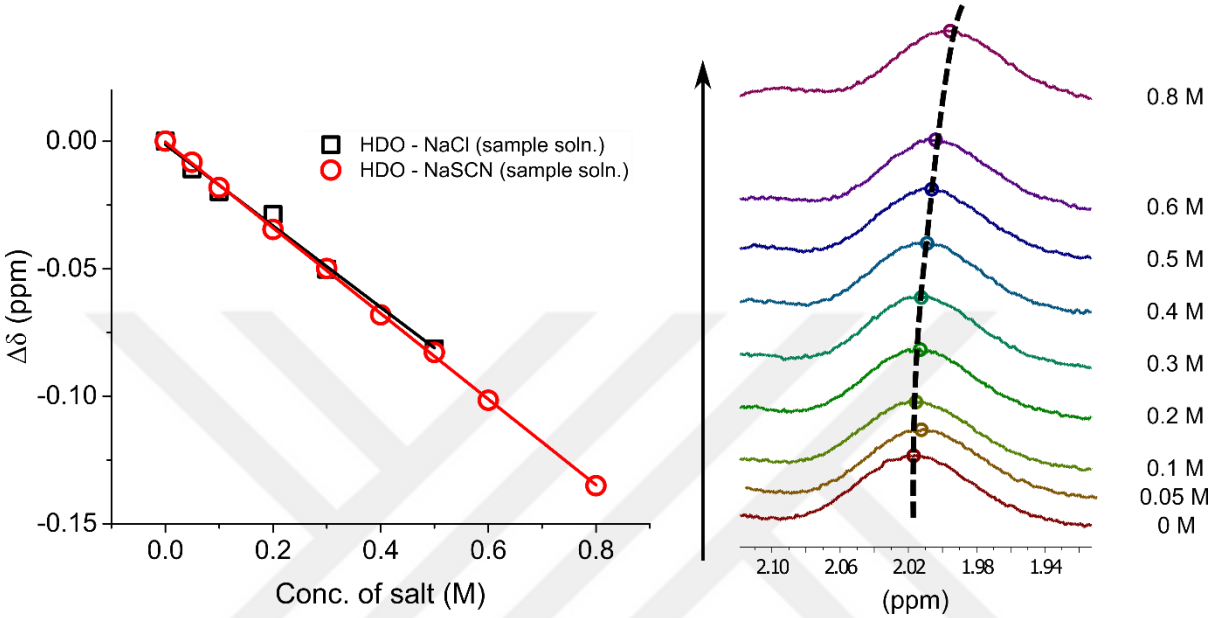

Figure 17: Left: The chemical shift changes observed in the water $^{1}H^{2}DO$ peak (of the sample solution) vs. concentration of NaCl and NaSCN in the sample. Right: The shift of the normalized backbone -CH- signal (originally at ~2.016 ppm, in neat D_2O) with increasing concentrations of NaSCN. Vertical offset of spectra is scaled according to the concentrations given on the right. Approximate peak positions and tracking curve (dashed) are included as guides to the eye.

With regard to the chemical shift effects on polymer signals (as depicted in Figure 17, right panel), the mechanism is putatively very similar. Hydration by water induces a net deshielding effect due to increased polarization of polymer hydrogens, and a negative chemical shift change (i.e., shielding) is contributed with increasing salt concentration due to the weakening of water's ability to preferentially hydrate the polymer. In addition, specific interaction with anions electronically induces a positive chemical shift contribution (i.e., deshielding) from the electrostatics of the interaction. Overall, these effects additively combine into the observed net 'average' as reported by the ^{1}H-NMR signals, and thus elucidate the concentration-dependent dynamics at play—the saturable Langmuir-type binding, and the linear salting-out effect—when investigated by NMR titration.

Having demonstrated that our in-house instrumentation and ^{1}H-NMR methodology could successfully distinguish and quantitatively characterize ion-macromolecule interactions, we were able to proceed to the investigation of the novel effects of the QA salts with confidence. The following sections will describe the multiple experimental approaches employed, and the quantitative ^{1}H-NMR methodology described here is used again in section 3.2.3.

3.2 Hydrophobic Cations: Interactions of Tetraalkylammonium Cations with Macromolecules (PNIPAM)

3.2.1 LCST Measurements: Evidence of a Major Cation-Driven Salting-in Effect

The discussion presented in Chapter 1 – Introduction endeavored to provide the historical and contemporary context for the motivation of the present study. In beginning our studies of the Hofmeister effects of quaternary tetraalkylammonium salts, our first experimental approach was to study their macroscopic thermodynamic effects on our model macromolecular system, the thermoresponsive polymer PNIPAM. Indeed, the original discoveries of specific ion effects traces to their thermodynamic manifestations, namely on the solubilities of proteins as in Franz Hofmeister's seminal studies.[20–22,25] The utility of such macroscopic approaches lies in their function as direct Litmus tests for the overall thermodynamic driving forces that predominate in a given system. In particular, the attractiveness of one such method employed here—phase transition temperature measurements; the lower critical solution temperature (LCST) of thermoresponsive polymers—is its clear, practical and reliable correspondence to the thermodynamic interplay of solution ion-macromolecule interactions. As previous studies have amply exemplified, the straight-forwardness of neutral macromolecule phase transition measurement techniques can provide a coherent route to elucidating molecular-level behavior, without the complications imposed by multidimensionality of protein systems (be it charge/pH considerations or topological complexity) which—although scientifically valuable for study—has much convoluted incremental progress in the long history of Hofmeister effect research.

To this end, LCST measurements of 5 mg/mL PNIPAM‡ were carried out with six salts. As representative controls and to serve as the least weakly-hydrated amongst the salts studied, NaCl and NH_4Cl were included. Both of these salts occupy the weakly-hydrated and (barring some exceptional cases) non-interacting, salting-out class of cations in typical Hofmeister orderings. Then, measurements were extended to four tetraalkylammonium chloride salts with incremental lengthening of their symmetric alkyl chains: NMe_4Cl, NEt_4Cl, $N(n\text{-}Pr)_4Cl$ and $N(n\text{-}Bu)_4Cl$ (hereon, abbreviated to NPr_4Cl and NBu_4Cl). The resulting PNIPAM LCST curves are shown in Figure 18 below.

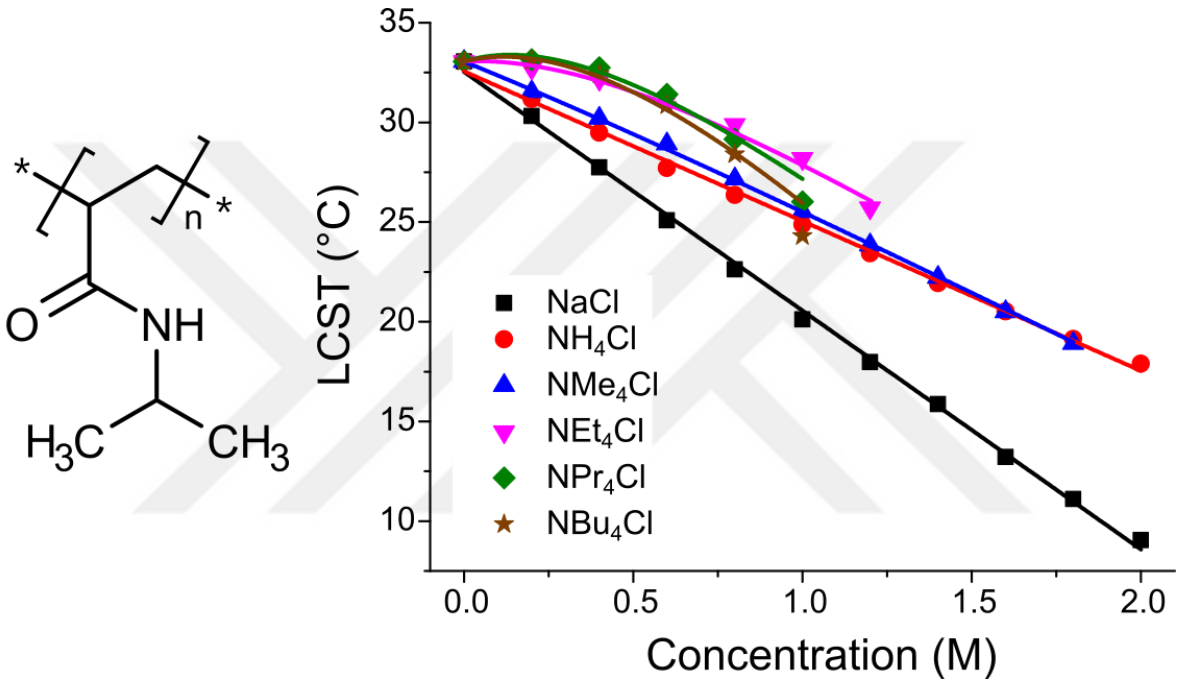

Figure 18: Left: The structure of poly(*N*-isopropylacrylamide) (PNIPAM). Right: fitted lower critical solution temperature (LCST) curves for PNIPAM with varying concentrations of six chloride salts as cosolute in aqueous solution. Error bars, though included, are smaller than the data symbols for all points.

In the absence of salt, the LCST of the PNIPAM is found to be 33.05 °C. As can be seen in the figure, both NaCl and NH_4Cl produce almost entirely linear LCST curves, with a slight curvature at higher salt concentrations. Recalling that this behavior was recently explored for various metal chloride salts by Bruce et al.,[10] the slight upward curvature of the trends can be

‡ As mentioned in section 2.1.2, PNIPAM used for the LCST measurements discussed here was sourced from the vendor Polymer Source Inc. However, LCST measurements were also carried out with PNIPAM purchased from Sigma-Aldrich and qualitatively reproduced largely the same results. These measurements are included in Appendix A: LCST Measurements with Sigma-Aldrich PNIPAM.

readily interpreted as related to solvent-shared ion pairing behavior at higher concentration (in accordance with Equation 7, section 1.3). The smallest tetraalkylammonium salt, NMe_4Cl, exhibits a similarly linear trend with a slope marginally shallower than NH_4Cl's, indicating that NMe_4^+ also predominantly salts-out. Starting with NEt_4Cl, however, the LCST profile changes remarkably: a significant deviation from linearity appears at low (0 – 0.4 M) salt concentrations; that is, the cosolute partially salts-in PNIPAM. Furthermore, it appears that the NPr_4Cl salt affects the LCST of PNIPAM even more strongly, with sharper nonlinearity. The effect is strong enough that the overall behavior becomes nonmonotonic; a local LCST maximum (33.15°C) is attained at 0.2 M NPr_4Cl. The salt of the most hydrophobic, i.e., 'greasiest' cation, NBu_4Cl influences the LCST trend similarly, where once again the nonlinearity is significant enough that an LCST maximum (33.12°C) is attained at 0.2 M salt, and a steeper downward curvature compared to NPr_4Cl is also observed at higher concentrations.

Strikingly, it is evident that the nature of the nonlinear LCST behavior observed for these NR_4Cl salts differs from the known strongly-hydrated cation salting-in effect previously demonstrated for metal salts such as $CaCl_2$, $MgCl_2$ and LiCl.[10] For these metal chloride salts, the initial LCST trend is linear and a deviation—in the form of an upward curvature—is increasingly significant only at higher concentrations. In contrast, these tetraalkylammonium chloride salts produce a nonlinearity in the LCST response dominant at lower concentrations, and appear to shift toward linear salting-out at higher concentrations with a sharp downward trend. This indicates that the salting-in mechanism valid for Ca^{2+}, Mg^{2+} and Li^+ does not hold for chloride salts of tetraalkylammonium cations. On the contrary, the behavior exhibited here is reminiscent to those observed for the sodium salts of weakly-hydrated anions such as I^-, ClO_4^-, or SCN^-.[9,16,103] As discussed previously, the underlying molecular mechanism for the action of these salts was shown to involve saturable anion binding at particular specific, susceptible sites on the macromolecule, and the overall LCST behavior of the polymer can be modeled with the following equation:

$$T = T_0 + c[\mathrm{M}] + \frac{B_{\max}[\mathrm{M}]}{K_\mathrm{D} + [\mathrm{M}]} \qquad (9)^{\S}$$

§ Note that this equation is, of course, of the same form as Equations 3 and 4 given in Chapter 1 – Introduction. However, it bears repeating here for clarity and because this will be the particular form of the equation that will be used for fitting of the data, presented subsequently.

where the LCST observed, T, is related to the transition temperature of the polymer in neat aqueous solution (T_0) plus the two additional terms. The first term is linear with the molar concentration of salt ([M]), having a negative coefficient c which corresponds to the salting-out effect contribution, which thus lowers the LCST. The second, nonlinear term expresses the salting-in contribution and is derived from a Langmuir binding isotherm; B_{max} is the maximum elevation in LCST at saturation and K_D is the (apparent) dissociation equilibrium constant for the binding event. By fitting the LCST curves shown in Figure 18 to this model, we are able to characterize the apparent binding strength of the NR_4Cl salts through the obtained values for K_D. The results of the fitting are shown below in Table 1.

Table 1: Fit values for the parameters c, K_D and B_{max} according to Equation 9, for LCST values of PNIPAM solutions of salt concentrations indicated in the second column. Values in parentheses are errors. For the first two salts, the fit is purely linear and thus there are no nonlinear terms (K_D, B_{max}). The R^2 values for the fits are all > 0.96.

Salt	Concentration range	c ($K \cdot M^{-1}$)	K_D (M)	B_{max} (K)
NaCl	0 – 2.0 M	-12.4 (0.1)	-	-
NH_4Cl	0 – 2.0 M	-8.1 (0.1)	-	-
NMe_4Cl	0 – 1.8 M	-8.84	-	-
NEt_4Cl	0 – 1.4 M	-12.5	1.2 (0.2)	15.9 (2.1)
NPr_4Cl	0 – 1.0 M	-15.4	0.8 (0.2)	17.6 (2.4)
NBu_4Cl	0 – 1.0 M	-20.8	1.2 (0.15)	30.3 (2.7)

The fitting methodology employed was described previously in section 2.3. However, an additional aspect of the procedure should be discussed here in further detail. As can be seen, several of the c parameter values reported for the NR_4Cl salts do not have an accompanying error value. This is related to the curvature of the LCST plots for these salts; it was observed that at the highest salt concentrations tested, the LCST profiles exhibited excessive downward curvature. This is both qualitatively anomalous and quantitatively outside the scope of the model presented in Equation 9, which only encompasses linear salting-out contributions at higher concentrations. For this reason, the fitting algorithm cannot be employed to the full range of concentrations for which data was obtained, and between one and two of the highest concentration points were excluded from the analysis.[**] It is also known that the

[**] The higher concentration LCST measurements are included in full in Appendix B: LCST of PNIPAM at High Salt Concentrations.

tetraalkylammonium salts form clathrate-type hydrates at elevated salt concentrations (as discussed in section 1.3.3), and the concentration regime where this unique aqueous behavior is present is purposely omitted. Mathematically, it was necessary to impose a lower bound to the *c* parameter, which would otherwise tend to unbounded negative values in an attempt to optimize the fit. This was done by taking the tangential slope of the data at the edge of the fitted range, where the nonlinear term should have saturated and the slope should give the best approximation for the *c* parameter.

The apparent K_D values obtained for the nonlinear (i.e., binding) salts are: 1.2 M, 0.8 M and 1.2 M for NBu_4Cl, NPr_4Cl and NEt_4Cl, respectively. In the case of NBu_4Cl in particular, the determined apparent K_D straddles the concentration range considered and thus the numerical value should be taken with additional discretion; from simple chemical equilibrium considerations, it can be derived that the K_D value for a bimolecular binding is equivalent to the concentration at which half of the binding sites are occupied. Therefore, without inclusion of concentrations at or above the K_D, the apparent value from the fit can be regarded as an estimate with a larger degree of error likely associated with it. Nevertheless, the fitting of the results to the model in Equation 9 is informative, because it shows that a saturable binding event is implicated with the observed thermodynamic effects of these salts on PNIPAM. Moreover, because the anion is kept constant between salts and chloride anion is known to be generally non-binding to such neutral macromolecules,[1,9,16,103] it can be inferred that this highly significant effect is driven by the properties of the cations. With increasing alkyl chain length, and thus the corresponding cation size, the K_D values generally decrease and the B_{max} values increase (reflected in the growing nonlinearity of the LCST profiles), indicating that the apparent binding becomes stronger and more effectual with increasing cation size. Indeed, the LCST experiments represent an unprecedented set of evidence for the salting-in effects of the most weakly-hydrated cations, mediated by a mechanism that correlated with the cation hydrophobicity and weakness of hydration. Thus, our findings point in the direction of a cation-driven, saturable, Langmuir-type binding of NR_4Cl salts to PNIPAM. Yet, the phase transition measurements are not capable of demonstrating the binding site on the PNIPAM macromolecule for a detailed molecular-level mechanistic picture. To this end, spectroscopic approaches provide powerful tools and were employed next, as described in the following sections.

3.2.2 ATR-FTIR Measurements: Probing the Carbonyl Group as a Potential Site for Cation Interaction

As discussed previously in Chapter 1 – Introduction, whilst the effects of Hofmeister cations have been known to frequently be overshadowed by the more significant anion effects, the strongly-hydrated cations in particular are known for their role as weak salting-in agents.[1,3,10,16,188] In later mechanistic studies, it was determined that the most strongly-hydrated cations exhibit a very weak but measurable affinity for interaction with the carbonyl groups of small amide molecules, oligopeptides as well as larger polyamide-type neutral macromolecules.[10,88,89,188] As the most salient electronegative group present in many biologically relevant molecules—most importantly, being present in the peptide bond common to all proteins—the carbonyl moiety is indeed a rational means to account for specific interactions of positively-charged cosolutes, in the absence of negatively charged groups. Due to its demonstrated central role in the cationic Hofmeister effects of metal chlorides,[188] it is a logical target to explore for interactions with the apparent strong binding of tetraalkylammonium cations as well.

Additionally, the amide carbonyl moiety has the further advantage of its characteristic vibrational signature, which provides a means to probe it spectroscopically *in situ*. For this purpose, attenuated total reflectance Fourier transform infrared spectroscopy (ATR-FTIR) was employed (as illustrated below in Figure 19a). The amide I vibrational mode of PNIPAM samples in D_2O was probed in the presence of QA salt solutions. In a D_2O environment, the amide I resonance consists primarily of the carbonyl C=O stretching mode, with diminished contribution from vibrational modes involving other amide-group atoms. Additionally, measurements benefit from being done in D_2O[††] because the approximate wavenumbers where the amide I bands typically appear nearly coincide with the bending mode of non-deuterated water (H_2O), at ~1650 cm^{-1}. The water bending mode in D_2O is redshifted to ~1200 cm^{-1}, and barring excessive proton contamination provides a better environment to isolate the amide I

[††] It is remarked here that LCST measurements on PNIPAM described in section 3.2.1 were carried out in regular aqueous (H_2O) media, as opposed to D_2O solutions. However, the latter measurements were also carried out, and are shown in Appendix C: LCST Measurements of PNIPAM in D2O Media. The general trends as deduced in section 3.2.1 hold for D_2O solutions as well, but because they were not found to provide additional evidence for the mechanistic interpretations in the present case their discussion is relegated to the mentioned section.

band in IR spectroscopy. The vibrational signals mentioned, as well as other bands that appear in the region are shown below in Figure 19b.

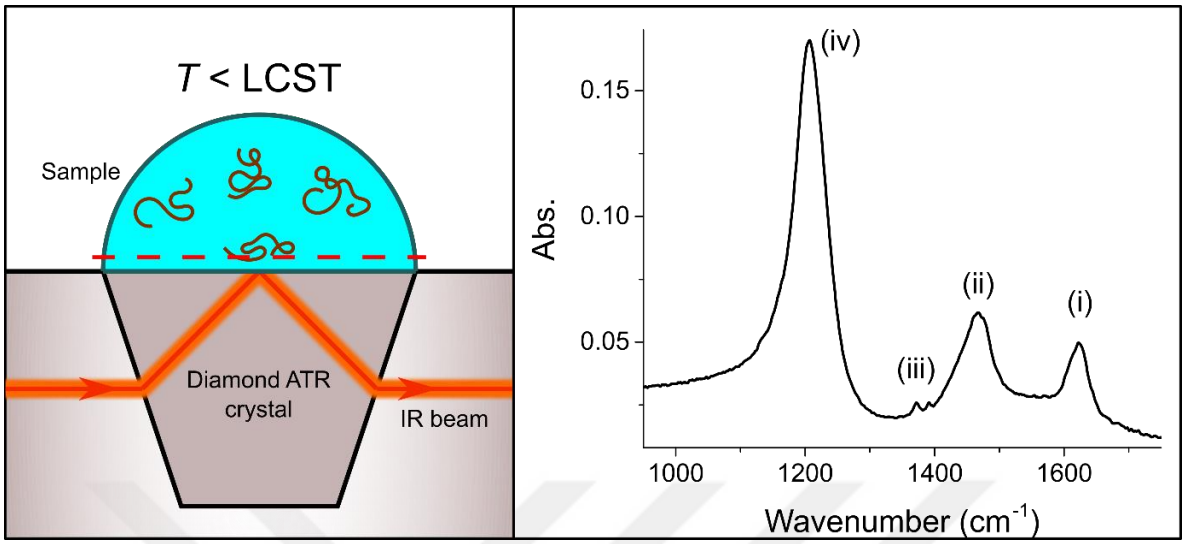

Figure 19: (a) Schematic representation of ATR-FTIR of PNIPAM solutions. Due to the principle of the method (attenuated total reflectance), the IR beam only interacts with a small layer of the sample near the crystal (red dashed line). The distance penetrated by the beam (in the form of an 'evanescent wave') depends on frequency, refractive index and incident angle but is generally in the range of ~0.5 – 2 µm. (b) An ATR-FTIR spectrum of 20 mg/mL PNIPAM at ~5°C, showing frequency window relevant for the present investigation. The amide I band is labeled (i), and appears at ~1625 cm^{-1}. The other labeled signals are: (ii) amide II, at ~1467 cm^{-1} (iii) the antisymmetric *i*-Pr group deformation modes, at ~1392 and ~1373 cm^{-1} and (iv) the D_2O bending mode, at ~1206 cm^{-1}.[255,256]

Below, Figure 20 shows the normalized ATR-FTIR spectra of 20 mg/mL PNIPAM solutions in neat D_2O and in 1 M of each of the salts used in LCST experiments previously in D_2O media. The measurements were all carried out at 4 – 5°C to ensure the polymer remains below its LCST and does not aggregate. The fully dissolved PNIPAM amide I band in neat D_2O appears at ~1625 cm^{-1}. In the presence of 1 M NaCl, NH_4Cl and NMe_4Cl, the IR band remains identical with that in neat D_2O, as can be seen from the extremely close superposition of the spectra in Figure 20a. Such unaltered amide I bands indicate an absence of direct interaction. Figure 20b shows the amide I band of PNIPAM in the presence of 1M NEt_4Cl salt and again a lack of a change at the amide I band is observed, despite its distinctly nonlinear LCST influence. Figure 20c – d show the normalized ATR-FTIR bands in the presence of the two salts with the largest NR_4^+ ions; in this case, there is a small yet distinguishable emergence

of a distortion in the amide I band. However, the magnitudes of the residual change (i.e., the difference between the normalized spectra, with and without 1 M salt; these are shown for the four tetraalkylammonium chlorides in Figure 21) cannot be justified with the apparent K_D values from the thermodynamic LCST data. That is, if the carbonyl group is the primary interaction site for the binding of the larger NR_4^+ cations with K_D values ~1 M, we should see a comparable population of cation-bound carbonyl groups in the IR spectrum of the 1 M salt solutions. As shown by Okur et al.[188], the cation binding event produces a blueshift to ~1645 cm^{-1} in the amide I band, which appears as a sizeable shoulder band alongside the main feature at high concentrations. In our case, despite the apparent binding being significantly stronger, there is no comparable effect. From Figure 21, it can be seen that both the magnitude of the blueshift (of a presumed shoulder band; note that this is different from the residuals depicted) and the low population corresponding to the shoulder area are not in accordance with a direct carbonyl interaction model.

Nevertheless, the presence of the cation in the vicinity of the molecular surface should be expected to alter the hydration of the macromolecule. Consequently, whilst the amide oxygen is indeed found not to be the primary binding site of NR_4^+ cations on PNIPAM, it may still be exhibiting a secondary effect related to the largest NR_4^+ cations' binding at some other, nearby site. Considering the molecular size of the largest of these cations, their approach toward any specific site on the polymer side-chain would likely affect the hydration state of other nearby sites to varying degrees. However, it is clear that further investigation is needed in order to properly characterize the preferential orientation of the cation-macromolecule interaction. To achieve this, ^{1}H-NMR spectroscopy proved an invaluable tool, and was utilized in systematic measurements described in the following section.

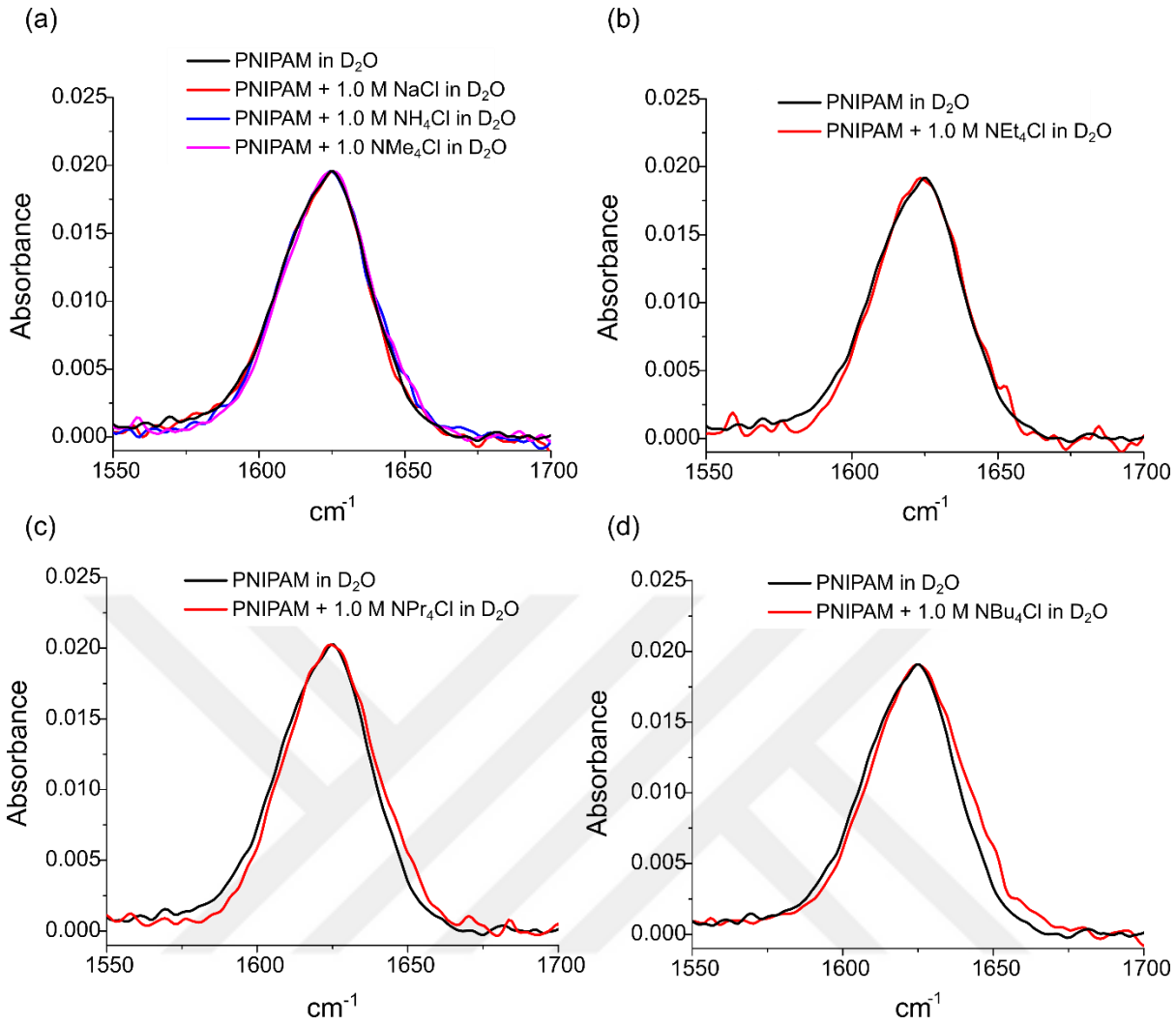

Figure 20: Normalized amide I ATR-FTIR bands of PNIPAM in various D_2O solutions, measured well below the polymer LCST points. The bands were normalized to the reference peak, which is the same representative PNIPAM amide I band in neat D_2O in all cases and plotted in each panel, together with: (a) PNIPAM amide I in 1.0 M solutions of NaCl, NH_4Cl, NMe_4Cl in D_2O, depicting no change in the peak shape or position; (b) PNIPAM amide I in 1.0 M NEt_4Cl solution, depicting no observable change; (c) PNIPAM amide I in 1.0 M NPr_4Cl solution, depicting a small change in band shape; (d) PNIPAM amide I in 1.0 M NBu_4Cl solution, depicting the slightly larger distortion in the peak. Also see Figure 21 for comparison with additional PNIPAM amide I spectra in neat D_2O and residuals.

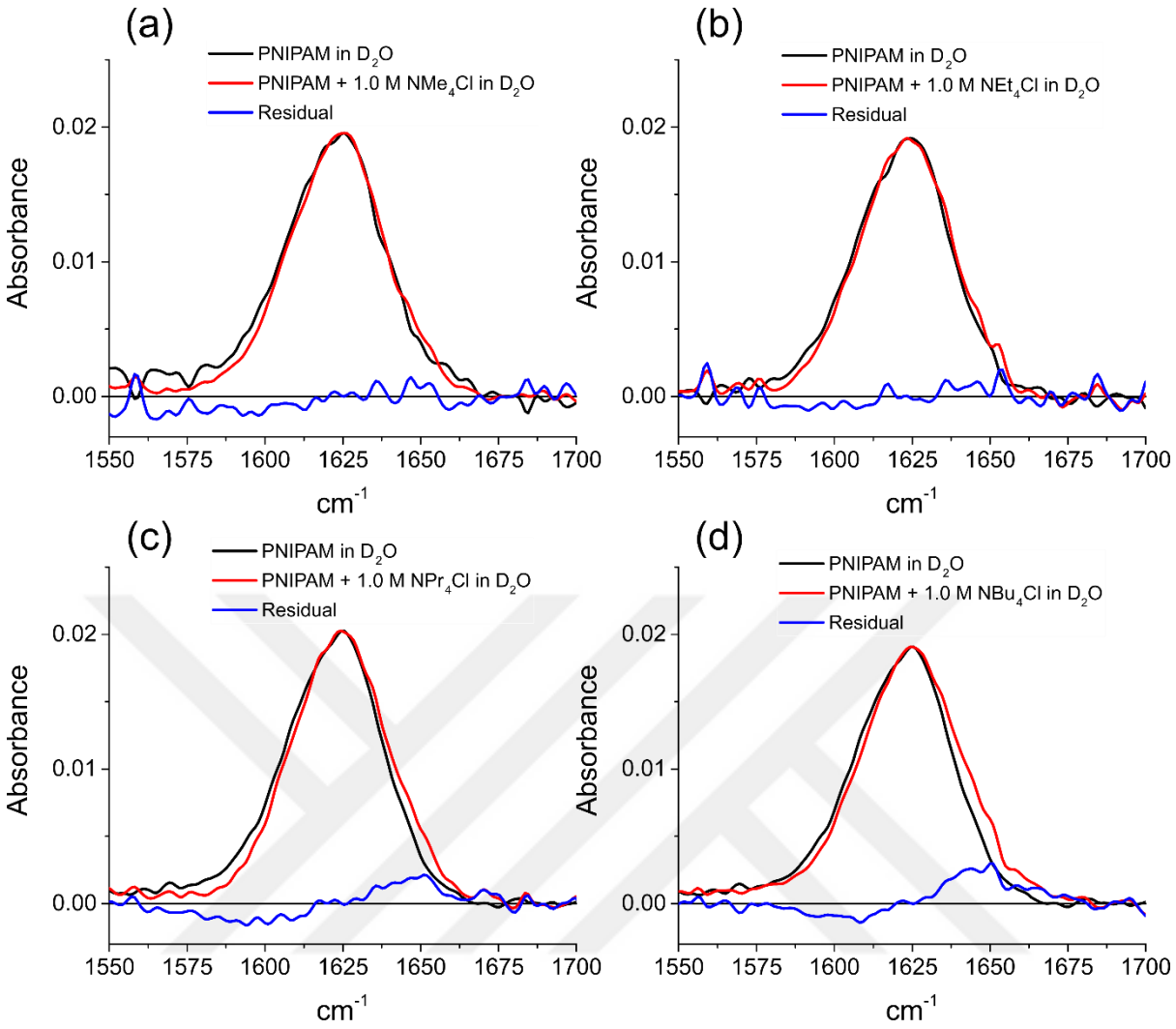

Figure 21: The PNIPAM + 1 M salt in D_2O amide I bands from Figure 20 are plotted with different PNIPAM in neat D_2O amide I spectra measured on the same day. The conclusions are the same as in Figure 20, with the added visualization granted by the 'residual' plotted in each panel. The residual is simply obtained by subtracting the reference spectrum from the sample spectrum, thus producing a visual indication of the change between the two curves. The residuals in (a) and (b) are flat lines at 0 absorbance within error, confirming that the amide I bands are unchanged by the presence of 1 M NMe_4Cl and NEt_4Cl salts. In (c), the residual shape indicates a slight blueshifting component in the presence of 1 M NPr_4Cl, and (d) indicates the effect is slightly larger with 1 M NBu_4Cl.

3.2.3 ^{1}H-NMR Measurements: Probing the Whole Polymer & Hydrophobic Interaction Mechanism

As described in section 3.1, a quantitative externally-referenced ^{1}H-NMR spectroscopic methodology was successfully implemented to study ion specific effects and binding behavior toward the model macromolecule. Crucially, the methodology was able to distinguish the behavior of nonbinding, purely salting-out salts from the effect of a binding salt by distinguishing a specific polymer site for the preferential interaction, and furthermore elicited quantitative information regarding the strength of the binding.

This methodology is, again, of great use here because it allows all hydrogens on the PNIPAM macromolecule to be screened for the primary site of interaction. Thus, the same methodology described in section 3.1 was applied to PNIPAM – NR_4Cl salt NMR titration measurements. Figure 22 depicts the effect of each salt on the four polymer ^{1}H-NMR signals' chemical shifts, from measurements of 3.3 mg/mL PNIPAM samples in D_2O media. Measurements and data processing were carried out as described in sections 2.5 and 3.1.1. As can be seen, the majority of the polymer chemical shifts undergo a linear, monotonic decrease with all four of the NR_4Cl salts. The magnitudes of the chemical shift changes up to 0.6 or 0.8 M salt are also comparable between the salts (~0.04 – 0.05 ppm decrease in chemical shifts, maximum), except for NMe_4Cl (~0.01 ppm shift, maximum) which appears to have a distinctly diminished effect on the polymer chemical shifts—this is striking in that NMe_4^+ is also the only tetraalkylammonium cation observed as non-binding on the basis of its entirely linear LCST curve (Figure 18). Also, note that this much smaller change in the chemical shift in the case of NMe_4Cl is the reason why its curves appear noisier in Figure 22a.

The first hint of a different chemical shift response appears in NPr_4Cl. Here, both the N-CH and backbone -CH- signals are once again highly linear with salt concentration whilst, in sharp contrast, the *i*-Pr terminal -CH_3 signal exhibits a slight but noticeable curvature. Moreover, it is a curvature similar to that observed in the LCST curves of the binding salts. That is, there is a nonlinear component to the chemical shift curve that is more readily evident at lower concentrations, but appears to reach saturation and is overtaken by the dominant linear component at higher concentrations. While this feature of the *i*-Pr -CH_3 curve is a mild difference for NPr_4Cl, the curvature is even more pronounced for NBu_4Cl. Here, the effect of the binding of the cation to the site appears to have an even greater effect on the observed chemical shift of the local hydrogens.

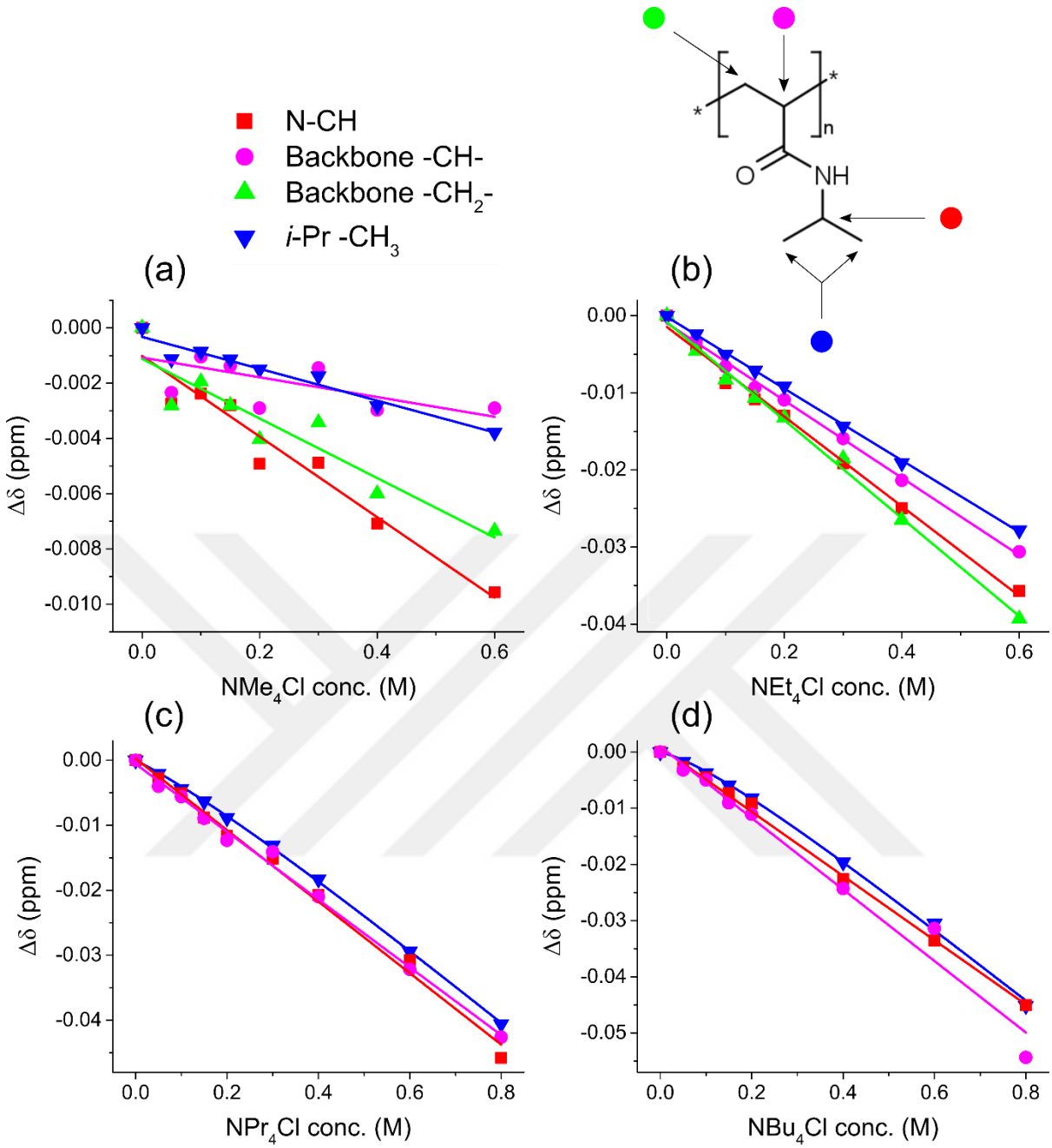

Figure 22: The ^{1}H-NMR chemical shifts for the four PNIPAM signals (legend and color-annotated structure of PNIPAM are included at the top) as a function of concentration of (a) NMe_4Cl, (b) NEt_4Cl, (c) NPr_4Cl, and (d) NBu_4Cl. Overview of the trends depicted here are given in the text. Note that the backbone -CH_2- signal is absent in (c) and (d), because the signal coincides with a large salt peak and is unobservable in these cases.

In order to illuminate the striking distinction in the chemical shift responses of the two largest QA cations, Figure 23a depicts only the *i*-Pr terminal methyl and N-CH group's chemical shift curves against concentration of NBu_4Cl and NaCl. Here, the difference between the purely non-binding NaCl salt and the binding NBu_4Cl salt is made all the more evident;

whereas both polymer signals' chemical shifts fall linearly with NaCl concentration, the distinctive nonlinearity, particularly significant at lower concentrations—i.e., the hallmark of saturable-type binding behavior—is apparent in the case of NBu_4Cl. The feature is more dominant for terminal methyl groups of the isopropyl chain, but may also be observed in the central, N-bonded -CH- position of the isopropyl group. Therefore, these findings constitute a strong indication that the chemical environment of the isopropyl group alters as a function of NBu_4Cl concentration in the manner of a saturable binding site. As discussed previously, similar binding events have been demonstrated through the NMR titration approach for the case of Langmuir-type binding of weakly-hydrated anions to PNIPAM, as well as other macromolecules. The cosolute ions induce a net shielding effect—due to their modulating effect on the macromolecule's hydration by water, i.e., salting-out—at all sites except for the binding site, where the saturable interaction contributes an independent partial deshielding effect, due to the electronic influence of a binding ion on the polymer. The resultant, net chemical shift profiles for the binding site is, thus, comprised of the sum of these two competing effects and can be modeled as such. Hence, the relation that will used to fit the binding curves is:

$$\Delta\delta_{\mathrm{H}} = c'[\mathrm{M}] + \frac{\Delta\delta_{\max}[\mathrm{M}]}{K'_{\mathrm{D}} + [\mathrm{M}]} \tag{10}$$

The results of the fits to Equation 10 are shown in Table 2. Parameters are tabulated for the salt-polymer signal pairs that generate a nonlinear chemical shift response. It is additionally illustrative to calculate the 'residuals'; that is, the nonlinear contribution to the data points (if any), which is simply obtained by subtracting the linear portion of the fit (i.e., $c'\cdot[\mathrm{M}]$) from the data. The residuals for the series plotted in Figure 23a are shown in Figure 23b. Here, we can clearly see that the residual, nonlinear component of the NBu_4Cl – *i*-Pr terminal methyl data (and, to a lesser but still significant extent, the same salt's N-CH series) matches a Langmuir-type saturable binding isotherm reasonably well. In contrast, the residuals obtained for the non-binding NaCl chemical shifts are flat lines, with the individual residual points oscillating around the *x*-axis due to the inherent noise present in the measurements.

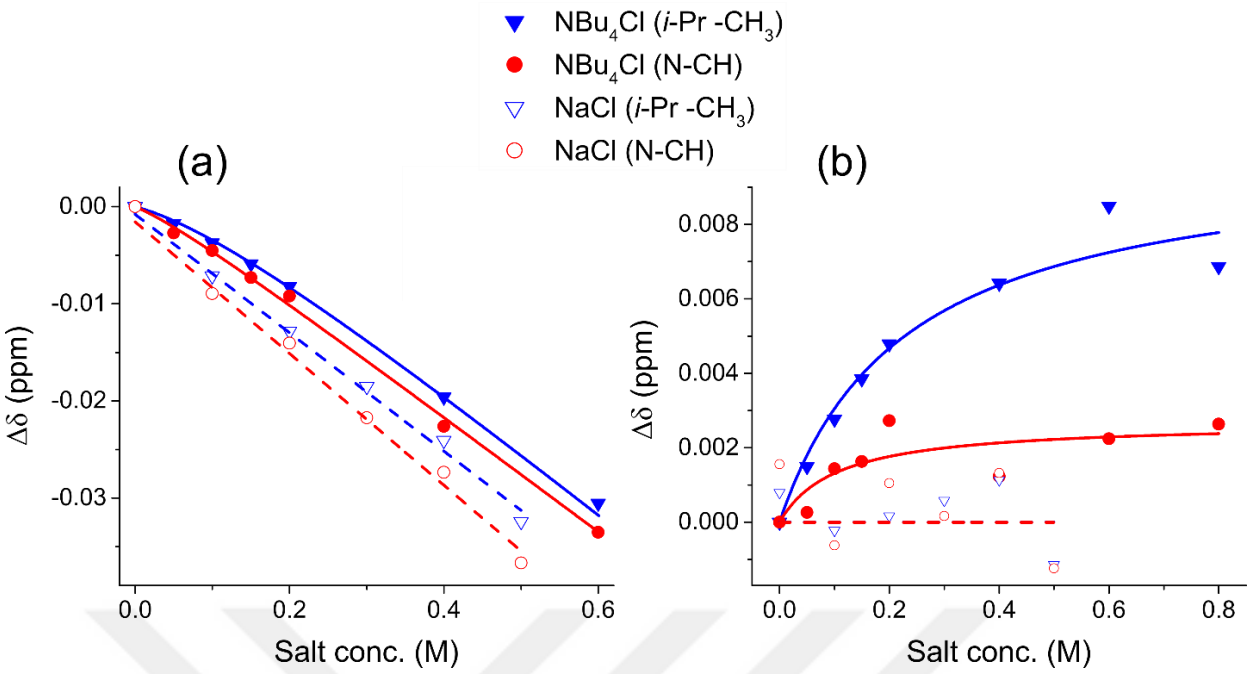

Figure 23: Top inset gives the legend for both panels: (a) Chemical shift vs. salt concentration curves for the *i*-Pr terminal -CH_3 and N-CH signals of PNIPAM + NBu_4Cl and NaCl. Here, the NaCl data depicted are the average of two separate measurement series; the aim is to reduce the presence of random noise so as not to obscure the general trend, but due to the highly precise nature of chemical shift changes some noisy oscillation persists in the data series regardless. (b) Residuals for the curves in panel (a), calculated according to fits to Equation 10 in the case of NBu_4Cl, and to a purely linear fit in the case of NaCl.

It is also noteworthy that although the *i*-Pr terminal methyl groups appear to be the more significant interaction sites based on the larger chemical shift response, the neighboring N-CH groups are also correlated with the salt. Moreover, their apparent K_D values are similar within error, as such one can argue that it results from the same binding event. The binding site of the large tetraalkylammonium cations may thus be best described as a hybrid of the terminal and central positions of the isopropyl side-chain. Considering the comparatively large size of the approaching cation, it is not difficult to rationalize that the hydration state of multiple close sites would be affected. This, furthermore, brings credence to the hypothesis presented in section 3.2.2 regarding the small distortion of the amide I bands being a secondary effect. The carbonyl group is the next closest neighbor along the PNIPAM side-chain, and its strongly-hydrated, highly polar nature in particular would likely make it responsive to alterations to the hydration structure in the vicinity. Its small but visible response may be interpreted as a partial

dehydration as a result of the occupancy of the cation at the macromolecule interface, and this would be in accordance with the small blueshifted character of the distortion.

Table 2: Tabulated results from the fitting of N-CH and *i*-Pr terminal methyl signals' chemical shift vs. salt concentration data to Equation 10. Values given in parentheses are errors. As can be seen, only NPr_4Cl and NBu_4Cl induce chemical shift responses that have a nonlinear component according to Equation 10.

Salt	N-CH		*i*-Pr terminal -CH_3	
	K_D' (M)	$\Delta\delta_{max}$ (ppm)	K_D' (M)	$\Delta\delta_{max}$ (ppm)
NaCl	-	-	-	-
NMe_4Cl	-	-	-	-
NEt_4Cl	-	-	-	-
NPr_4Cl	-	-	0.44 (0.05)	0.01
NBu_4Cl	0.1 (0.2)	0.003 (0.003)	0.23 (0.04)	0.01

Looking at the plots in Figure 22, Figure 23 and the tabulated results given in Table 2 together, it is indeed possible to arrive at some key insights regarding the Hofmeister behavior of these weakly-hydrated cations. Namely, their strong apparent interaction with neutral macromolecules and sizeable thermodynamic effect evinced by the LCST experiments are indeed revealed to be related to a novel mechanism. The interaction of these cations with PNIPAM is mediated by hydrophobic effects and correlated with the length of the alkyl chains—i.e., the size of the ion, and inversely related to its charge density. In stark contrast to the binding mechanism identified for the strongly-hydrated cations, binding is stronger for QA ions that are more weakly-hydrated: no binding-related salting-in effect is observed for the smallest QA salt, NMe_4Cl, which also affects the chemical shift response of the polymer only very weakly. NEt_4Cl exhibits significant salting-in on the macroscopic/thermodynamic scale, even though it does not translate to a clear detectable response in our ^{1}H-NMR methodology or instrumental capability. The next largest QA salt, NPr_4Cl binds strongly ($K_D \approx 0.44$ M) to the isopropyl terminal methyl groups, so as to be observable by quantitative ^{1}H-NMR. Finally, the largest and most hydrophobic cation NBu_4^+ has the strongest effect of all, and its binding to isopropyl methyls is the tightest ($K_D \approx 0.23$ M), and the chemical shift response of the neighboring N-CH hydrogen correlates with the binding equilibrium as well.

Whereas the salting-in effect of the tetraalkylammonium salts thus studied appears well-supported by the multiple lines of experimental evidence, the salting-out aspect of the

salts has thus far not been discussed. In fact, this aspect of the salts' behavior—which is noticeable even in the initial LCST measurements, as mentioned in passing in section 3.2.1—is not straight-forward and merits analysis of its own, and will be discussed in the following section.

3.2.4 Interpretation of the Salting-out Effect: Correlation Between *c* Values and Cation Properties, High-Temperature ATR-FTIR Studies

As summarized in the previous discussion, the various experimental findings indicate that the salting-in effect imparted by the tetraalkylammonium chloride salts is related to the hydrophobic, weakly-hydrated character of the cations. However, looking back at the LCST data and table of fitted parameters (Table 1) derived for the salts, we may notice an additional unexpected trend. The salting-out efficacy of the tetraalkylammonium salts, as encapsulated by the magnitude of the *c* parameter, *also increases* with increasing cation size and hydrophobicity. As can be observed from Figure 18, with increasing alkyl chain lengths, both the nonlinear effect in the lower concentration regime and the steepness of the linear-like curve at higher concentrations increases. It appears that the greasiest QA cations are both the strongest salting-in and salting-out agents, simultaneously. How might this occur?

It is worth recalling some mechanistic and phenomenological insights from the Hofmeister literature reviewed in Chapter 1 – Introduction. In a diverse range of Hofmeister studies spanning decades, seeking correlations between ionic properties and specific ion effects has been a fairly consistent strategy in the pursuit of fundamental models. Despite the largely unsuccessful outcomes of attempts to devise a single unifying explanation for all Hofmeister phenomena based on such correlations, significant relations between known ion properties and various manifestations of specific ion effects (SIE) have nevertheless contributed valuable clues to understanding the molecular-level mechanisms at large. Amongst the recent literature, several publications used this strategy to propose conceptual mechanisms for Hofmeister systems, and in many cases the correlations seem quite convincing. In the studies by Zhang et al.[9] and Cho et al.,[103] an apparently consistent set of correlations were used to explain the action of common anions on disparate macromolecular systems. As argued by these studies, the direct Hofmeister series for anions splits roughly at Cl^-, whereby the salting-out effect (i.e., value of parameter *c*) of anions more strongly-hydrated than Cl^- correlate with their *entropy of hydration*, whereas the salting-out effect of anions more weakly-hydrated than Cl^- correlate instead with their *surface tension increments*. The latter explanation is also consistent with the

solvophobic theory and microcavity-formation thermodynamics approaches developed in the mid-20th century, and is intuitively based on the understanding that the elevation of interfacial tension due to dissolved ions will thermodynamically favor the minimization of such interfaces and, thus, salting-out.

This latter correlation was also given consideration to explain the behavior of weakly-hydrated cations, which in terms of observed behavior appear to share the saturable binding and salting-in effect with the weakly-hydrated anions for which the correlation holds. However, in our case there is no such correlation between determined values for *c* and the surface tension effect of the QA cations. In fact, the QA cations larger than NMe_4^+ *decrease* the macroscopic air-water surface tension,[257] despite exhibiting salting-out behavior in the present system. Moreover, the surface tension lowering effect is very dramatic, in particular for the larger ions like NPr_4^+ and NBu_4^+.[257] This is generally contradictory to the thermodynamic behavior observed here; it is apparent that the surface tension-based conceptualization that holds true for weakly-hydrated anions cannot be the direct explanation for the pronounced salting-out behavior of the larger QA cations.

One possible route to an explanation that may come to mind relates to the *apparent* salting-out/solubility decrease caused by very strong, multivalent binding of cosolutes such as guanidinium cation.[216] Analogously, perhaps the largest QA cations could bind multiple hydrophobic patches of the polymer together so as to cause collapse. Yet, the effect observed in GndSCN-like systems, i.e., of strongly 'gluing' ions has been both experimentally and theoretically shown to manifest at lower concentrations, where the ratio of binding sites/host to guest is high. This is the complete opposite of the behavior observed with QA chlorides, but nevertheless could be related to a different inclusion-driven collapse mechanism specific to these salts. To test this possibility, we performed systematic ATR-FTIR measurements of PNIPAM in D_2O salt solutions above the LCST temperature. In contrast to the approach used in section 3.2.2, here the aim is to glean information specifically about the collapsed/aggregated form of the macromolecule. In essence, the main principle of such measurements is similar to that employed by Heyda et al.[216] to probe the accumulation/exclusion behavior of various ions from the collapsed form of macromolecules. In our case, systematically varied solutions of PNIPAM and cosolute salts are transferred to the ATR-FTIR plate which has already been heated to a stable ~45°C by the affixed circulator apparatus, as described previously in section 2.4 and illustrated in Figure 12c. Spectra acquisition is started immediately, and a full 32-scan FTIR spectrum of the sample is recorded every 2 minutes after the initial measurements. At

temperatures above the LCST, the thermoresponsive polymer promptly undergoes the collapse/aggregation transition and begins to accumulate on the ATR crystal interface, and a lower (denser) liquid layer separates from the bulk solution. Then, the ATR-FTIR spectra continuously probe the contents of this accumulating denser phase, which is richer in polymer and comparatively poorer in solution species (as depicted in Figure 24 below). The trends of various vibrational signals then provide information about the behavior of their corresponding species—including the QA cations of interest—during the transition.

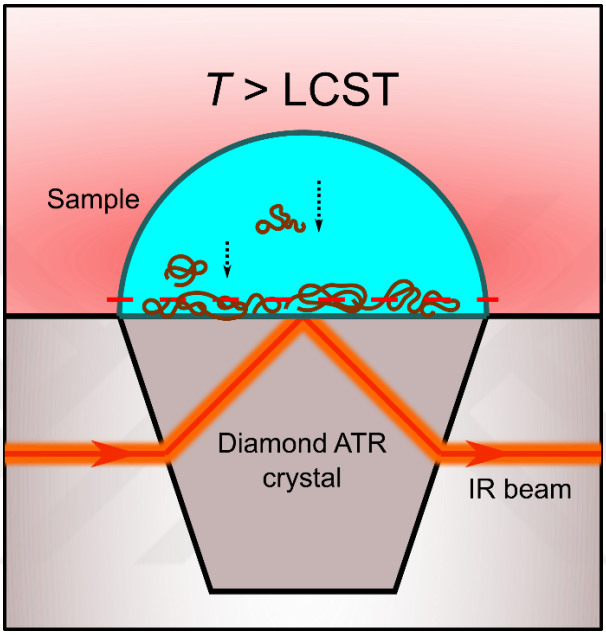

Figure 24: Schematic representation of the experimental principle of ATR-FTIR measurements above the LCST. PNIPAM in the sample rapidly undergoes hydrophobic collapse and begins to aggregate at the bottom of the sample, near the ATR crystal. Thus, the region of sample able to be penetrated by the IR evanescent wave (red dashed line) specifically probes the collapsed form of the polymer as it forms a lower subphase.

Measurements were performed for neat D_2O and PNIPAM in neat D_2O; 1.2 M salts in D_2O (except for NBu_4Cl, which was measured at 0.8 M, as discussed separately below); and PNIPAM in the same set of salt solutions. Figure 25a shows the spectral features of the collapsed form of PNIPAM in D_2O. As can be seen, there are several prominent vibrational bands which appear in the region ~1100 – 1800 cm^{-1}. These are assigned as: the amide I and amide II bands (at ~1620, ~1463 cm^{-1}, respectively), the isopropyl distortion bands (at ~1369, ~1389 cm^{-1}), D_2O bending band (~1203 cm^{-1}) and isopropyl skeletal vibrations (~1160 cm^{-1}, ~1132 cm^{-1}).[255,256] The amide I band shape is slightly altered compared to the below-LCST spectrum of PNIPAM shown in Figure 19b, due to the formation of ~10% amide-amide

hydrogen-bonded groups in the collapsed state.[258] The intensity of the bands provides a picture of how the collapsed state forms. Figure 25 shows spectra of 1.2 M NaCl, PNIPAM in neat D_2O, and PNIPAM in 1.2 M NaCl. As can be seen, the intensity of PNIPAM bands is significantly enhanced due to NaCl. This implies that the presence of the salt favors the collapsed form of the macromolecule. Unfortunately, the monoatomic ions (Na^+ and Cl^- in the set of salts used) cannot be observed by this method, and the behavior of these ions with regard to the PNIPAM collapse is not measurable here.

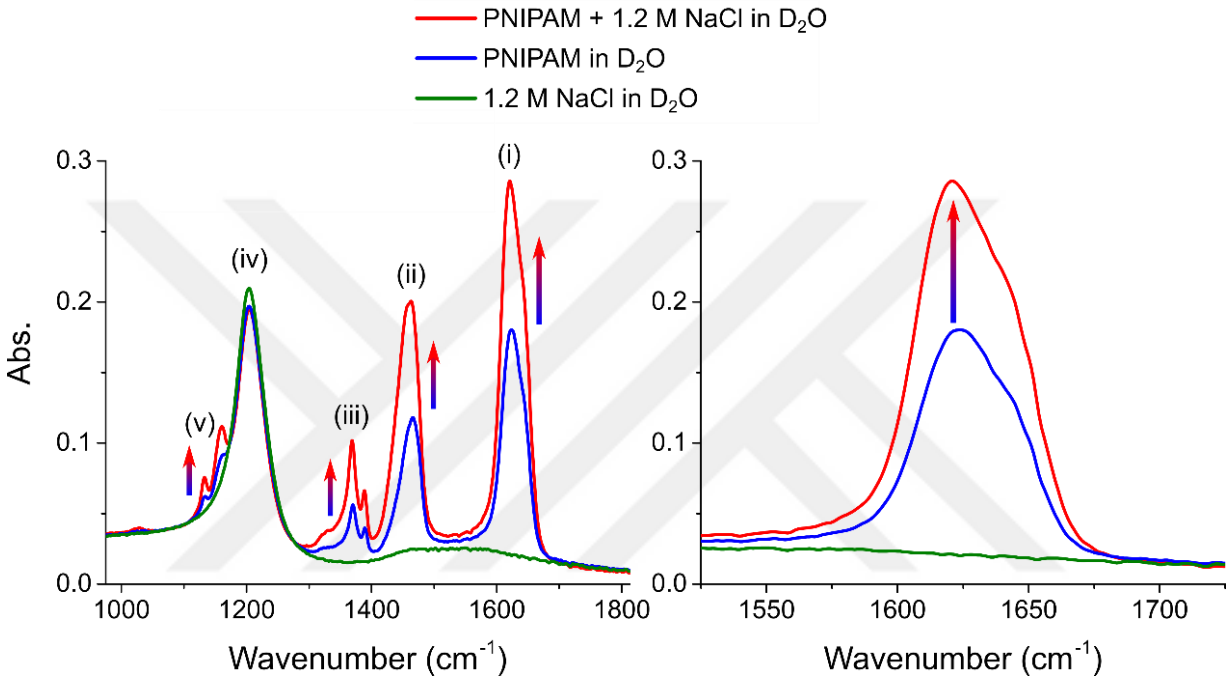

Figure 25: Left: A representative frequency window from the ATR-FTIR spectra measured above the LCST, showing the comparative intensity increase in PNIPAM vibrational bands due to the presence of NaCl. The legend for the spectra is given at the top. The assignments of the peaks (i) through (iv) are analogous to those given for Figure 19, i.e., below the LCST. The specific positions of the peaks shown here are also given in the text, above. The peaks labeled (v) are assigned as isopropyl skeletal vibrations (~1160 cm^{-1}, ~1132 cm^{-1}). Right: a frequency window showing the amide I band of PNIPAM and the distinct effect of 1.2 M NaCl. The arrow points in the direction of intensity change due to the presence of NaCl.

Figure 26a – b shows the analogous plots for PNIPAM and 1.2 M NH_4. In particular, Figure 26a demonstrates that the presence of NH_4Cl increases the intensity of the collapsed PNIPAM amide I bands almost two-fold. Here, the behavior of the salt is also observable: as can be seen from Figure 26b, the characteristic salt peak at ~1097 cm^{-1} (corresponding to the N-D bending modes[259]) is lower in intensity for the PNIPAM – salt mixture. This indicates that

the NH_4^+ cation is indeed preferentially depleted from the collapsed phase, consistent with an exclusion-driven salting-out mechanism. The same analysis can be made for NMe_4Cl in Figure 26c – d. Here the amide I band shows a moderate increase in intensity (~1.5 fold) due to the presence of the salt, and the observed intensity decrease in a vibrational signal characteristic for the cation in Figure 26d (at ~950 cm^{-1}, corresponding to the asymmetric N-C stretching mode[260,261]) confirms that this cation also salts-out due to preferential exclusion.

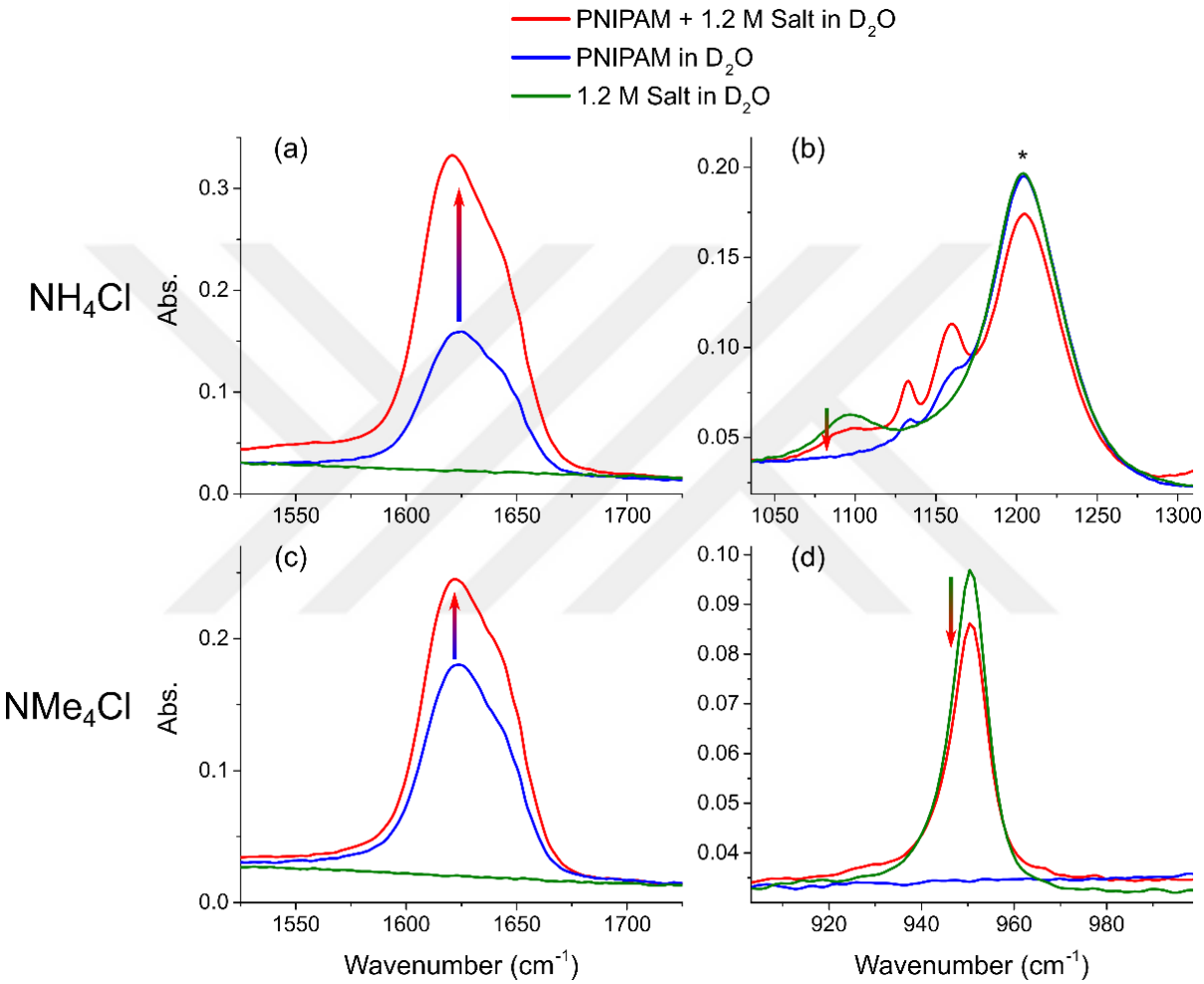

Figure 26: ATR-FTIR spectra above the LCST showing the effect on PNIPAM amide I bands in the presence of NH_4Cl (panel a) and NMe_4Cl (panel b), as well as the effect on signals specific to these salts (panels b and d, respectively) in the presence of PNIPAM. The legend for the spectra is given at the top. The large peak marked with * is the D_2O bending band. Arrows show the change in the signals specific to PNIPAM or the salt due to the presence of the other component in solution.

Figure 27 below shows the same set of spectra for PNIPAM - 1.2 M NEt_4Cl, NPr_4Cl samples. As shown in Figure 27a, NEt_4Cl increases the amide I intensity slightly and the

intensity comparison for the characteristic salt N-C stretching signal[259] at ~1002 cm^{-1} in Figure 27b shows that the concentration of the cation near the aggregated macromolecule is moderately lower than in the bulk solution. The result for NEt_4^+ is thus consistent with a modest depletion, which is in agreement with the minor salting-out effect evident from the amide I comparison. In striking contrast, 1.2 M NPr_4Cl has a major effect on the amide I intensity, increasing it more than two-fold. Concurrently, the decrease of intensity in the N-C stretch signal[259] at ~971 cm^{-1} indicates that the NPr_4^+ cation is strongly excluded from the collapsed macromolecule. This indicates that, indeed, this larger tetraalkylammonium salt is a very strong salting-out agent at high concentrations despite its being an effector of salting-in at low to moderate concentrations, and that the mechanism for salting-out involves exclusion from the macromolecular interface, and not an inclusion-driven one.

The same analysis could not be conducted for NBu_4Cl using 1.2 M salt solutions, because in 1.2 M NBu_4Cl PNIPAM is no longer fully soluble, and tends to remain in large part as an undissolved pellet or spontaneously precipitate out. Lower concentration samples were tested instead, and the results are shown in Figure 28 below. In 0.8 M NBu_4Cl, the PNIPAM bands are slightly intensified, and the salt peaks (the N-C stretching mode[259] at ~883 cm^{-1} is depicted in Figure 28b) are slightly diminished. This in consistent with NBu_4Cl slightly stabilizing the collapsed form of PNIPAM at 0.8 M through a weak preferential exclusion from the collapsed macromolecule.

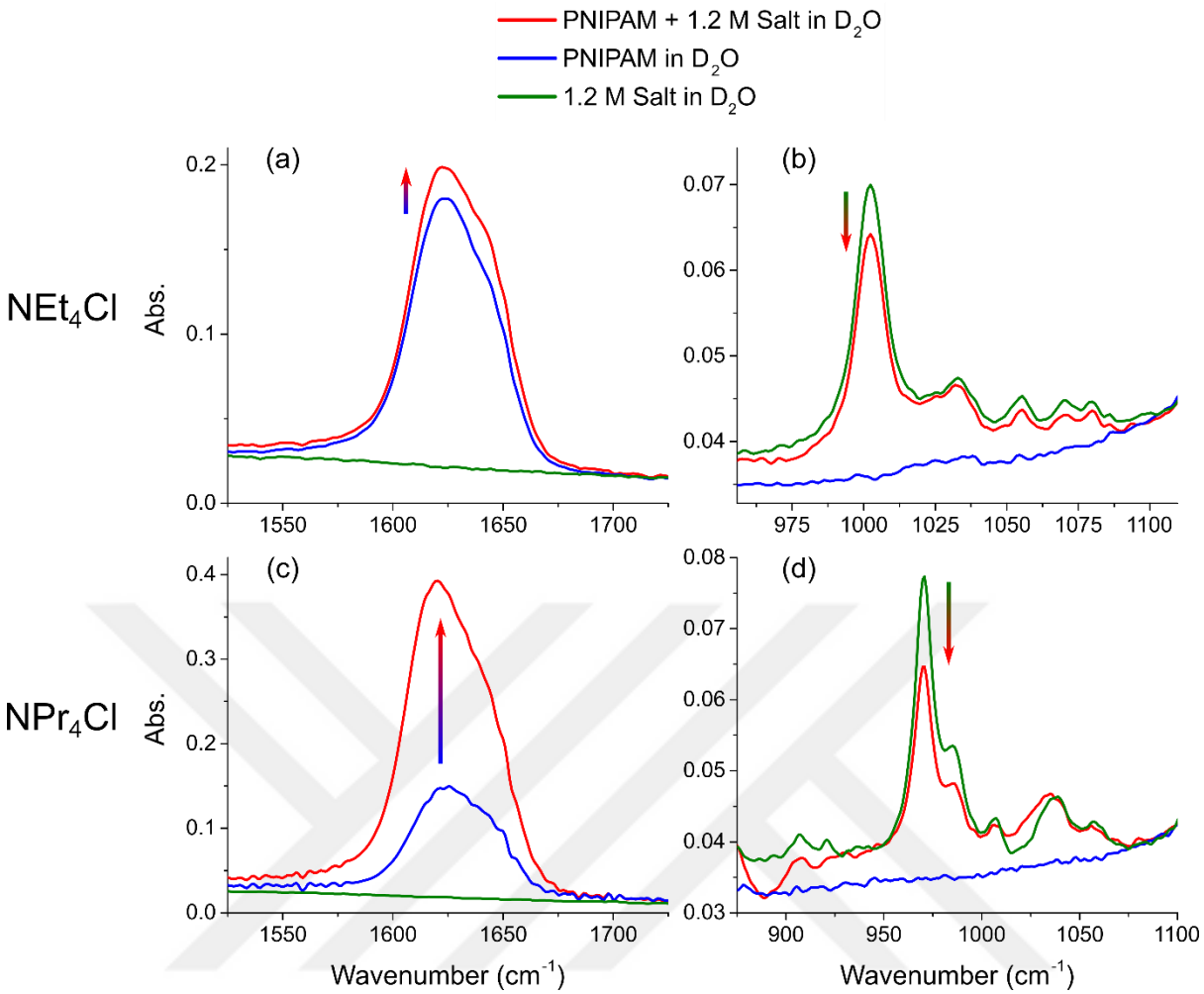

Figure 27: ATR-FTIR spectra above the LCST showing the PNIPAM amide I band in the presence of NEt_4Cl (panel a) and NPr_4Cl (panel b), as well as vibrational signals specific to the salts (panels b and d, respectively) in the presence of PNIPAM. Legend for the spectra is included at the top. Arrows indicate the change in the bands corresponding to PNIPAM or salt due to the presence of the other.

Thus, it can be concluded from the results of the high-temperature ATR-FTIR experiments that a mechanism involving 'gluing'/multivalent binding or some other form of inclusion-driven salting-out is not valid for these salts. Instead, the analysis of the spectra largely supports a depletion-based salting-out mechanism; the results for 1.2 M NEt_4Cl and, particularly decisively, for 1.2 M NPr_4Cl decisively indicates that the large tetraalkylammonium salts are effective drivers of salting-out due to their high degree of exclusion from the macromolecule interface at high concentrations. Intriguingly, this model for Hofmeister ion effects resembles the behavior of strongly-hydrated anions, such as the strongly salting-out anion SO_4^{2-}, despite the much more weakly-hydrated status attributed to

tetraalkylammonium cations. As mentioned before, the rank order of the strongly-hydrated anions correlates not with surface tension parameters but their entropy of hydration instead. Thus, we were interested to see if such a correlation existed for the tetraalkylammonium cations.

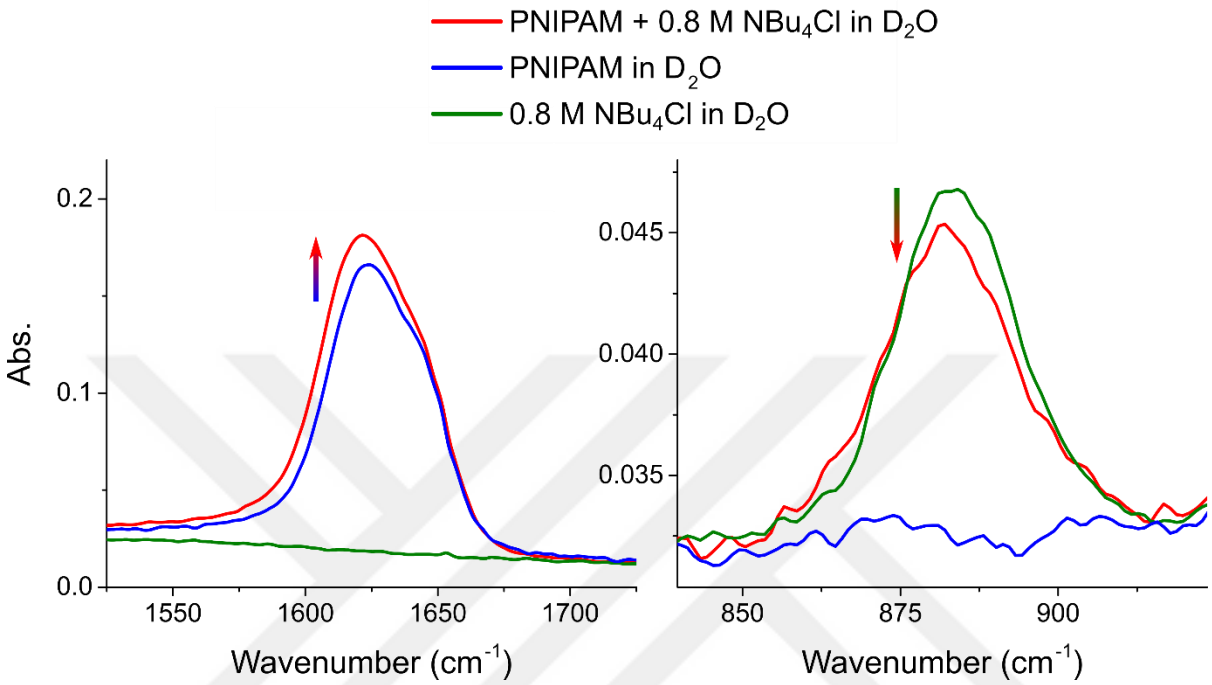

Figure 28: ATR-FTIR spectra measured above the LCST showing the change in the PNIPAM amide I band due to the presence of 0.8 M NBu_4Cl (left), and the change in a characteristic NBu_4Cl peak due to the presence of PNIPAM (right). Arrows indicate the direction of the changes.

Figure 29 shows the *c* parameters derived from the fitted LCST data for the six salts tested in this work against several physicochemical and physical parameters. As can be seen in Figure 29a, there indeed appears to be a correlation between the values of *c* and hydration entropies amongst the tetraalkylammonium cations. Panels (b) and (c) in Figure 29 depict additional possible correlations with polarizability and cation radii.

Zhang et al.[9] and Cho et al.[103] interpreted the correlation with hydration entropy as signifying the role of polarization of the macromolecule hydration shell by proximal anions. In this conjecture, anions sharing hydration water with the polymer destabilize its hydration by preferentially orienting water molecules through their stronger dipoles, and thus drive the minimization of the macromolecular solvated surface area. Hydration entropies, then, express the capacity of an ion to strongly order the orientation of surrounding water. While not

implausible, this mechanistic model was not supported with experimental or theoretical evidence in the years since. Instead, entropic driving forces are more often invoked in 'excluded volume' based conceptualizations of salting-out. In this viewpoint, the entropy of hydration (or more specialized, specifically defined entropy parameters, such as Marcus's structural entropy[262]) is understood as relating to the 'available volume' that a given solute takes up in its dissolution. Then, the entropic favorability of the dissolution of a cosolute is attenuated by the simple argument that the amount of free volume it can occupy has been reduced. Based on the combined findings of the present work, we are more partial to this model as a way to understand the behavior of the tetraalkylammonium cations. As can be seen from Figure 29, the hydration entropies of these cations are quite large and negative in value; although the structural effects of QA ions in solution remain contentious,[231,233] and potentially in need of further study to explore a molecular-level, detailed picture, we believe that this phenomenological correlation is in general accord with excluded volume-driven salting-out effects that can be expected from these large, hydrophobic cations.

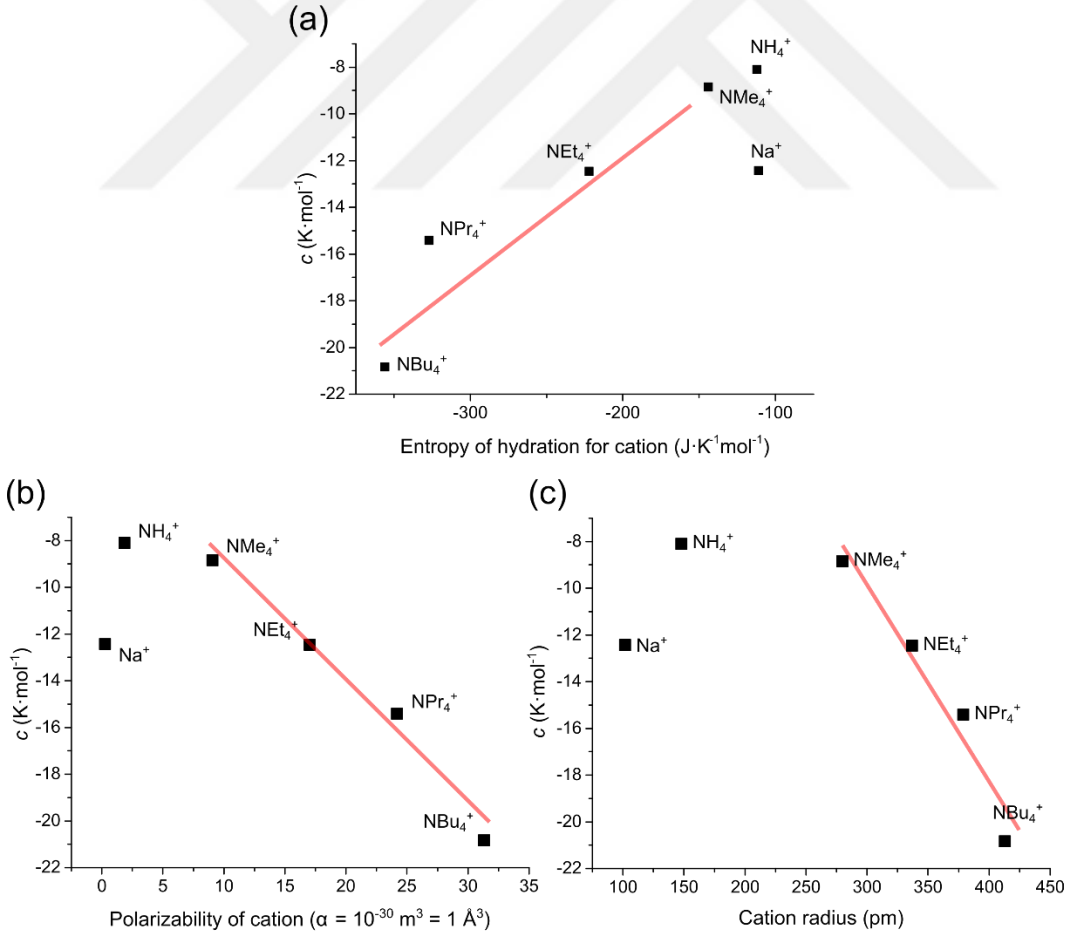

Figure 29: Plots of *c* values obtained by fitting the PNIPAM LCST's for the series of salts to Equation 9, as shown in Table 1, against: (a) the entropy of hydration, (b) polarizability, and

(c) ionic radius, for the respective cations. The source for the cation-specific values is Marcus,[232] who partitions experimental values between cation and anion pairs through explicit assumptions, some extra-thermodynamic. The ionic radii given for the tetraalkylammonium cations are their van der Waals radii. The red lines in each panel are a rough approximation of the correlation and meant to serve only as a guide to the eye.

3.3 Proposed Mechanism and Generality: Is This Effect Universal? Studies Using Other Polymers.

As a last branch of this thesis, we investigated the specific ion effects of the tetraalkylammonium chloride salts on other model macromolecules. Although PNIPAM is a well-studied, widespread and useful model for the generalized behavior of (bio)macromolecules, it is valid to ask whether the findings of this study might or might not extend to other macromolecular systems.

Moving beyond PNIPAM as our principle model, the first polymer that we incorporated into our testing was poly(*N,N*-diethylacrylamide) (PDEA), which is a closely related derivative of PNIPAM and a polymer that should also be familiar from the discourse of the Hofmeister effects literature given in Chapter 1 – Introduction. PDEA is also a thermoresponsive polymer, and its LCST (31.92 ± 0.08°C in neat water as determined by our measurements) is quite close to that of PNIPAM. Nevertheless, it has distinct structural and physical differences to PNIPAM that grant it chemical utility. For instance, PDEA has a tertiary amide moiety and thus does not possess an -NH- group as a hydrogen-bond donor. This fact was highlighted by Rembert et al.[112] in their previously discussed study of PNIPAM and PDEA, where they demonstrated that despite this structural difference the binding of weakly-hydrated anions to PDEA is not particularly impeded.

Figure 30 shows the structure of PDEA along with the measured LCST as a function of salt concentration for the same set of six salts investigated in section 3.2.1. As can be seen, the LCST effects of the six salts are qualitatively very similar to those observed with PNIPAM. Namely, whilst the classical, nonbinding weakly-hydrated salts NaCl and NH_4Cl elicit linearly decreasing LCST curves indicative of salting-out, starting with NEt_4Cl a distinct nonlinearity appears as a salting-in component at lower concentrations, followed by a fairly steep shift to salting-out. The effects of the larger salts are particularly striking; NPr_4Cl exhibits an even stronger nonlinearity/curvature such that it attains an LCST maximum at around 0.5 M, and the elevation in LCST at the maximum is larger than that observed with PNIPAM. The behavior

of NBu_4Cl is more striking still, so as to appear anomalous; within the concentration ranges tested, the LCST of PDEA – NBu_4Cl aqueous solutions appeared to rise monotonically and unbounded. No maximum could be observed within the testable range of temperature and concentration.

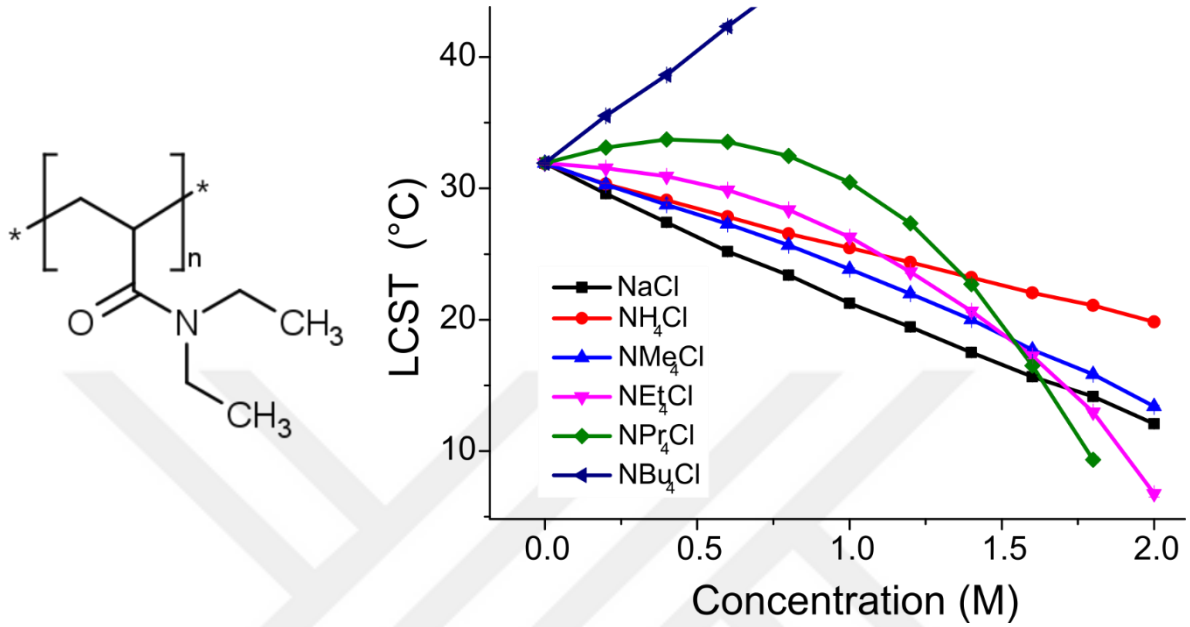

Figure 30: Left: Structure of poly(*N,N*-diethylacrylamide) (PDEA**)** Right: LCST of 5 mg/mL PDEA in aqueous solutions of the salts shown. Note that the trend lines are not mathematical fits, but meant only as a guide to the eye.

It appears, therefore, that PDEA's interaction with the tetraalkylammonium cations is similar to, if not more significant than those of PNIPAM. Again, we observe a distinct salting-in phenomenon, suggesting specific binding and correlating with the size and hydrophobic character of the cation. The extreme case of NBu_4Cl is anomalous and though much considered throughout the project duration, its elucidation is left outside the scope of this work.

The second model polymer chosen for a similar set of experiments is poly(ethylene oxide) (PEO) whose structure is shown below in Figure 31. As can be seen, this polymer is structurally totally disparate from the amide-based PNIPAM and PDEA. Although it finds similar use as a model macromolecule in specific ion effect studies[90]—owing to its thermoresponsive behavior and widespread availability at different molecular weights—the straight-chain simplicity of its structure and in particular the apparent lack of any locally hydrophobic environment within the polymer are striking. Figure 31 depicts the results of LCST measurements using the same six salts as before in aqueous solutions of 20 mg/mL PEO. Note that the LCST of PEO in neat water is quite high, at 98°C by our determination. This

unfortunately limits the range of concentrations that can be tested with strongly salting-in salts. Nevertheless, the data shown in Figure 31 are quite instructive; here again, we see a very similar qualitative picture emerge where from NEt_4Cl onwards, the tetraalkylammonium chloride salts effect a very significant salting-in on the macromolecule. In this case, the magnitudes of the salting-in contributions are the largest yet; for the first time amongst the tested polymers, NEt_4Cl's salting-in effect is strong enough to produce a significant nonmonotonic LCST curve having a late maximum at ~0.8 M NEt_4Cl. The LCST curves of the two largest salts rise upwards very steeply and rapidly extend beyond the measurable temperature window.

A point to consider is that due to the elevated temperatures involved in the LCST phase transitions of this polymer, the thermodynamic energy states of bulk water and its hydration behavior is likely to be distinct from those observed in PNIPAM and PDEA experiments. Nevertheless, what is remarkable is that the weakly-hydrated, highly hydrophobic tetraalkylammonium cations exhibit an (apparently strongest) binding to the PEO polymer, despite the evident lack of major hydrophobic moieties on the polymer chain, which we know are preferential interaction sites for these cations. This observation points to the generality and likely universality of the specific ion effects of the tetraalkylammonium cations on (bio)macromolecules, proteins, lipid assemblies and likely any other colloidal, (bio)interfacial system where the hydration behavior of soft matter is governed by a balance of hydrophilic and hydrophobic forces, or the molecular structure otherwise contains both polar and nonpolar motifs.

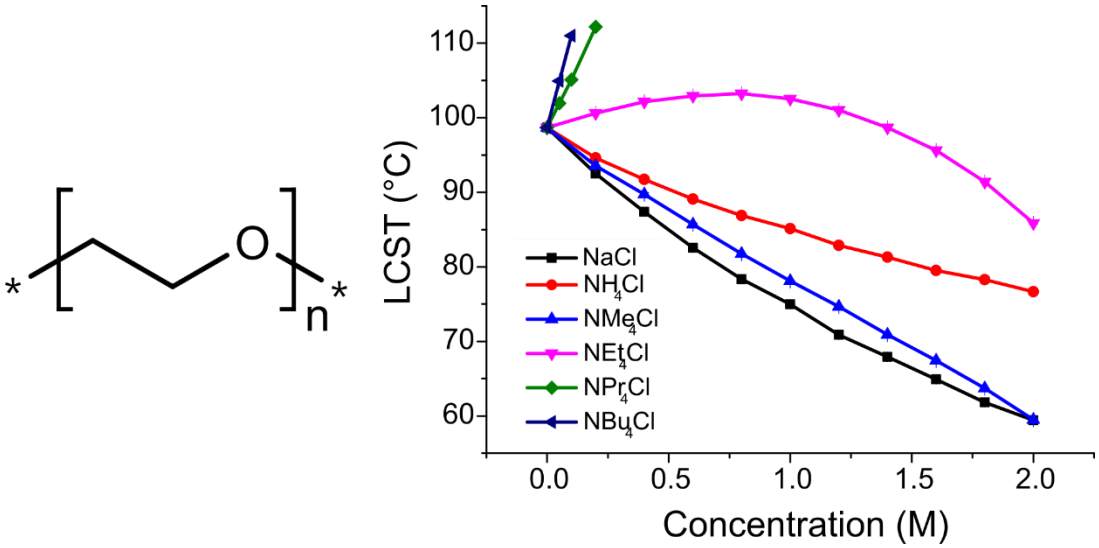

Figure 31: Left: Structure of poly(ethylene oxide) (PEO). Right: LCST of 20 mg/mL PEO in aqueous solutions of the salts shown. The data trend lines are not mathematical fits, and are

meant only as guides to the eye. The NPr_4Cl and NBu_4Cl series were measured to as high a salt concentration as possible, but boiling of the aqueous solutions swiftly limits the measurement.

From our results presented herein, we feel confident that the value of the work of expanding beyond limited understandings of classical Hofmeister cation effects is apparent. The findings presented in this thesis indicate that the traditional, linear Hofmeister rank order spanning weakly- to strongly-hydrated metal cations does not capture the complete diversity and richness of cation behavior. We envision that expanding beyond the weakly-hydrated metal cations, which cut-off cation interactions in most literature orderings, the purely salting-out behavior of the latter gives way to a new salting-in driving force that operates by a completely different mechanism than that of the strongly-hydrated cations (represented in Figure 32, as a summary of the main findings of this thesis). The behavior of sufficiently hydrophobic or 'greasy' cations is dominated by hydrophobic interactions at the weakly-hydrated centers of macromolecular interfaces, and rivals if not outright exceeds the effects of classical binding ions like weakly-hydrated anions in magnitude. In this sense, the 'inverted volcano-plot' of salting-in effects (Figure 33) stretches across the cation series and hints at the trove of rich physical chemistry at the biological interface that remains to be understood.

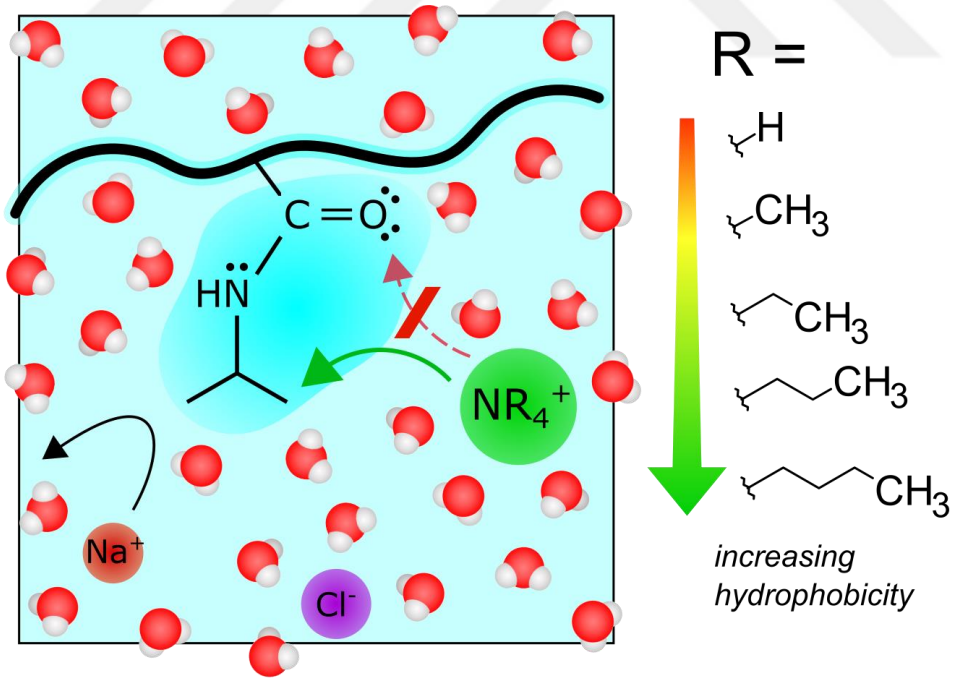

Figure 32: A schematic representation of the main findings of the present work: the molecular mechanism for the salting-in effects of the tetraalkylammonium chloride salts. Unlike weakly-hydrated metal cations like Na^+, which are depleted from the macromolecular interface, these 'greasy' weakly-hydrated cations interact preferentially with the most hydrophobic groups on

macromolecules, i.e., the isopropyl group on the PNIPAM side-chain. The propensity for interaction increases with the length of the alkyl substituents on the cation, i.e., increasing cation hydrophobicity. There is no primary binding to the carbonyl group, unlike that observed for strongly-hydrated anions.

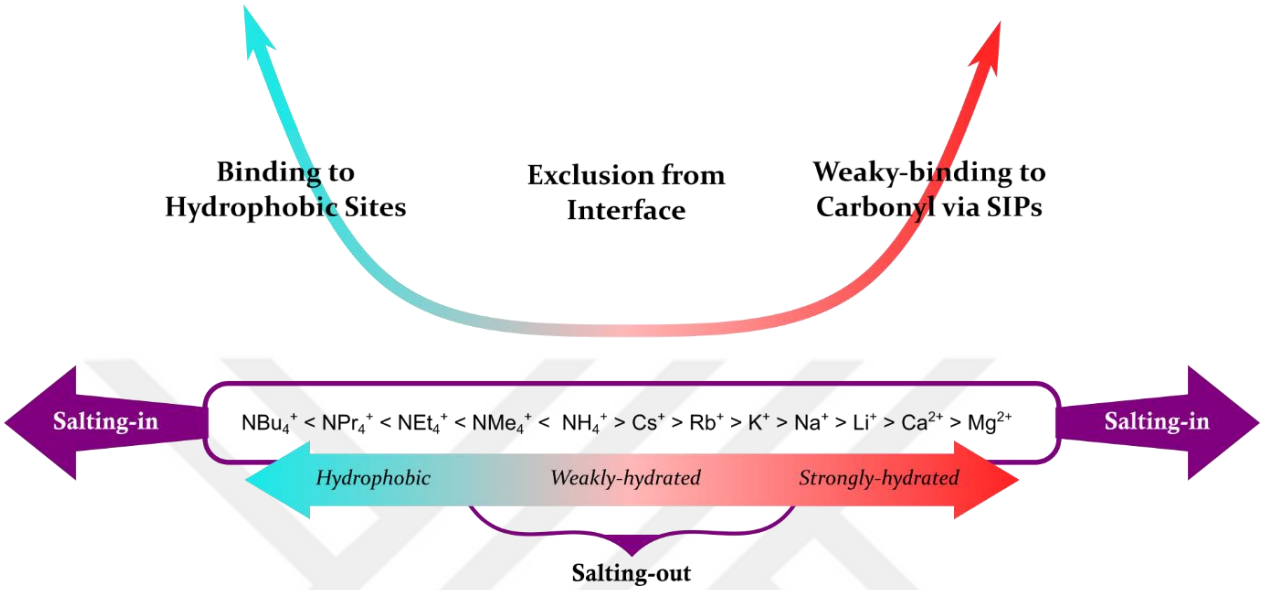

Figure 33: A new, expanded view of the Hofmeister cation series is proposed. On one end, strongly-hydrated cations exhibit weak binding to partially negatively-charged, polar groups (e.g., amide carbonyls) mediated through ion pairing with counter-anions, and thus produce a salting-in effect. In the middle regions of the series, weakly-hydrated cations do not exhibit any binding and are excluded from macromolecular interfaces, leading to salting-out. On the far weakly-hydrated end of the spectrum, large cations such as tetraalkylammonium cations salt-in at low to moderate concentrations by virtue of their binding to specific hydrophobic sites on macromolecules. This binding is facilitated through an entirely novel, hydrophobically-based interaction mechanism and scales with the 'greasiness' of the cations.

Chapter 4 – Conclusion

In the 130-year history of the pursuit of a molecular-level understanding of Hofmeister effects—the ubiquitous, unremittingly complex and deeply fundamental physical chemistry of ions in solution and everything that their effects dictate at the intersections of biophysics and chemistry—significant strides have been made in recent years. After the development of molecular-level models of anionic effects, the often-overlooked cationic series has recently begun to be better characterized. The work presented in this thesis represents our contribution to this nascent field, by presenting a broader and more complete picture of cation Hofmeister effects. Classical conceptions of kosmotropic and chaotropic metal cations have only recently been better characterized as a series spanning, from one end, the strongly-hydrated cations which display some binding to specific polar centers (e.g., amide carbonyl groups), to the non-interacting, weakly-hydrated cations on the other, traditionally understood only as passive contributors to salting-out effects. Thus, the Hofmeister chemistry of cation hydrophobicity, i.e., the region that lies beyond traditional cut-off points at the chaotropic edge of the series remained, until the present work, unexplored.

Herein, we systematically characterized the effects of increasingly 'greasy', large hydrophobic cations using a variety of experimental techniques and demonstrate that entirely different, novel mechanisms govern their behavior. We carried out the systematic study of quaternary ammonium (QA) chloride salts, in the form of a series of tetraalkylammonium chlorides with incremental alkyl chain lengths, thus encompassing a broad range of cation sizes and properties. Namely, our scope spanned salts of the form: NR_4Cl where R = H, Me, Et, *n*-Pr, and *n*-Bu. Phase transition temperature (LCST) measurements of the model neutral, thermoresponsive polymer PNIPAM clearly demonstrated that these very weakly-hydrated cations, most strikingly, exhibit significant salting-in of macromolecules at low-to-midrange concentrations, and this effect intensifies with increasing cation hydrophobicity. Moreover, the interaction mechanism was subsequently found to be strictly distinct from that recently elucidated for the strongly-hydrated cations. ATR-FTIR investigations of the polymer in salt solutions below its LCST point evinced that the carbonyl—the most obvious partial-negative center—is not the primary site of interaction for these cations. The amide I band of PNIPAM (occurring at 1625 cm^{-1} in neat D_2O and consisting primarily of the carbonyl C=O stretch) was observed to be unchanged by the presence of the salts, and no statistically-consistent population of cation-bound carbonyl signature was observed. The largest of the QA salts (NPr_4Cl and

NBu_4Cl) were found to produce a slight distortion in the amide I bands, and this was later understood as resulting from the proximal binding at a different site on the polymer. Specifically, a quantitative, externally-referenced ^{1}H-NMR titration methodology was developed and shown to successfully distinguish and quantify ion-macromolecule interactions in solution, which was then employed in order to extensively probe all molecular groups on the PNIPAM polymer in the presence of the QA salts. The results revealed that, indeed, the QA cations bind to the most hydrophobic moiety on the polymer (consisting primarily of the isopropyl terminal methyl groups, and secondarily involving the adjacent methine group connected to the amide nitrogen), and that the interaction magnitude scaled with the cation hydrophobicity. With the largest cations, the binding dissociation constant was calculated to be as tight at $K_D \approx 0.23$ M. Thus, a completely novel mechanism for cation interaction in the form of a saturable, hydrophobically-driven binding of QA cations to these specific polymer sites was demonstrated.

The mechanism of the salting-out effect of the QA salts at higher concentrations, where the effect can exceed and overcome the salting-in component, was found to correlate with the entropy of hydration of the cations. Based on similar correlations found to hold for the salting-out effects of strongly-hydrated anions, the mechanism was phenomenologically understood as an excluded volume effect. That is, crowding by high concentrations of these bulky ions in solution is able to entropically disfavor the solvation of macromolecules through reducing the effective free solution volume. Lastly, the universality of our conclusions was investigated by studying additional model polymers with methods similar to those utilized for PNIPAM. With both poly(*N,N*-diethylacrylamide) (PDEA; a polymer structurally related to PNIPAM) and poly(ethylene oxide) (PEO; an entirely dissimilar one), the trends were qualitatively the same: the QA salts were observed to salt in all of the tested polymers with the same apparent behavior, indicative of saturable binding at lower concentrations and excluded volume-driven salting-out at higher ones. The interaction was confirmed once more to correlate with the cation hydrophobicity, and was furthermore more pronounced with PDEA, as well as PEO. Thus, even with structurally very distinct macromolecules, the generalized mechanism of the Hofmeister effects of the QA cations was found to hold.

As a result of these findings presented herein, we conceive of the Hofmeister cation series as extending beyond the limits of the commonly studied metal cations and thus forming an ‘inverted volcano curve’ of cation interactivity whereby, on the strongly-hydrated end, cations exhibit a weak affinity for negative, polar groups driven electrostatically, whereas in

the far weakly-hydrated region where the tetraalkylammonium cations reside, the cations gain affinity for macromolecular moieties mediated by hydrophobic interactions. Thus, a more holistic understanding of specific cation effects is reached, and what we see as a valuable piece of the puzzle of understanding the rich diversity of specific ion effects present in nature—which commonly employs weakly-hydrated, 'greasy' cationic motifs in osmolytes, lipids and other important biomolecules—is contributed, with promising future prospects for fundamental studies of Hofmeister ion effects in the scientific field at large.

References

1. Collins, K. D. & Washabaugh, M. W. The Hofmeister effect and the behaviour of water at interfaces. *Q Rev Biophys* **18**, 323–422 (1985).

2. Baldwin, R. L. How Hofmeister ion interactions affect protein stability. *Biophys J* **71**, 2056–2063 (1996).

3. Cacace, M. G., Landau, E. M. & Ramsden, J. J. The Hofmeister series: Salt and solvent effects on interfacial phenomena. *Q Rev Biophys* **30**, 241–277 (1997).

4. Kunz, W., Lo Nostro, P. & Ninham, B. W. The present state of affairs with Hofmeister effects. *Curr Opin Colloid Interface Sci* **9**, 1–18 (2004).

5. Zhang, Y. & Cremer, P. S. Interactions between macromolecules and ions: the Hofmeister series. *Curr Opin Chem Biol* **10**, 658–663 (2006).

6. Nostro, P. Lo *et al.* Hofmeister specific ion effects in two biological systems. *Curr Opin Colloid Interface Sci* **9**, 97–101 (2004).

7. Nostro, P. Lo *et al.* Specific ion effects on the growth rates of Staphylococcus aureus and Pseudomonas aeruginosa. *Phys Biol* **2**, 1 (2005).

8. Jungwirth, P., Rosenfeld, D. & Buch, V. A possible new molecular mechanism of thundercloud electrification. *Atmos Res* **76**, 190–205 (2005).

9. Zhang, Y., Furyk, S., Bergbreiter, D. E. & Cremer, P. S. Specific Ion Effects on the Water Solubility of Macromolecules: PNIPAM and the Hofmeister Series. *J Am Chem Soc* **127**, 14505–14510 (2005).

10. Bruce, E. E. *et al.* Molecular Mechanism for the Interactions of Hofmeister Cations with Macromolecules in Aqueous Solution. *J Am Chem Soc* **142**, 19094–19100 (2020).

11. Challis, J. Report on the present state of the analytical theory of hydrostatics and hydrodynamics. *British Association Reports IV* 253 (1834).

12. Lo Nostro, P. & Ninham, B. W. Hofmeister Phenomena: An Update on Ion Specificity in Biology. *Chem Rev* **112**, 2286–2322 (2012).

13. Wilson, E. K. A Renaissance for Hofmeister. *Chemical & Engineering News Archive* **85**, 47–49 (2007).

14. Lo Nostro, P. & Ninham, B. W. Editorial: Electrolytes and specific ion effects. New and old horizons. *Curr Opin Colloid Interface Sci* **23**, A1–A5 (2016).

15. Jungwirth, P. & Cremer, P. S. Beyond Hofmeister. *Nat Chem* **6**, 261–263 (2014).

16. Okur, H. I. *et al.* Beyond the Hofmeister Series: Ion-Specific Effects on Proteins and Their Biological Functions. *J Phys Chem B* **121**, 1997–2014 (2017).

17. Assaf, K. I. & Nau, W. M. The Chaotropic Effect as an Assembly Motif in Chemistry. *Angewandte Chemie International Edition* **57**, 13968–13981 (2018).

18. Leontidis, E. Chaotropic salts interacting with soft matter: Beyond the lyotropic series. *Curr Opin Colloid Interface Sci* **23**, 100–109 (2016).

19. Drummond, C., Pérez-Fuentes, L. & Bastos-González, D. Can Polyoxometalates Be Considered as Superchaotropic Ions? *The Journal of Physical Chemistry C* **123**, 28744–28752 (2019).

20. Hofmeister, F. Zur Lehre von der Wirkung der Salze. *Archiv für experimentelle Pathologie und Pharmakologie* **25**, 1–30 (1888).

21. Hofmeister, F. Zur Lehre von der Wirkung der Salze. *Archiv für experimentelle Pathologie und Pharmakologie* **24**, 247–260 (1888).

22. Kunz, W., Henle, J. & Ninham, B. W. 'Zur Lehre von der Wirkung der Salze' (about the science of the effect of salts): Franz Hofmeister's historical papers. *Curr Opin Colloid Interface Sci* **9**, 19–37 (2004).

23. v. Limbeck, R. Zur Lehre von der Wirkung der Salze. *Archiv für experimentelle Pathologie und Pharmakologie* **25**, 69–86 (1888).

24. Hofmeister, F. 24. Zur Lehre von der Wirkung der Salze. *Archiv für experimentelle Pathologie und Pharmakologie* **27**, 395–413 (1890).

25. Hofmeister, F. Zur Lehre von der Wirkung der Salze. *Archiv für experimentelle Pathologie und Pharmakologie* **28**, 210–238 (1891).

26. Voet, A. Quantative Lyotropy. *Chem Rev* **20**, 169–179 (1937).

27. Green, A. A. Studies in the Physical Chemistry of the Proteins: X. The Solubility of Hemoglobin in Solutions of Chlorides and Sulfates of Varying Concentration. *Journal of Biological Chemistry* **95**, 47–66 (1932).

28. Cohn, E. J. & Edsall, J. T. *Proteins, amino acids and peptides as ions and dipolar ions*. (Reinhold Publishing Corporation, 1943).

29. Setschenow, J. Über die konstitution der salzlösungen auf grund ihres verhaltens zu kohlensäure. *Zeitschrift für Physikalische Chemie* **4**, 117–125 (1889).

30. McDevit, W. F. & Long, F. A. The Activity Coefficient of Benzene in Aqueous Salt Solutions. *J Am Chem Soc* **74**, 1773–1777 (1952).

31. Darmois, E. Salt effect and rotatory power. *Transactions of the Faraday Society* **26**, 384–390 (1930).

32. Gustavson, K. H. *The Chemistry and Reactivity of Collagen*. (Academic Press, 1956).

33. Bello, J., Riese, H. C. A. & Vinograd, J. R. Mechanism of Gelation of Gelatin. Influence of Certain Electrolytes on the Melting Points of Gels of Gelatin and Chemically Modified Gelatins. *J Phys Chem* **60**, 1299–1306 (1956).

34. von Hippel, P. H. & Wong, K.-Y. The Effect of Ions on the Kinetics of Formation and the Stability of the Collagen-Fold. *Biochemistry* **1**, 664–674 (1962).

35. von Hippel, P. H. & Wong, K.-Y. The Collagen Gelatin Phase Transition. I. Further Studies of the Effects of Solvent Environment and Polypeptide Chain Composition. *Biochemistry* **2**, 1387–1398 (1963).

36. von Hippel, P. H. & Wong, K.-Y. Neutral Salts: The Generality of Their Effects on the Stability of Macromolecular Conformations. *Science* **145**, 577–580 (1964).

37. von Hippel, P. H. & Wong, K.-Y. On the Conformational Stability of Globular Proteins: The Effects of Various Electrolytes and Nonelectrolytes on the Thermal Ribonuclease Transition. *Journal of Biological Chemistry* **240**, 3909–3923 (1965).

38. Sinanoglu, O. & Abdulnur, S. Effect of water and other solvents on the structure of biopolymers. in *Federation proceedings* vol. 24 S12–S23 (1965).

39. Robinson, D. R. & Jencks, W. P. The effect of concentrated salt solutions on the activity coefficient of acetyltetraglycine ethyl ester. *J Am Chem Soc* **87**, 2470–2479 (1965).

40. Cox, W. M. & Wolfenden, J. H. The viscosity of strong electrolytes measured by a differential method. *Proceedings of the Royal Society of London. Series A, Containing Papers of a Mathematical and Physical Character* **145**, 475–488 (1934).

41. Gurney, R. W. *Ionic Processes in Solution*. (McGraw-Hill, 1953).

42. Marcus, Y. *Ions in Solution and their Solvation*. (John Wiley & Sons, 2015).

43. Derjaguin, B. V. Theory of the stability of strongly charged lyophobic sol and of the adhesion of strongly charged particles in solutions of electrolytes. *Acta phys. chim. URSS* **14**, 633 (1941).

44. Derjaguin, B. V & Landau, L. D. Theory of Stability of Highly Charged Lyophobic Sols and Aggregation of Highly Charged Particles in Electrolyte Solutions. *Zh. Eksp. Teor. Fiz.* **11**, 802–821 (1941).

45. Derjaguin, B. & Landau, L. A theory of the stability of highly charged lyophobic sols and of the adhesion of particles in electrolyte solutions. *Zh Eksp Teor Fiz* **15**, 662 (1945).

46. Verwey, E. J. W. Theory of the stability of lyophobic colloids. *J Phys Chem* **51**, 631–636 (1947).

47. Israelachvili, J. N. *Intermolecular and surface forces*. (Academic Press, 1991).

48. Ninham, B. W. & Yaminsky, V. Ion Binding and Ion Specificity: The Hofmeister Effect and Onsager and Lifshitz Theories. *Langmuir* **13**, 2097–2108 (1997).

49. Boström, M., Williams, D. R. M. & Ninham, B. W. Specific Ion Effects: Why DLVO Theory Fails for Biology and Colloid Systems. *Phys Rev Lett* **87**, 168103 (2001).

50. Boström, M., Williams, D. R. M. & Ninham, B. W. Ion specificity of micelles explained by ionic dispersion forces. *Langmuir* **18**, 6010–6014 (2002).

51. Boström, M., Lonetti, B., Fratini, E., Baglioni, P. & Ninham, B. W. Why pH titration in protein solutions follows a Hofmeister series. *J Phys Chem B* **110**, 7563–7566 (2006).

52. Salis, A. *et al.* Specific anion effects on glass electrode pH measurements of buffer solutions: bulk and surface phenomena. *J Phys Chem B* **110**, 2949–2956 (2006).

53. Boström, M., Williams, D. R. M. & Ninham, B. W. Specific ion effects: why the properties of lysozyme in salt solutions follow a Hofmeister series. *Biophys J* **85**, 686–694 (2003).

54. Boström, M., Williams, D. R. M. & Ninham, B. W. The influence of ionic dispersion potentials on counterion condensation on polyelectrolytes. *J Phys Chem B* **106**, 7908–7912 (2002).

55. Boström, M., Kunz, W. & Ninham, B. W. Hofmeister effects in surface tension of aqueous electrolyte solution. *Langmuir* **21**, 2619–2623 (2005).

56. Jungwirth, P. & Tobias, D. J. Specific ion effects at the air/water interface. *Chem Rev* **106**, 1259–1281 (2006).

57. Ghosal, S. *et al.* Electron spectroscopy of aqueous solution interfaces reveals surface enhancement of halides. *Science* **307**, 563–566 (2005).

58. Sinanoglu, O. Solvent effects on molecular associations. in *Molecular Associations in Biology* (ed. Pullman, B.) 427–445 (1968).

59. Fernández, A. & Sinanoğlu, O. Denaturation of proteins in methanol/water mixtures. *Biophys Chem* **21**, 163–166 (1985).

60. Sinanoğlu, O. & Fernández, A. The denaturation maxima of proteins and of drug-biomolecule complex formation in a wide range of methanol/water mixtures: Solvophobic theory predictions as compared to experiments. *Biophys Chem* **21**, 157–162 (1985).

61. Nandi, P. K. & Robinson, D. R. Effects of salts on the free energies of nonpolar groups in model peptides. *J Am Chem Soc* **94**, 1308–1315 (1972).

62. Sharp, K. A., Nicholls, A., Fine, R. F. & Honig, B. Reconciling the Magnitude of the Microscopic and Macroscopic Hydrophobic Effects. *Science* **252**, 106–109 (1991).

63. Pratt, L. R. & Pohorille, A. Theory of hydrophobicity: Transient cavities in molecular liquids. *Proceedings of the National Academy of Sciences* **89**, 2995–2999 (1992).

64. Sinanoğlu, O. Microscopic surface tension down to molecular dimensions and microthermodynamic surface areas of molecules or clusters. *J Chem Phys* **75**, 463–468 (1981).

65. Arakawa, T. & Timasheff, S. N. Preferential interactions of proteins with salts in concentrated solutions. *Biochemistry* **21**, 6545–6552 (1982).

66. Omta, A. W., Kropman, M. F., Woutersen, S. & Bakker, H. J. Negligible Effect of Ions on the Hydrogen-Bond Structure in Liquid Water. *Science* **301**, 347–349 (2003).

67. Kropman, M. F. & Bakker, H. J. Effect of Ions on the Vibrational Relaxation of Liquid Water. *J Am Chem Soc* **126**, 9135–9141 (2004).

68. Kropman, M. F. & Bakker, H. J. Femtosecond mid-infrared spectroscopy of aqueous solvation shells. *J Chem Phys* **115**, 8942–8948 (2001).

69. Omta, A. W., Kropman, M. F., Woutersen, S. & Bakker, H. J. Influence of ions on the hydrogen-bond structure in liquid water. *J Chem Phys* **119**, 12457–12461 (2003).

70. Kropman, M. F. & Bakker, H. J. Vibrational relaxation of liquid water in ionic solvation shells. *Chem Phys Lett* **370**, 741–746 (2003).

71. Kropman, M. F. & Bakker, H. J. Dynamics of Water Molecules in Aqueous Solvation Shells. *Science* **291**, 2118–2120 (2001).

72. Batchelor, J. D., Olteanu, A., Tripathy, A. & Pielak, G. J. Impact of Protein Denaturants and Stabilizers on Water Structure. *J Am Chem Soc* **126**, 1958–1961 (2004).

73. Chalikian, T. V. Structural Thermodynamics of Hydration. *J Phys Chem B* **105**, 12566–12578 (2001).

74. Head-Gordon, T. & Hura, G. Water Structure from Scattering Experiments and Simulation. *Chem Rev* **102**, 2651–2670 (2002).

75. Gurau, M. C. *et al.* On the Mechanism of the Hofmeister Effect. *J Am Chem Soc* **126**, 10522–10523 (2004).

76. Gurau, M. C. *et al.* Thermodynamics of Phase Transitions in Langmuir Monolayers Observed by Vibrational Sum Frequency Spectroscopy. *J Am Chem Soc* **125**, 11166–11167 (2003).

77. Aroti, A., Leontidis, E., Maltseva, E. & Brezesinski, G. Effects of Hofmeister Anions on DPPC Langmuir Monolayers at the Air−Water Interface. *J Phys Chem B* **108**, 15238–15245 (2004).

78. Neilson, G. W., Broadbent, R. D., Howell, I. & Tromp, R. H. Faraday research article. Structural and dynamical aspects of aqueous ionic solutions. *Journal of the Chemical Society, Faraday Transactions* **89**, 2927–2936 (1993).

79. Leberman, R. & Soper, A. K. Effect of high salt concentrations on water structure. *Nature* **378**, 364–366 (1995).

80. Mancinelli, R., Botti, A., Bruni, F., Ricci, M. A. & Soper, A. K. Perturbation of water structure due to monovalent ions in solution. *Physical Chemistry Chemical Physics* **9**, 2959–2967 (2007).

81. Chen, Y. *et al.* Electrolytes induce long-range orientational order and free energy changes in the H-bond network of bulk water. *Sci Adv* **2**, e1501891 (2016).

82. Chen, Y., Okur, H. I., Liang, C. & Roke, S. Orientational ordering of water in extended hydration shells of cations is ion-specific and is correlated directly with viscosity and hydration free energy. *Physical Chemistry Chemical Physics* **19**, 24678–24688 (2017).

83. Chen, Y., Dupertuis, N., Okur, H. I. & Roke, S. Temperature dependence of water-water and ion-water correlations in bulk water and electrolyte solutions probed by femtosecond elastic second harmonic scattering. *J Chem Phys* **148**, 222835 (2018).

84. Robertson, T. B. Contributions to the Theory of the Mode of Action of Inorganic Salts upon Proteins in Solution. *Journal of Biological Chemistry* **9**, 303–326 (1911).

85. Ries-Kautt, M. M. & Ducruix, A. F. Relative Effectiveness of Various Ions on the Solubility and Crystal Growth of Lysozyme. *Journal of Biological Chemistry* **264**, 745–748 (1989).

86. Nandi, P. K. & Robinson, D. R. Effects of salts on the free energy of the peptide group. *J Am Chem Soc* **94**, 1299–1308 (1972).

87. Gregor, H. P., Belle, J. & Marcus, R. A. Studies on ion-exchange resins. XIII. Selectivity coefficients of quaternary base anion-exchange resins toward univalent anions. *J Am Chem Soc* **77**, 2713–2719 (1955).

88. Hladílková, J. *et al.* Effects of End-Group Termination on Salting-Out Constants for Triglycine. *J Phys Chem Lett* **4**, 4069–4073 (2013).

89. Paterová, J. *et al.* Reversal of the Hofmeister Series: Specific Ion Effects on Peptides. *J Phys Chem B* **117**, 8150–8158 (2013).

90. Rogers, B. A. *et al.* Weakly hydrated anions bind to polymers but not monomers in aqueous solutions. *Nat Chem* **14**, 40–45 (2022).

91. Bergbreiter, D. E., Hughes, R., Besinaiz, J., Li, C. & Osburn, P. L. Phase-Selective Solubility of Poly(N-alkylacrylamide)s. *J Am Chem Soc* **125**, 8244–8249 (2003).

92. Yang, Y. *et al.* Reversible Changes in Solution pH Resulting from Changes in Thermoresponsive Polymer Solubility. *J Am Chem Soc* **134**, 7378–7383 (2012).

93. Sun, J. *et al.* Effect of Molecular Structure on Thermoresponsive Behaviors of Pyrrolidone-Based Water-Soluble Polymers. *Macromolecules* **43**, 4041–4049 (2010).

94. Kadam, Y. *et al.* Induced micellization and micellar transitions in aqueous solutions of non-linear block copolymer Tetronic® T904. *J Colloid Interface Sci* **351**, 449–456 (2010).

95. Patel, K., Bharatiya, B., Kadam, Y. & Bahadur, P. Micellization and Clouding Behavior of EO–PO Block Copolymer in Aqueous Salt Solutions. *J Surfactants Deterg* **13**, 89–95 (2010).

96. Yan, Y., Li & Hoffmann, H. Clouding: Origin of Phase Separation in Oppositely Charged Polyelectrolyte/Surfactant Mixed Solutions. *J Phys Chem B* **110**, 1949–1954 (2006).

97. Bloksma, M. M., Bakker, D. J., Weber, C., Hoogenboom, R. & Schubert, U. S. The Effect of Hofmeister Salts on the LCST Transition of Poly(2-oxazoline)s with Varying Hydrophilicity. *Macromol Rapid Commun* **31**, 724–728 (2010).

98. Roy, D., Brooks, W. L. A. & Sumerlin, B. S. New directions in thermoresponsive polymers. *Chem Soc Rev* **42**, 7214–7243 (2013).

99. Tiktopulo, E. I. *et al.* 'Domain' Coil-Globule Transition in Homopolymers. *Macromolecules* **28**, 7519–7524 (1995).

100. Von Hippel, P. H., Peticolas, V., Schack, L. & Karlson, L. Model studies on the effects of neutral salts on the conformational stability of biological macromolecules. I. Ion binding to polyacrylamide and polystyrene columns. *Biochemistry* **12**, 1256–1264 (1973).

101. Song, J. D., Ryoo, R. & Jhon, M. S. Anion binding properties of poly(vinylpyrrolidone) in aqueous solution studied by halide NMR spectroscopy. *Macromolecules* **24**, 1727–1730 (1991).

102. Breslow, R. & Guo, T. Surface tension measurements show that chaotropic salting-in denaturants are not just water-structure breakers. *Proceedings of the National Academy of Sciences* **87**, 167–169 (1990).

103. Cho, Y. *et al.* Effects of Hofmeister Anions on the Phase Transition Temperature of Elastin-like Polypeptides. *J Phys Chem B* **112**, 13765–13771 (2008).

104. Meyer, D. E. & Chilkoti, A. Quantification of the Effects of Chain Length and Concentration on the Thermal Behavior of Elastin-like Polypeptides. *Biomacromolecules* **5**, 846–851 (2004).

105. Meyer, D. E. & Chilkoti, A. Genetically Encoded Synthesis of Protein-Based Polymers with Precisely Specified Molecular Weight and Sequence by Recursive Directional Ligation: Examples from the Elastin-like Polypeptide System. *Biomacromolecules* **3**, 357–367 (2002).

106. Yao, X. L. & Hong, M. Structure Distribution in an Elastin-Mimetic Peptide (VPGVG)3 Investigated by Solid-State NMR. *J Am Chem Soc* **126**, 4199–4210 (2004).

107. Ohgo, K., Ashida, J., Kumashiro, K. K. & Asakura, T. Structural Determination of an Elastin-Mimetic Model Peptide, (Val-Pro-Gly-Val-Gly)6, Studied by 13C CP/MAS NMR Chemical Shifts, Two-Dimensional off Magic Angle Spinning Spin-Diffusion NMR, Rotational Echo Double Resonance, and Statistical Distribution of Torsion Angles from Protein Data Bank. *Macromolecules* **38**, 6038–6047 (2005).

108. Flamia, R., Zhdan, P. A., Martino, M., Castle, J. E. & Tamburro, A. M. AFM Study of the Elastin-like Biopolymer Poly(ValGlyGlyValGly). *Biomacromolecules* **5**, 1511–1518 (2004).

109. Li, B., Alonso, D. O. V, Bennion, B. J. & Daggett, V. Hydrophobic Hydration Is an Important Source of Elasticity in Elastin-Based Biopolymers. *J Am Chem Soc* **123**, 11991–11998 (2001).

110. Schmidt, P., Dybal, J., Rodriguez-Cabello, J. C. & Reboto, V. Role of Water in Structural Changes of Poly(AVGVP) and Poly(GVGVP) Studied by FTIR and Raman Spectroscopy and ab Initio Calculations. *Biomacromolecules* **6**, 697–706 (2005).

111. Rembert, K. B. *et al.* Molecular Mechanisms of Ion-Specific Effects on Proteins. *J Am Chem Soc* **134**, 10039–10046 (2012).

112. Rembert, K. B., Okur, H. I., Hilty, C. & Cremer, P. S. An NH Moiety Is Not Required for Anion Binding to Amides in Aqueous Solution. *Langmuir* **31**, 3459–3464 (2015).

113. Schwierz, N., Horinek, D. & Netz, R. R. Reversed Anionic Hofmeister Series: The Interplay of Surface Charge and Surface Polarity. *Langmuir* **26**, 7370–7379 (2010).

114. von Hansen, Y., Kalcher, I. & Dzubiella, J. Ion Specificity in α-Helical Folding Kinetics. *J Phys Chem B* **114**, 13815–13822 (2010).

115. Heyda, J., Hrobárik, T. & Jungwirth, P. Ion-Specific Interactions between Halides and Basic Amino Acids in Water. *J Phys Chem A* **113**, 1969–1975 (2009).

116. Dzubiella, J. Salt-Specific Stability and Denaturation of a Short Salt-Bridge-Forming α-Helix. *J Am Chem Soc* **130**, 14000–14007 (2008).

117. Boström, M. *et al.* Why forces between proteins follow different Hofmeister series for pH above and below pI. *Biophys Chem* **117**, 217–224 (2005).

118. Zhang, Y. & Cremer, P. S. The inverse and direct Hofmeister series for lysozyme. *Proceedings of the National Academy of Sciences* **106**, 15249–15253 (2009).

119. Marcus, Y. *Ion solvation*. (Wiley, 1985).

120. Perez-Jimenez, R., Godoy-Ruiz, R., Ibarra-Molero, B. & Sanchez-Ruiz, J. M. The Efficiency of Different Salts to Screen Charge Interactions in Proteins: A Hofmeister Effect? *Biophys J* **86**, 2414–2429 (2004).

121. Chandler, D. Interfaces and the driving force of hydrophobic assembly. *Nature* **437**, 640–647 (2005).

122. Hande, V. R. & Chakrabarty, S. Structural Order of Water Molecules around Hydrophobic Solutes: Length-Scale Dependence and Solute–Solvent Coupling. *J Phys Chem B* **119**, 11346–11357 (2015).

123. Davis, J. G., Gierszal, K. P., Wang, P. & Ben-Amotz, D. Water structural transformation at molecular hydrophobic interfaces. *Nature* **491**, 582–585 (2012).

124. Stillinger, F. H. Structure in aqueous solutions of nonpolar solutes from the standpoint of scaled-particle theory. *J Solution Chem* **2**, 141–158 (1973).

125. Duboué-Dijon, E. & Laage, D. Characterization of the Local Structure in Liquid Water by Various Order Parameters. *J Phys Chem B* **119**, 8406–8418 (2015).

126. Gibb, C. L. D. & Gibb, B. C. Anion Binding to Hydrophobic Concavity Is Central to the Salting-in Effects of Hofmeister Chaotropes. *J Am Chem Soc* **133**, 7344–7347 (2011).

127. Sokkalingam, P., Shraberg, J., Rick, S. W. & Gibb, B. C. Binding Hydrated Anions with Hydrophobic Pockets. *J Am Chem Soc* **138**, 48–51 (2016).

128. Sullivan, M. R., Yao, W., Tang, D., Ashbaugh, H. S. & Gibb, B. C. The Thermodynamics of Anion Complexation to Nonpolar Pockets. *J Phys Chem B* **122**, 1702–1713 (2018).

129. Fox, J. M. *et al.* Interactions between Hofmeister Anions and the Binding Pocket of a Protein. *J Am Chem Soc* **137**, 3859–3866 (2015).

130. Assaf, K. I. *et al.* Water Structure Recovery in Chaotropic Anion Recognition: High-Affinity Binding of Dodecaborate Clusters to γ-Cyclodextrin. *Angewandte Chemie International Edition* **54**, 6852–6856 (2015).

131. Naskar, B., Diat, O., Nardello-Rataj, V. & Bauduin, P. Nanometer-Size Polyoxometalate Anions Adsorb Strongly on Neutral Soft Surfaces. *The Journal of Physical Chemistry C* **119**, 20985–20992 (2015).

132. Taraszewska, J. & Wójcik, J. Complexation of inorganic anions by β-cyclodextrin studied by polarography and 1H NMR. *Supramol Chem* **2**, 337–343 (1993).

133. Assaf, K. I., Gabel, D., Zimmermann, W. & Nau, W. M. High-affinity host–guest chemistry of large-ring cyclodextrins. *Org Biomol Chem* **14**, 7702–7706 (2016).

134. Assaf, K. I. *et al.* Hierarchical host–guest assemblies formed on dodecaborate-coated gold nanoparticles. *Chemical Communications* **53**, 4616–4619 (2017).

135. Warneke, J., Jenne, C., Bernarding, J., Azov, V. A. & Plaumann, M. Evidence for an intrinsic binding force between dodecaborate dianions and receptors with hydrophobic binding pockets. *Chemical Communications* **52**, 6300–6303 (2016).

136. Eyrilmez, S. M. *et al.* Binary twinned-icosahedral [B21H18]− interacts with cyclodextrins as a precedent for its complexation with other organic motifs. *Physical Chemistry Chemical Physics* **19**, 11748–11752 (2017).

137. Fan, P. *et al.* Interaction of dodecaborate cluster compounds on hydrophilic column materials in water. *J Chromatogr A* **1256**, 98–104 (2012).

138. Collins, K. D. Sticky ions in biological systems. *Proceedings of the National Academy of Sciences* **92**, 5553–5557 (1995).

139. Wu, Y. *et al.* Complexation of Polyoxometalates with Cyclodextrins. *J Am Chem Soc* **137**, 4111–4118 (2015).

140. Moussawi, M. A. *et al.* Polyoxometalate, Cationic Cluster, and γ-Cyclodextrin: From Primary Interactions to Supramolecular Hybrid Materials. *J Am Chem Soc* **139**, 12793–12803 (2017).

141. Moussawi, M. A. *et al.* Nonconventional Three-Component Hierarchical Host–Guest Assembly Based on Mo-Blue Ring-Shaped Giant Anion, γ-Cyclodextrin, and Dawson-type Polyoxometalate. *J Am Chem Soc* **139**, 14376–14379 (2017).

142. Wang, W. *et al.* Orthogonal Molecular Recognition of Chaotropic and Hydrophobic Guests Enables Supramolecular Architectures. *ChemNanoMat* **5**, 124–129 (2019).

143. Wang, W. *et al.* The chaotropic effect as an orthogonal assembly motif for multi-responsive dodecaborate-cucurbituril supramolecular networks. *Chemical Communications* **54**, 2098–2101 (2018).

144. Goel, T., Barooah, N., Mallia, M. B., Bhasikuttan, A. C. & Mohanty, J. Recognition-mediated cucurbit[7]uril-heptamolybdate hybrid material: a facile supramolecular strategy for 99mTc separation. *Chemical Communications* **52**, 7306–7309 (2016).

145. Fang, X., Kögerler, P., Isaacs, L., Uchida, S. & Mizuno, N. Cucurbit[n]uril−Polyoxoanion Hybrids. *J Am Chem Soc* **131**, 432–433 (2009).

146. Kuperman, M. V *et al.* Effective binding of perhalogenated closo-borates to serum albumins revealed by spectroscopic and ITC studies. *J Mol Struct* **1141**, 75–80 (2017).

147. Goszczyński, T. M., Fink, K., Kowalski, K., Leśnikowski, Z. J. & Boratyński, J. Interactions of Boron Clusters and their Derivatives with Serum Albumin. *Sci Rep* **7**, 9800 (2017).

148. Awad, D. *et al.* Halogenated Dodecaborate Clusters as Agents to Trigger Release of Liposomal Contents. *Chempluschem* **80**, 656–664 (2015).

149. Nabika, H., Inomata, Y., Itoh, E. & Unoura, K. Activity of Keggin and Dawson polyoxometalates toward model cell membrane. *RSC Adv* **3**, 21271–21274 (2013).

150. Barba-Bon, A. *et al.* Boron clusters as broadband membrane carriers. *Nature* **603**, 637–642 (2022).

151. Hohenschutz, M., Dufrêche, J.-F., Diat, O. & Bauduin, P. When Ions Defy Electrostatics: The Case of Superchaotropic Nanoion Adsorption. *J Phys Chem Lett* **14**, 3602–3608 (2023).

152. Malinenko, A. *et al.* Are Keggin's POMs Charged Nanocolloids or Multicharged Anions? *Langmuir* **34**, 2026–2038 (2018).

153. Hohenschutz, M., Grillo, I., Diat, O. & Bauduin, P. How Nano-Ions Act Like Ionic Surfactants. *Angewandte Chemie International Edition* **59**, 8084–8088 (2020).

154. Fernandez-Alvarez, R., Ďorďovič, V., Uchman, M. & Matějíček, P. Amphiphiles without Head-and-Tail Design: Nanostructures Based on the Self-Assembly of Anionic Boron Cluster Compounds. *Langmuir* **34**, 3541–3554 (2018).

155. Uchman, M., Abrikosov, A. I., Lepšík, M., Lund, M. & Matějíček, P. Nonclassical Hydrophobic Effect in Micellization: Molecular Arrangement of Non-Amphiphilic Structures. *Adv Theory Simul* **1**, 1700002 (2018).

156. Bauduin, P. *et al.* A Theta-Shaped Amphiphilic Cobaltabisdicarbollide Anion: Transition From Monolayer Vesicles to Micelles. *Angewandte Chemie International Edition* **50**, 5298–5300 (2011).

157. Brusselle, D. *et al.* Lyotropic Lamellar Phase Formed from Monolayered θ-Shaped Carborane-Cage Amphiphiles. *Angewandte Chemie International Edition* **52**, 12114–12118 (2013).

158. Zhang, Y. & Cremer, P. S. Chemistry of Hofmeister Anions and Osmolytes. *Annu Rev Phys Chem* **61**, 63–83 (2010).

159. Jungwirth, P. & Tobias, D. J. Ions at the Air/Water Interface. *J Phys Chem B* **106**, 6361–6373 (2002).

160. Ghosal, S. *et al.* Electron Spectroscopy of Aqueous Solution Interfaces Reveals Surface Enhancement of Halides. *Science* **307**, 563–566 (2005).

161. Collins, K. D., Neilson, G. W. & Enderby, J. E. Ions in water: Characterizing the forces that control chemical processes and biological structure. *Biophys Chem* **128**, 95–104 (2007).

162. Conway, B. E. The evaluation and use of properties of individual ions in solution. *J Solution Chem* **7**, 721–770 (1978).

163. Combariza, J. E., Kestner, N. R. & Jortner, J. Energy-structure relationships for microscopic solvation of anions in water clusters. *J Chem Phys* **100**, 2851–2864 (1994).

164. Luck, W. A. P. The influence of ions on water structure and on aqueous systems. in *Water and Ions in Biological Systems* 95–126 (Springer, 1985).

165. Luck, W. Zur Assoziation des Wassers II. Salzeffekte auf die Ultrarotbanden des Wassers. *Berichte der Bunsengesellschaft für physikalische Chemie* **69**, 69–76 (1965).

166. Terpstra, P., Combes, D. & Zwick, A. Effect of salts on dynamics of water: A Raman spectroscopy study. *J Chem Phys* **92**, 65–70 (1990).

167. Chen, X., Yang, T., Kataoka, S. & Cremer, P. S. Specific Ion Effects on Interfacial Water Structure near Macromolecules. *J Am Chem Soc* **129**, 12272–12279 (2007).

168. Onorato, R. M., Otten, D. E. & Saykally, R. J. Adsorption of thiocyanate ions to the dodecanol/water interface characterized by UV second harmonic generation. *Proceedings of the National Academy of Sciences* **106**, 15176–15180 (2009).

169. Fesinmeyer, R. M. *et al.* Effect of Ions on Agitation- and Temperature-Induced Aggregation Reactions of Antibodies. *Pharm Res* **26**, 903–913 (2009).

170. Schwierz, N., Horinek, D. & Netz, R. R. Anionic and Cationic Hofmeister Effects on Hydrophobic and Hydrophilic Surfaces. *Langmuir* **29**, 2602–2614 (2013).

171. Shahir, A. A., Khristov, K., Nguyen, K. T., Nguyen, A. V & Mileva, E. Combined Sum Frequency Generation and Thin Liquid Film Study of the Specific Effect of Monovalent Cations on the Interfacial Water Structure. *Langmuir* **34**, 6844–6855 (2018).

172. Hua, W., Verreault, D., Huang, Z., Adams, E. M. & Allen, H. C. Cation Effects on Interfacial Water Organization of Aqueous Chloride Solutions. I. Monovalent Cations: Li+, Na+, K+, and NH4+. *J Phys Chem B* **118**, 8433–8440 (2014).

173. Perrine, K. A. *et al.* Specific cation effects at aqueous solution−vapor interfaces: Surfactant-like behavior of Li+ revealed by experiments and simulations. *Proceedings of the National Academy of Sciences* **114**, 13363–13368 (2017).

174. Flores, S. C., Kherb, J., Konelick, N., Chen, X. & Cremer, P. S. The Effects of Hofmeister Cations at Negatively Charged Hydrophilic Surfaces. *The Journal of Physical Chemistry C* **116**, 5730–5734 (2012).

175. Götte, L. *et al.* Solvent-Shared Ion Pairs at the Air–Solution Interface of Magnesium Chloride and Sulfate Solutions Revealed by Sum Frequency Spectroscopy and Molecular Dynamics Simulations. *J Phys Chem A* **121**, 6450–6459 (2017).

176. Ganguly, P., Hajari, T. & van der Vegt, N. F. A. Molecular Simulation Study on Hofmeister Cations and the Aqueous Solubility of Benzene. *J Phys Chem B* **118**, 5331–5339 (2014).

177. Altekar, W. Fluorescence of proteins in aqueous neutral salt solutions. II. Influence of monovalent cation chlorides, particularly cesium chloride. *Biopolymers* **16**, 369–386 (1977).

178. Vrbka, L., Vondrášek, J., Jagoda-Cwiklik, B., Vácha, R. & Jungwirth, P. Quantification and rationalization of the higher affinity of sodium over potassium to protein surfaces. *Proceedings of the National Academy of Sciences* **103**, 15440–15444 (2006).

179. Klasczyk, B., Knecht, V., Lipowsky, R. & Dimova, R. Interactions of Alkali Metal Chlorides with Phosphatidylcholine Vesicles. *Langmuir* **26**, 18951–18958 (2010).

180. Bello, J. & Bello, H. R. Evidence from Model Peptides relating to the Denaturation of Proteins by Lithium Salts. *Nature* **194**, 681–682 (1962).

181. Bello, J., Haas, D. & Bello, H. R. Interactions of Protein-Denaturing Salts with Model Amides. *Biochemistry* **5**, 2539–2548 (1966).

182. Haas, D. J. Interactions between Lithium Salts and a Model Peptide: Crystal Structure of Lithium Chloride–N-Methylacetamide Complex. *Nature* **201**, 64–65 (1964).

183. Kurtz, J. & Harrington, W. F. Interaction of poly-L-proline with lithium bromide. *J Mol Biol* **17**, 440–455 (1966).

184. Schleich, T., Gentzler, R. & Von Hippel, P. H. Proton exchange of N-methylacetamide in concentrated aqueous electrolyte solutions. I. Acid catalysis. *J Am Chem Soc* **90**, 5954–5960 (1968).

185. Schleich, T., Rollefson, B. & Von Hippel, P. H. Proton exchange of N-methylacetamide in concentrated aqueous electrolyte solutions. II. Acid catalysis in water-dioxane mixtures and base catalysis. *J Am Chem Soc* **93**, 7070–7074 (1971).

186. Rao, Ch. P., Balaram, P. & Rao, C. N. R. 13C nuclear magnetic resonance studies of the binding of alkali and alkaline earth metal salts to amides. *Journal of the Chemical Society, Faraday Transactions 1: Physical Chemistry in Condensed Phases* **76**, 1008–1013 (1980).

187. Arakawa, T. & Timasheff, S. N. Mechanism of protein salting in and salting out by divalent cation salts: balance between hydration and salt binding. *Biochemistry* **23**, 5912–5923 (1984).

188. Okur, H. I., Kherb, J. & Cremer, P. S. Cations Bind Only Weakly to Amides in Aqueous Solutions. *J Am Chem Soc* **135**, 5062–5067 (2013).

189. Pluhařová, E., Baer, M. D., Mundy, C. J., Schmidt, B. & Jungwirth, P. Aqueous Cation-Amide Binding: Free Energies and IR Spectral Signatures by Ab Initio Molecular Dynamics. *J Phys Chem Lett* **5**, 2235–2240 (2014).

190. Balos, V., Bonn, M. & Hunger, J. Quantifying transient interactions between amide groups and the guanidinium cation. *Physical Chemistry Chemical Physics* **17**, 28539–28543 (2015).

191. Balos, V., Bonn, M. & Hunger, J. Correction: Quantifying transient interactions between amide groups and the guanidinium cation. *Physical Chemistry Chemical Physics* **18**, 1346–1347 (2016).

192. Balos, V., Kim, H., Bonn, M. & Hunger, J. Dissecting Hofmeister Effects: Direct Anion–Amide Interactions Are Weaker than Cation–Amide Binding. *Angewandte Chemie International Edition* **55**, 8125–8128 (2016).

193. Heyda, J. & Dzubiella, J. Ion-specific counterion condensation on charged peptides: Poisson–Boltzmann vs. atomistic simulations. *Soft Matter* **8**, 9338–9344 (2012).

194. Uejio, J. S. *et al.* Characterization of selective binding of alkali cations with carboxylate by x-ray absorption spectroscopy of liquid microjets. *Proceedings of the National Academy of Sciences* **105**, 6809–6812 (2008).

195. Aziz, E. F. *et al.* Cation-Specific Interactions with Carboxylate in Amino Acid and Acetate Aqueous Solutions: X-ray Absorption and ab initio Calculations. *J Phys Chem B* **112**, 12567–12570 (2008).

196. Hess, B. & van der Vegt, N. F. A. Cation specific binding with protein surface charges. *Proceedings of the National Academy of Sciences* **106**, 13296–13300 (2009).

197. Kubíčková, A. *et al.* Overcharging in Biological Systems: Reversal of Electrophoretic Mobility of Aqueous Polyaspartate by Multivalent Cations. *Phys Rev Lett* **108**, 186101 (2012).

198. Fedorov, M. V, Goodman, J. M. & Schumm, S. The effect of sodium chloride on poly-l-glutamate conformation. *Chemical Communications* 896–898 (2009) doi:10.1039/B816055D.

199. Fedorov, M. V, Goodman, J. M. & Schumm, S. To Switch or Not To Switch: The Effects of Potassium and Sodium Ions on α-Poly-l-glutamate Conformations in Aqueous Solutions. *J Am Chem Soc* **131**, 10854–10856 (2009).

200. Dzubiella, J. Molecular Insights into the Ion-Specific Kinetics of Anionic Peptides. *J Phys Chem B* **114**, 7098–7103 (2010).

201. Gaborek, T. J., Chipot, C. & Madura, J. D. Conformational Free-Energy Landscapes for a Peptide in Saline Environments. *Biophys J* **103**, 2513–2520 (2012).

202. Crevenna, A. H., Naredi-Rainer, N., Lamb, D. C., Wedlich-Söldner, R. & Dzubiella, J. Effects of Hofmeister Ions on the α-Helical Structure of Proteins. *Biophys J* **102**, 907–915 (2012).

203. Dzubiella, J. Salt-Specific Stability of Short and Charged Alanine-Based α-Helices. *J Phys Chem B* **113**, 16689–16694 (2009).

204. Kherb, J., Flores, S. C. & Cremer, P. S. Role of Carboxylate Side Chains in the Cation Hofmeister Series. *J Phys Chem B* **116**, 7389–7397 (2012).

205. van der Vegt, N. F. A. *et al.* Water-Mediated Ion Pairing: Occurrence and Relevance. *Chem Rev* **116**, 7626–7641 (2016).

206. He, Q., Vargas-Zúñiga, G. I., Kim, S. H., Kim, S. K. & Sessler, J. L. Macrocycles as Ion Pair Receptors. *Chem Rev* **119**, 9753–9835 (2019).

207. Bruce, E. E., Bui, P. T., Cao, M., Cremer, P. S. & van der Vegt, N. F. A. Contact Ion Pairs in the Bulk Affect Anion Interactions with Poly(N-isopropylacrylamide). *J Phys Chem B* **125**, 680–688 (2021).

208. Mason, P. E., Neilson, G. W., Dempsey, C. E., Barnes, A. C. & Cruickshank, J. M. The hydration structure of guanidinium and thiocyanate ions: Implications for protein stability in aqueous solution. *Proceedings of the National Academy of Sciences* **100**, 4557–4561 (2003).

209. Wernersson, E. *et al.* Orientational Dependence of the Affinity of Guanidinium Ions to the Water Surface. *J Phys Chem B* **115**, 12521–12526 (2011).

210. Vazdar, M., Uhlig, F. & Jungwirth, P. Like-Charge Ion Pairing in Water: An Ab Initio Molecular Dynamics Study of Aqueous Guanidinium Cations. *J Phys Chem Lett* **3**, 2021–2024 (2012).

211. Mason, P. E., Dempsey, C. E., Neilson, G. W., Kline, S. R. & Brady, J. W. Preferential Interactions of Guanidinum Ions with Aromatic Groups over Aliphatic Groups. *J Am Chem Soc* **131**, 16689–16696 (2009).

212. Dooley, K. H. & Castellino, F. J. Solubility of amino acids in aqueous guanidinium thiocyanate solutions. *Biochemistry* **11**, 1870–1874 (1972).

213. Mason, P. E., Dempsey, C. E., Neilson, G. W. & Brady, J. W. Nanometer-Scale Ion Aggregates in Aqueous Electrolyte Solutions: Guanidinium Sulfate and Guanidinium Thiocyanate. *J Phys Chem B* **109**, 24185–24196 (2005).

214. Dempsey, C. E., Mason, P. E., Brady, J. W. & Neilson, G. W. The Reversal by Sulfate of the Denaturant Activity of Guanidinium. *J Am Chem Soc* **129**, 15895–15902 (2007).

215. Mason, P. E. *et al.* Specificity of Ion−Protein Interactions: Complementary and Competitive Effects of Tetrapropylammonium, Guanidinium, Sulfate, and Chloride Ions. *J Phys Chem B* **113**, 3227–3234 (2009).

216. Heyda, J. *et al.* Guanidinium can both Cause and Prevent the Hydrophobic Collapse of Biomacromolecules. *J Am Chem Soc* **139**, 863–870 (2017).

217. Long, F. A. & McDevit, W. F. Activity Coefficients of Nonelectrolyte Solutes in Aqueous Salt Solutions. *Chem Rev* **51**, 119–169 (1952).

218. Neuberg, C. Hydrotropic phenomena. *Biochem. Z* **76**, 107–108 (1916).

219. Saylor, J. H., Whitten, A. I., Claiborne, I. & Gross, P. M. The Solubilities of Benzene, Nitrobenzene and Ethylene Chloride in Aqueous Salt Solutions. *J Am Chem Soc* **74**, 1778–1781 (1952).

220. Bockris, J. O., Bowler-Reed, J. & Kitchener, J. A. The salting-in effect. *Transactions of the Faraday Society* **47**, 184–192 (1951).

221. Linderstrom-Lang, K. . *Compt. rend. trav. lab. Carlsberg* **15**, (1923).

222. Deno, N. C. & Spink, C. H. The McDevit-Long Equation for Salt Effects on Non-Electrolytes. *J Phys Chem* **67**, 1347–1349 (1963).

223. Bergen Jr, R. L. & Long, F. A. The salting in of substituted benzenes by large ion salts. *J Phys Chem* **60**, 1131–1135 (1956).

224. Desnoyers, J. E., Pelletier, G. E. & Jolicoeur, C. Salting-In by Quaternary Ammonium Salts. *Can J Chem* **43**, 3232–3237 (1965).

225. Conway, B. E., Novak, D. M. & Laliberté, L. Salting-out and ionic volume behavior of some tetraalkylammonium salts. *J Solution Chem* **3**, 683–711 (1974).

226. Wen, W.-Y. & Hung, J. H. Thermodynamics of hydrocarbon gases in aqueous tetraalkylammonium salt solutions. *J Phys Chem* **74**, 170–180 (1970).

227. von Hippel, P. H. & Wong, K.-Y. The Collagen Gelatin Phase Transition. II. Shape of the Melting Curves and Effect of Chain Length. *Biochemistry* **2**, 1399–1413 (1963).

228. Schrier, E. E. & Scheraga, H. A. The effect of aqueous alcohol solutions on the thermal transition of ribonuclease. *Biochim Biophys Acta* **64**, 406–408 (1962).

229. Frank, H. S. & Evans, M. W. Free volume and entropy in condensed systems III. Entropy in binary liquid mixtures; partial molal entropy in dilute solutions; structure and thermodynamics in aqueous electrolytes. *J Chem Phys* **13**, 507–532 (1945).

230. Jain, S. & Ahluwalia, J. C. Differential scanning calorimetric ammonium and tetraalkylammonium lysozyme studies on the effect of halides on the stability of lysozyme. *Biophys Chem* **59**, 17–177 (1996).

231. Frank, H. S. & Wen, W.-Y. Ion-solvent interaction. Structural aspects of ion-solvent interaction in aqueous solutions: a suggested picture of water structure. *Discuss Faraday Soc* **24**, 133–140 (1957).

232. Marcus, Y. *Ion Properties*. (Marcel Dekker, 1997).

233. Marcus, Y. Tetraalkylammonium Ions in Aqueous and Non-aqueous Solutions. *J Solution Chem* **37**, 1071–1098 (2008).

234. Fowler, D. L., Loebenstein, W. V, Pall, D. B. & Kraus, C. A. Some Unusual Hydrates of Quaternary Ammonium Salts. *J Am Chem Soc* **62**, 1140–1142 (1940).

235. McMullan, R. & Jeffrey, G. A. Hydrates of the Tetra n-butyl and Tetra i-amyl Quaternary Ammonium Salts. *J Chem Phys* **31**, 1231–1234 (1959).

236. Feil, D. & Jeffrey, G. A. Polyhedral Clathrate Hydrates. II. Structure of the Hydrate of Tetra Iso-Amyl Ammonium Fluoride. *J Chem Phys* **35**, 1863–1873 (1961).

237. Bonamico, M., Jeffrey, G. A. & McMullan, R. K. Polyhedral Clathrate Hydrates. III. Structure of the Tetra n-Butyl Ammonium Benzoate Hydrate. *J Chem Phys* **37**, 2219–2231 (1962).

238. Jeffrey, G. A. & McMullan, R. K. Polyhedral Clathrate Hydrates. IV. The Structure of the Tri n-Butyl Sulfonium Fluoride Hydrate. *J Chem Phys* **37**, 2231–2239 (1962).

239. McMullan, R. K., Bonamico, M. & Jeffrey, G. A. Polyhedral clathrate hydrates. V. structure of the tetra-n-butyl ammonium fluoride hydrate. *J Chem Phys* **39**, 3295–3310 (1963).

240. Beurskens, G., Jeffrey, G. A. & McMullan, R. K. Polyhedral clathrate hydrates. VI. Lattice type and ion distribution in some new peralkyl ammonium, phosphonium, and sulfonium salt hydrates. *J Chem Phys* **39**, 3311–3315 (1963).

241. Englezos, P. Clathrate hydrates. *Ind Eng Chem Res* **32**, 1251–1274 (1993).

242. Wen, W.-Y. & Saito, S. Apparent and partial molal volumes of five symmetrical tetraalkylammonium bromides in aqueous solutions. *J Phys Chem* **68**, 2639–2644 (1964).

243. Wen, W.-Y. Structural aspects of aqueous tetraalkylammonium salt solutions. *J Solution Chem* **2**, 253–276 (1973).

244. Nair, H. K., Seravalli, J., Arbuckle, T. & Quinn, D. M. Molecular Recognition in Acetylcholinesterase Catalysis: Free-Energy Correlations for Substrate Turnover and Inhibition by Trifluoro Ketone Transition-State Analogs. *Biochemistry* **33**, 8566–8576 (1994).

245. Cavallito, C. J. Quaternary ammonium salts — advances in chemistry and pharmacology since 1960. in *Progress in Drug Research / Fortschritte der Arzneimittelforschung / Progrès des recherches pharmaceutiques* (eds. Berde, B. et al.) 267–373 (Birkhäuser Basel, 1980).

246. Armstrong, C. M. Interaction of Tetraethylammonium Ion Derivatives with the Potassium Channels of Giant Axons. *Journal of General Physiology* **58**, 413–437 (1971).

247. Adams, C. M., Price, M. P., Snyder, P. M. & Welsh, M. J. Tetraethylammonium Block of the BNC1 Channel. *Biophys J* **76**, 1377–1383 (1999).

248. Zhou, M., Morais-Cabral, J. H., Mann, S. & MacKinnon, R. Potassium channel receptor site for the inactivation gate and quaternary amine inhibitors. *Nature* **411**, 657–661 (2001).

249. Faraldo-Gómez, J. D. *et al.* Mechanism of Intracellular Block of the KcsA K+ Channel by Tetrabutylammonium: Insights from X-ray Crystallography, Electrophysiology and Replica-exchange Molecular Dynamics Simulations. *J Mol Biol* **365**, 649–662 (2007).

250. Gottlieb, H. E., Kotlyar, V. & Nudelman, A. NMR chemical shifts of common laboratory solvents as trace impurities. *Journal of organic chemistry* **62**, 7512–7515 (1997).

251. Reddy, P. M., Taha, M., Venkatesu, P., Kumar, A. & Lee, M.-J. Destruction of hydrogen bonds of poly(N-isopropylacrylamide) aqueous solution by trimethylamine N-oxide. *J Chem Phys* **136**, 234904 (2012).

252. Rice, C. V. Phase-Transition Thermodynamics of N-Isopropylacrylamide Hydrogels. *Biomacromolecules* **7**, 2923–2925 (2006).

253. Mäemets, V. & Koppel, I. Effect of ions on the 17O and 1H NMR chemical shifts of water. *Journal of the Chemical Society, Faraday Transactions* **94**, 3261–3269 (1998).

254. Shoolery, J. N. & Alder, B. J. Nuclear Magnetic Resonance in Concentrated Aqueous Electrolytes. *J Chem Phys* **23**, 805–811 (2004).

255. Maeda, Y., Higuchi, T. & Ikeda, I. Change in Hydration State during the Coil−Globule Transition of Aqueous Solutions of Poly(N-isopropylacrylamide) as Evidenced by FTIR Spectroscopy. *Langmuir* **16**, 7503–7509 (2000).

256. Maeda, Y., Nakamura, T. & Ikeda, I. Change in Solvation of Poly(N,N-diethylacrylamide) during Phase Transition in Aqueous Solutions As Observed by IR Spectroscopy. *Macromolecules* **35**, 10172–10177 (2002).

257. Tamaki, K. The Surface Activity of Tetra-n-alkylammonium Halides in Aqueous Solutions. The Effect of Hydrophobic Hydration. *Bull Chem Soc Jpn* **47**, 2764–2767 (1974).

258. Sagle, L. B. *et al.* Investigating the Hydrogen-Bonding Model of Urea Denaturation. *J Am Chem Soc* **131**, 9304–9310 (2009).

259. Guenzler, H. & Gremlich, H. U. *IR Spectroscopy An introduction*. (Wiley-VCH, 2002).

260. Kabisch, G. & Klose, M. A Raman spectroscopic study of aqueous and methanolic tetramethylammonium chloride solutions. *Journal of Raman Spectroscopy* **7**, 311–315 (1978).

261. Bottger, G. L. & Geddes, A. L. The infrared spectra of the crystalline tetramethylammonium halides. *Spectrochimica Acta* **21**, 1701–1708 (1965).

262. Marcus, Y. Viscosity B-coefficients, structural entropies and heat capacities, and the effects of ions on the structure of water. *J Solution Chem* **23**, 831–848 (1994).

Appendix A: LCST Measurements with Sigma-Aldrich PNIPAM

As mentioned in sections 2.1.2 and 3.2.1, the LCST measurements shown in the main text were performed using PNIPAM from the vendor Polymer Source Inc., whereas all other measurements (namely, the ATR-FTIR and ^{1}H-NMR spectroscopy experiments) were done on PNIPAM sourced from Sigma-Aldrich. These two instances of the polymer partially differ in their average molecular masses and PDI's (see 2.1.2), and possibly in finer aspects of their structure such as the specific end groups or polymer tacticity, but are otherwise identical. As shown below in Figure 34, LCST measurements were also tested with the Sigma-Aldrich PNIPAM and the trends amongst the salts are qualitatively the same as those described in 3.2.1. The principal reason for preferring the Polymer Source Inc. sourced PNIPAM for the LCST investigations presented in the main text is that the LCST of Sigma-Aldrich PNIPAM in neat water, ~34.1°C, is slightly higher than the average literature value commonly reported. While this is not strictly an issue, possible confusion with salt-driven LCST shifts were preferred to be avoided, and so the Polymer Source Inc. sourced PNIPAM was selected.

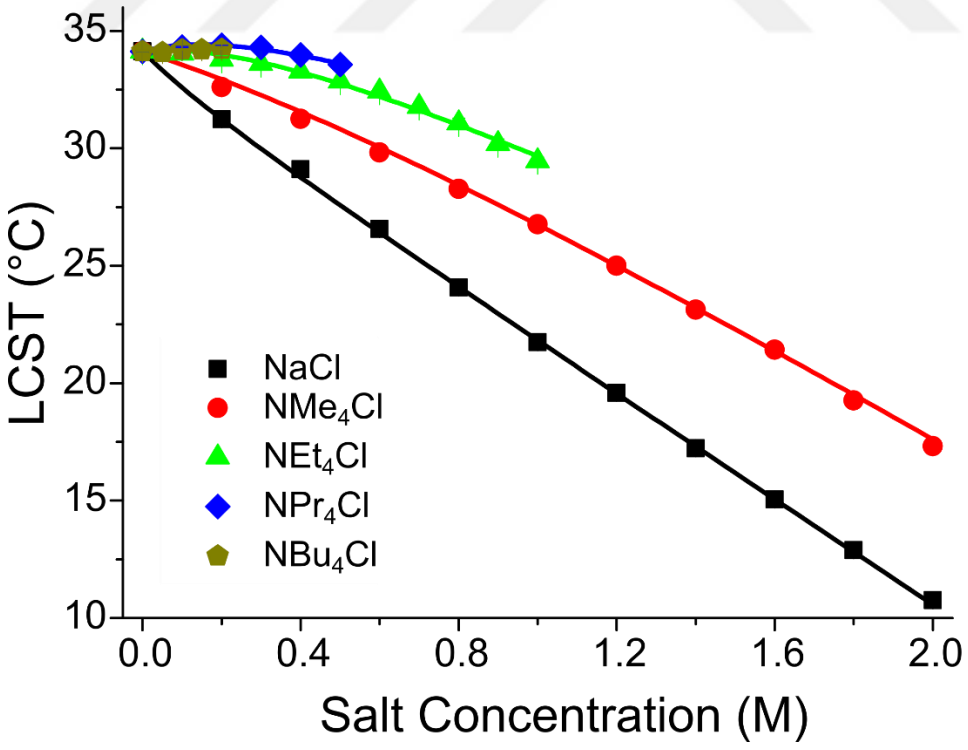

Figure 34: LCST measurements of 5 mg/mL PNIPAM (Sigma-Aldrich) in aqueous solutions of the salt shown. The measurement details are the same as described previously (2.3).

Appendix B: LCST of PNIPAM at High Salt Concentrations

As discussed in section 3.2.1, the LCST of PNIPAM in the presence of very high concentrations of QA chloride salts resulted in rather anomalous effects that were deemed outside the model presented for the salting-in and salting-out effects predominant at the lower concentrations. Figure 35 below shows the LCST of PNIPAM in solutions of the same six salts up to the highest concentrations of the QA chlorides that could yield measurable LCST values. As can be seen, this was determined roughly to be only ~1.4 M for NPr_4Cl and ~1.2 M for NBu_4Cl. In fact, above these concentrations (and perhaps even partially at these points) PNIPAM was rapidly insolubilized out of bulk solution; that is, solid lyophilized PNIPAM would dissolve not at all or only partially at these salt concentrations. This can likely be understood as the extreme case of the salting-out effect of these salts. LCST measurements near the solubility limit were also generally less reliable, as values tended to become increasingly imprecise and some PNIPAM samples could spontaneously precipitate out the polymer from the solution. Instead of attempting to account for the high concentration extremes within the model employed for lower concentrations, it might be speculated as related to the unique hydration-state behavior of highly concentrated solutions of very large tetraalkylammonium salts, as described in section 1.3.3. In fact, the clathrate hydrate formation of NBu_4Cl at and above 1.2 M stock solutions was observed when the solutions were cooled near 0 – 5°C, whereby the bulk solution would spontaneously solidify in an amorphous/semi-crystalline appearing mass that could be re-liquified by heating. The elucidation of this unique behavior at high concentration limits is interesting but beyond the scope of this present work, and may be better explored through use of hydration-state spectroscopic studies, such as Raman-MCR methodologies.[123]

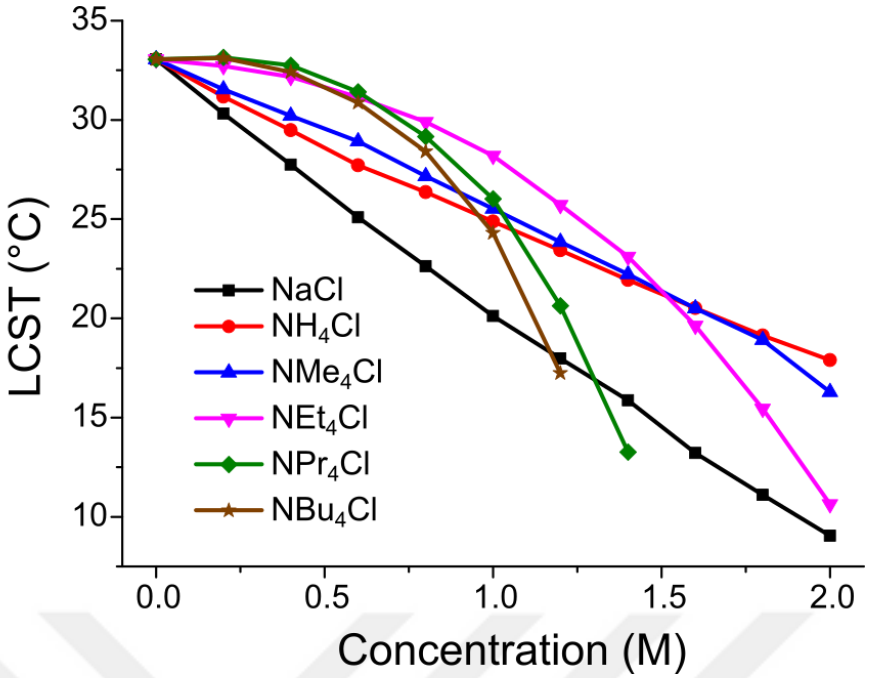

Figure 35: LCST of 5 mg/mL PNIPAM in solutions of the salts shown at the largest range of concentrations for which measurements could be conducted. Note that the data points are not plotted with fit lines as in Figure 18, as the trends could not fit by the model employed for the lower concentration regime. Instead, data are shown in full and connected with straight-line segments only as a guide to the eye.

Appendix C: LCST Measurements of PNIPAM in D_2O Media

As mentioned in passing in section 3.2.1, LCST measurements of PNIPAM were also conducted in D_2O media for some of the salts studied, instead of regular aqueous (i.e., H_2O) solutions. The motivation for testing this was two-fold: (i) Firstly, it is reasonable to deem it necessary to verify that the general behavior and salt effect trends observed in regular H_2O media are not qualitatively different in D_2O, and (ii) Solvent isotopic substitution methods have previously found use in examining solvent-dominated effects of polymer hydration dynamics, in order to distinguish or couple cosolute effects from purely solvent-directed ones. For instance, Zhang et al.[9] employed a similar D_2O-medium LCST study of PNIPAM in their work to argue that the two-step phase transition observed in high concentration of strongly-hydrated anions' sodium salts comprised an initial partial dehydration step involving breakage of hydrogen bonds with the solvent, followed by the dehydration of the hydrophobic polymer backbone. However, in our present case the D_2O isotopic solvent substitution does not provide categorical or qualitatively distinguishing information. A representative comparison of the H_2O vs. D_2O media LCST's of PNIPAM with NaCl and NPr_4Cl cosolutes are shown below in Figure 36. As can be seen, the LCST is affected slightly by the solvent change, as is expected, in both the neat solvent and salt cosolute solutions. The general effect is a positive shift in the LCST, mostly within +2°C. Accounting for the values of the shifts under concurrent solvent isotope, salt identity and concentration changes is not a simple task, and the effect cannot readily be partitioned between the thermodynamic contributions of polymer, salt and water-water hydration/interaction changes without additional thermodynamic measurements beyond LCST temperatures. Nevertheless, we see that the general trends observed in H_2O media indeed extend to D_2O media as well, which validates our use of both media in the methods employed.

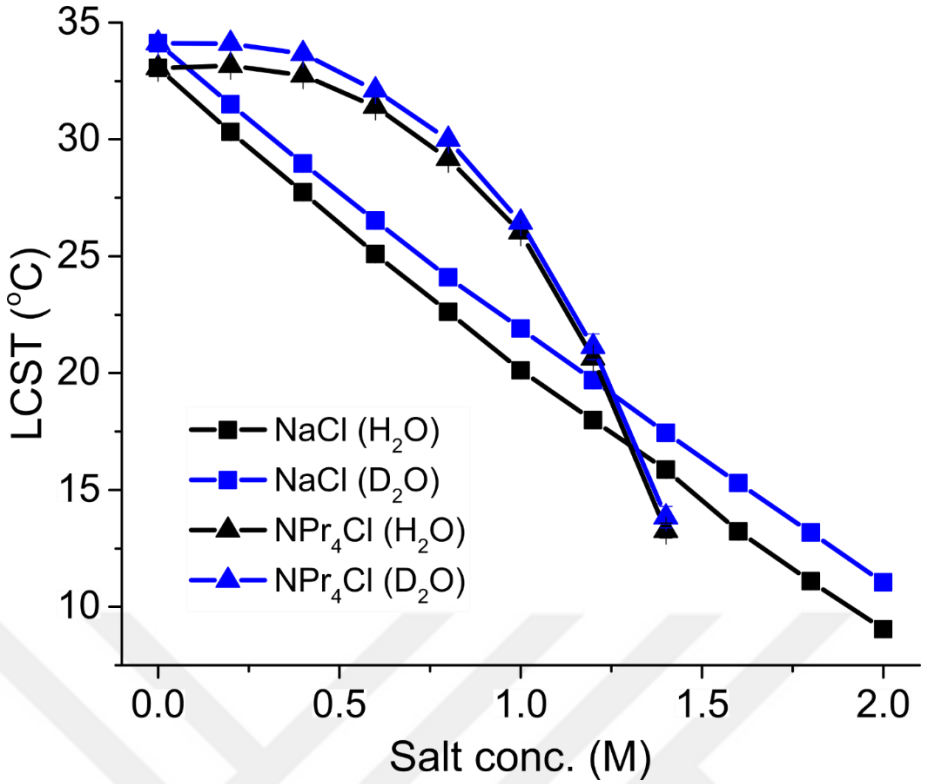

Figure 36: LCST measurements of 5 mg/mL PNIPAM in H_2O and D_2O solutions of the two salts shown. The effect of the solvent isotopic substitution is to shift the LCST of PNIPAM (within + 2°C), but the overall trend of the salt effects is the same as shown in Figure 18.